NASA CONTRACTOR REPORT

NASA CR-423

RESEARCH AND DEVELOPMENT OF AN INSTRUMENT FOR DETECTION OF EXTRATERRESTRIAL LIFE BY OPTICAL ROTATORY DISPERSION

Prepared under Contract No. NASw-842 *by*
MELPAR, INC.
Falls Church, Va.
for

NATIONAL AERONAUTICS AND SPACE ADMINISTRATION • WASHINGTON, D. C. • APRIL 1966

NASA CR-423

RESEARCH AND DEVELOPMENT OF AN INSTRUMENT FOR DETECTION OF EXTRATERRESTRIAL LIFE BY OPTICAL ROTATORY DISPERSION

Prepared under Contract No. NASw-842 by
MELPAR, INC.
Falls Church, Va.

for

NATIONAL AERONAUTICS AND SPACE ADMINISTRATION

For sale by the Clearinghouse for Federal Scientific and Technical Information
Springfield, Virginia 22151 – Price $1.45

ABSTRACT

A novel single-beam polarimeter capable of development to meet the requirements of a space mission to seek optical activity in extraterrestrial soil samples is described. Optical rotatory dispersion curves of extracts of soil and ancient strata were obtained with this instrument. The polarimeter is relatively insensitive to scattering, dichroism and absorption. It can make measurements of optical rotation in the presence of optical densities of approximately 5, provided the light source has sufficient spectral purity.

It is concluded that the feasibility of producing an experiment to seek for optical activity in an extraterrestrial soil sample has been demonstrated. Further scientific effort should be devoted to elucidating the chemistry of the extracts and to relate the chemistry more closely to the complex optical rotatory dispersion curves.

1. INTRODUCTION

This document is submitted as the final technical report on the NASA Contract NASw-842. The purpose of this contract is to provide the National Aeronautics and Space Administration with a research effort, the anticipated outcome of which is the development of an instrument for detection of biological molecules by means of optical rotation. This system will consist of a soil sample processor to dissolve the soluble components of the soil sample and an electronic sensor with associated phase change detector and with automatic program operation.

The specific objectives of the present program were:

A. Design, fabrication and testing of a breadboard model of an instrument for the detection of biological molecules by means of optical rotation.

B. Design of a laboratory-flight-development unit after tests had been conducted on the breadboard model to prove design feasibility.

C. Delivery of one tested laboratory-flight-development instrument.

1.1 Summary of Work Performed

The research conducted under this contract has resulted in the successful development of an instrument for detecting biological molecules by means of optical rotation. While further research is needed, particularly with respect to the scientific aspects of an extraterrestrial measurement of optical rotation, it is believed that a firm basis for considering such an experiment has been provided. This conclusion rests on the results obtained to date: First, optical activity has been demonstrated in extracts of a variety of soils and sediments. For example, rotations of approximately 0.6 degree were obtained from 30-second extracts of desert soil containing only 0.4% organic matter. (The extraction procedure is simple and rapid. The reagents can be sterilized with heat.) Second, the simple, automatic instrumentation which has been developed can readily be adapted to meet the requirements of a space mission. It is estimated that a flight unit would have the following specifications:

Weight	2 pounds
Volume	0.1 cubic foot
Power consumption	16 watt-hours

A more detailed summary of the work is given below.

A. A novel, single-beam polarimeter has been developed. The purpose of this development was to devise a method for measuring optical rotation that eliminates or minimizes the shortcomings of conventional instrumentation and is capable of being readily adapted to meet the requirements of a space mission.

B. A breadboard of the new, single-beam polarimeter was constructed and feasibility of this approach demonstrated.

C. The breadboard instrument was adapted to function as a spectropolarimeter over the wavelength range of approximately 250mμ to 600 mμ.

D. A limited number of aqueous soil extraction procedures was investigated with respect to the amount of optical activity of the extract and the freedom from nonspecific absorption. Of these, EDTA (Ethylenediamine tetraacetate)-citrate at pH 5.0 was found to be best.

E. Optical rotatory dispersion and absorption spectra of EDTA-citrate extracts were investigated as a function of processing time and soil-to-solvent ratio. Both parameters were found to be of importance. Appreciable optical activity was obtainable with short extraction times (approximately one minute) and large solvent-to-soil ratios. Short extraction times also favored the production of extracts of relatively low optical density.

F. Optical rotatory dispersion curves of EDTA-citrate extracts of a variety of desert soils and of local Virginia soils were obtained.

G. Qualitative and quantitative chemical analyses for total organic matter, total protein and total carbohydrates were performed on the soils from which extracts were made. No significant correlation with optical activity was discernable, indicating that more detailed chemical analyses and separation are required in future work.

H. In collaboration with Dr. Hoering of the Carnegie Institution of Washington, optical rotatory dispersion curves of organic extracts of ancient sedimentary strata were obtained. Cotton regions were found in the visible portion of the spectrum. These correlated well with the absorption spectra.

I. Based upon data obtained with the breadboard instrument, a laboratory-flight-development unit was designed, constructed and placed in operation.

J. A patent disclosure has been filed on the single-beam polarimeter developed under this contract.

K. A paper entitled, "A Polarimeter for Detection of Extraterrestrial Life" was presented at the 18th Annual Conference on Engineering in Medicine and Biology (Nov. 10-12, 1965). An abstract appears in the proceedings.

2. STATEMENT OF THE PROBLEM

In general, optical activity of solutes is considered related to living material or its residues. This is the reason for considering that the optical activity found in petroleums strongly indicates their biologic origin. The same reason is the basis for seeking optical activity in extracts of precambrian strata. Finding optical activity in such strata could be interpreted as strongly suggesting the presence of molecules of biological origin.

Assuming no new chemistry is involved in the composition of Mars, an experiment designed to measure optical activity in an extraterrestrial environment is attractive for the reasons listed below:

A. It makes few basic assumptions. The assumptions made can be compared with laboratory data on terrestrial samples.

B. Optical activity is a fundamental and highly generalized experiment. On earth, optical activity is ubiquitously present in all known biological species. It is also present in ancient as well as contemporary biological residues.

C. Optical activity is a simple rapid determination requiring only a few minutes. The extraction procedure can be a one-step, single-solution process.

D. Optical activity is a physical measurement which does not depend on the physiological state of the material being measured.

E. By virtue of the simplicity of the experiment and the economy of its means, it is possible to repeat a measurement a number of times on a given mission without unduly burdening the space, weight, and power capacities of a spacecraft.

F. A positive result would provide a firm basis for a logical sequence of more sophisticated additional experiments. These could be designed to provide physical-chemical characterization of the substances detected.

G. Sensitivity is high. Work to date has demonstrated as much as 0.6 degrees of optical rotation in a 30-second extract of desert soil containing 0.4 per cent organic matter. The ratio of soil to extractant was 1:40.

H. The speed of the entire experiment is such that it requires only a few minutes.

I. The entire experiment can be reduced to a weight of 2 pounds occupying only 0.1 cubic foot.

J. The logistic requirements are minimal. Reagents are stable, quantities are small, and the experiment is self contained. Only a soil sample (approximately one gram) and electrical power (approximately 16 watt-hours must be furnished).

In pursuit of these broad objectives Melpar has addressed itself to a research effort to demonstrate the feasability of such an experiment and to provide scientific data useful for designing a specific experiment and interpreting its results; and an instrumentation development program to provide the means for carrying out the scientific effort and to demonstrate the potential for an exobiological experiment. The remainder of this report is a detailed summary of the work performed under this context.

3. THEORETICAL ANALYSIS

For maximum sensitivity, measurements will probably be performed in the far blue or near ultraviolet regions of the spectrum. At these wavelengths, extraterrestrial samples may be expected to exhibit appreciable amounts of circular dichroism, scattering, and nonspecific absorption of light. These phenomena may mask or degrade the measurement of optical activity. Thus, it is of prime importance that an instrument designed to measure optical activity of extraterrestrial samples discriminate against such interfering phenomena. Ability to perform in this fashion must be coupled with high sensitivity and simplicity of design and operation. A novel single-beam polarimeter which meets these criteria has been developed. Also, it is largely insensitive to any noise that results in amplitude modulation of the signal.

Figure 1 is a block diagram that shows the operation of the single-beam polarimeter. The polarimeter consists of a monochromatic light source, a sample cell and a rotating analyzer. Fixed to the outer circumference of the rotating analyzer housing is a magnetic track, that, in conjunction with the magnetic head shown, functions as a magnetic recorder. The amplitude of the light leaving the rotating analyzer varies sinusoidally as a function of time. The phototube and its associated circuits produce an electrical analog of the light impinging on the face of the phototube and record the phase of this signal on the magnetic track. Thus, this indication of phase is fixed in space and becomes an integral part of the rotating analyzer. When an optically active sample is introduced between the polarizer and the rotating analyzer, the phase of the signal is altered. The phase of this new signal is also recorded on the magnetic track. These recordings consist of pulses with fast rise-times that mark the point on the sinusoidal waveform where it crosses the zero axis in the positive direction. The crossing occurs at an angular displacement of 45° between the plane of the analyzer and the plane of the plane-polarized light incident on its face.

Since the analyzer rotates at a constant speed, the phase between the sample and reference signals may be measured as a function of time and constitutes a direct measurement of the optical rotation produced by the sample. This is accomplished, as shown in figure 1, by reproducing the pulses and utilizing them to open and close a gate to a decade counter. Clock pulses from a stable crystal oscillator are counted only during the time between pulses. The stability of readily available crystal oscillators is in the neighborhood of 1 part in 10^8, and is so high that the time measuring system represented by the electronic counter and crystal oscillator combination need not be considered in determining the limitations on the accuracy of the overall system. Operation of the polarimeter is rapid, since a measurement is obtained in 1/2 second for a rotational speed of 1 revolution per second, and also, since the determination of phase is made at that instant in time when the plane of the analyzer is displaced by 45° from the plane of the plane-polarized light incident on it. The system is very conservative of radiant energy and can either deal with high optical density or, for solutions of low optical density, utilize a relatively weak light source.

$$I^2 = I_o^2 \cos^2(\omega t + \theta)$$

$$I^2 = \frac{I_o^2}{2} + \frac{I_o^2}{2} \cos(2\omega t + 2\theta)$$

$$E_s = kI^2$$

$$E_s' = \frac{kI_o^2}{2} \cos(2\omega t + 2\theta)$$

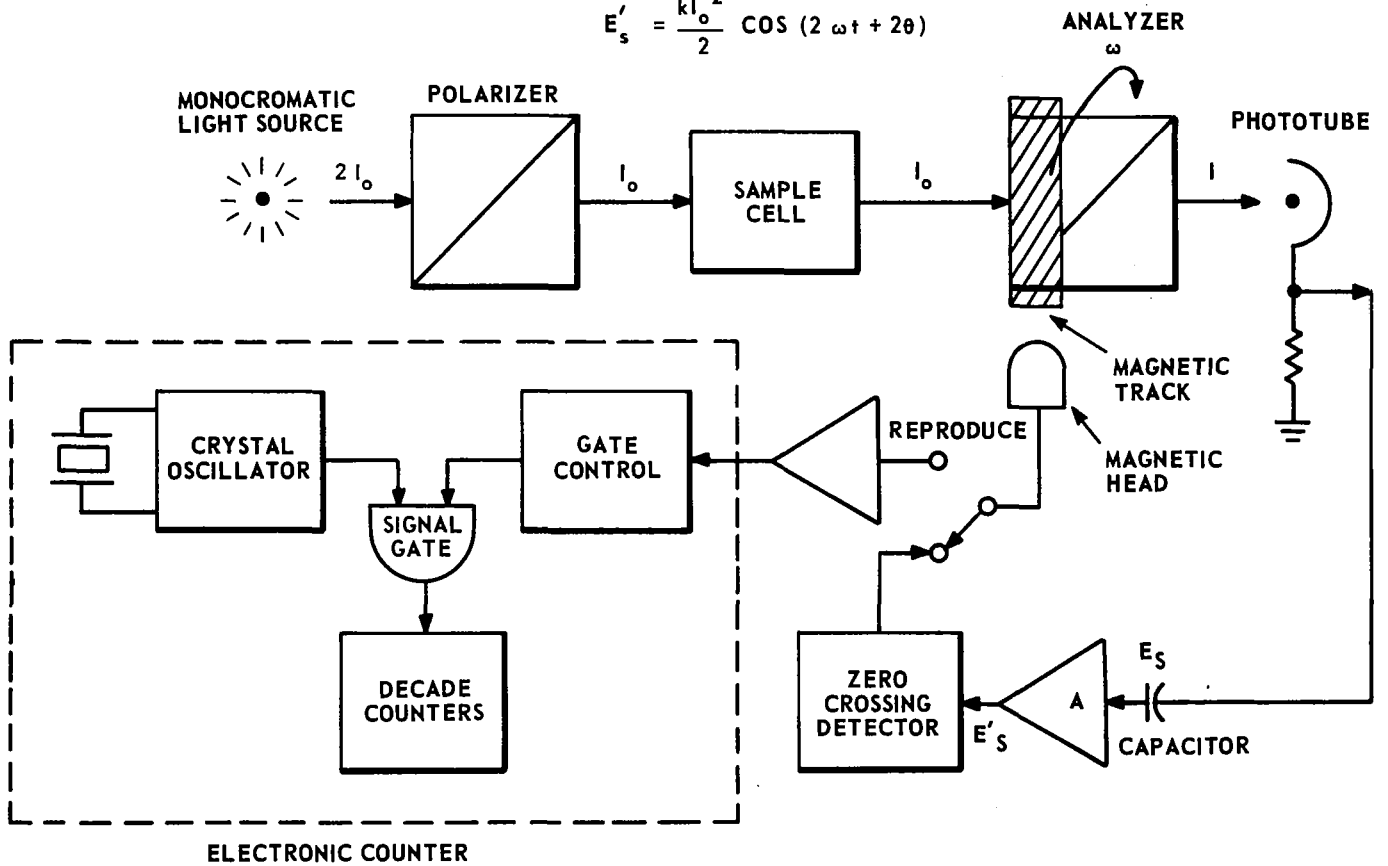

Figure 1. Block Diagram Showing Principles of Operation

Utilizing the symbols as shown in figure 1, the intensity of light I^2 leaving the analyzer prism, is related to the intensity of light incident on the analyzer, Io^2, as shown in equation (1).

$$I^2 = Io^2 \cos^2 \phi, \tag{1}$$

where Io = amplitude of plane-polarized light incident on analyzer prism polarized;

I = amplitude of the polarized light transmitted by the analyzer prism;

and ϕ = the angle between the plane of polarization of the incident light and the plane of polarization defined by the analyzer

This is the familiar law of Malus.

When the analyzer is rotated at a constant speed, w ($w = 2\pi f$, where f is the rotational frequency), then equation (1) becomes

$$I^2 = Io^2 \cos^2 (wt + \theta), \tag{2}$$

where t = time in seconds,

and θ = the phase angle

Using a trigonometric identity, equation (2) may be transformed to

$$I = \frac{Io^2}{2} + \frac{Io^2}{2} \cos (2wt + 2\theta) \tag{3}$$

With an optically inactive or reference solution in the sample cell, the angle θ may be made zero. Now, if an optically active substance is placed between the polarizer and analyzer, θ takes on values other than zero. The optical rotation of the sample is given by equation (4).

$$\text{Optical Rotation (OR)} = 2\theta$$

Voltage of the signal, E_s, produced by the photoelectric device in the range of linear operation is

$$E_s = \frac{k R Io^2}{2} + \frac{Io^2}{2} \cos (2wt + 2\theta), \tag{5}$$

where k is the transducer constant in μamps/μwatt, and R is the resistance of the phototube load resistor

After passage through the capacitor, the dc term is lost, and the signal E's (in volts) is given by

$$E_s' = (k\ R\ Io^2/2)\cos\ (2wt + 2\theta). \qquad (6)$$

The signal (in volts) applied to the input of the zero-crossing detector is simply

$$AE_s' = (AkRIo^2/2)\cos\ (2wt + 2\theta), \qquad (7)$$

where A = amplifier gain.

The zero-crossing detector generates a pulse with fast rise-time whenever the signal, AE'_s crosses the baseline in the positive direction. The pulse is recorded on the magnetic track that is an integral part of the rotating analyzer assembly. Since the electronic signal transmission is essentially instantaneous, the position of the pulse on the magnetic track fixes in space the position of the analyzer where its plane of polarization is rotated 45 degrees with respect to the plane of polarization of the incident beam. A given amount of optically active material in the sample cell produces a pulse with a unique position on the circumference described by the magnetic track. The distance on the magnetic track between a reference and a sample pulse is highly insensitive to changes in amplitude of the signal applied to the zero-crossing detector over a wide dynamic range.

The rotational frequency, f, is limited on the high side by the response of the magnetic recording system, and on the low-frequency end by the increasing indeterminacy of detecting the point of zero-crossing as the slope at the zero-crossing becomes smaller. A rotational frequency, f, of one revolution per second has been chosen. This is in keeping with a crystal frequency of one megacycle per second and the pulse response of the magnetic recording system employed. In a perfect system, the smallest angle of optical rotation that could be measured under these conditions is 0.36 millidegrees ± 0.36 millidegrees, which represents #1 count. This is not considered the theoretical limit on sensitivity. The practical limit is not yet known. The very small magnitude of the minimum angle requires additional investigation to determine the practical limits.

Figure 2 shows the waveforms in the system, the derivation of the pulses marking the zero-crossings, and the angle 2θ.

The time measurement which measures the optical rotation will always contain a small amount of indeterminacy, or error, as do all practical systems. It is impossible to eliminate all noise. For the system under discussion here, this may be termed trigger-level error. Figure 3 is a graphic representation of the effect of noise from various sources on the definition of the zero-crossing point. The symbols and their definitions

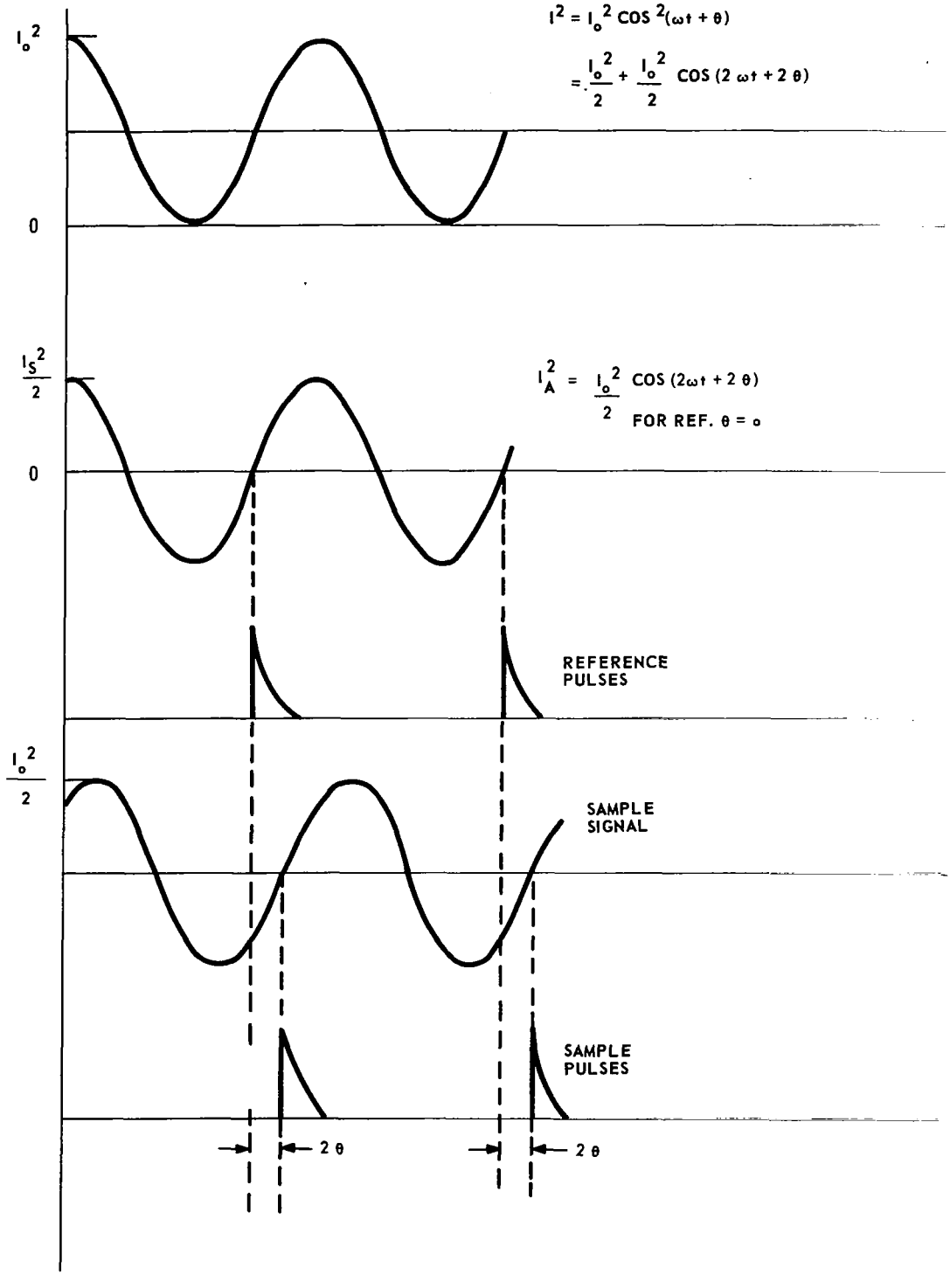

Figure 2. Waveforms of Single Beam Polarimeter

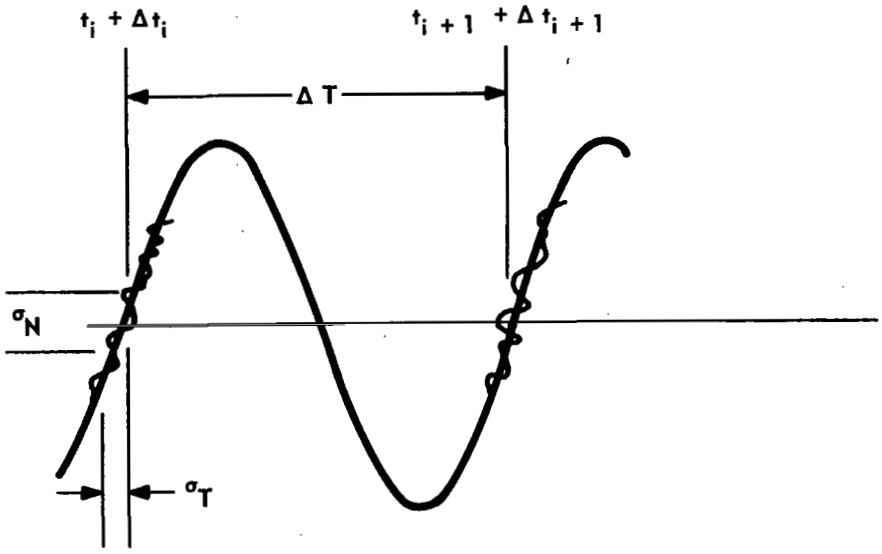

$$\sigma_N = \sqrt{\sigma_t^2 + A^2(\sigma_S^2 + \sigma_L^2 + \sigma_a^2)} \text{ VOLTS}$$

σ_t = STANDARD DEVIATION OF TRIGGER POINT VARIATION

σ_S = STANDARD DEVIATION OF THE PHOTOTUBE NOISE.

σ_L = STANDARD DEVIATION OF THE VARIATION IN THE PHASE OF I DUE TO VARIATION IN ω

σ_a = STANDARD DEVIATION IN THE AMPLIFIER NOISE REFERRED TO THE INPUT

A = AMPLIFIER GAIN

$\sigma_T = \sigma_{\Delta t_i} = \sigma_{\Delta t_{i+1}}$ = STANDARD DEVIATION OF THE TIME ERROR IN THE TRIGGER POINT.

σ_M = STANDARD DEVIATION OF TIME MEASUREMENT ERROR.

$$\sigma_M = \sqrt{2}\ \sigma_T = \sqrt{2}\ \frac{\sigma_N}{AS} \text{ SEC}$$

S = SLOPE AT AMPLIFIER INPUT IN VOLTS/SEC.

Figure 3. Detection of Zero Crossing

are defined as shown in the figure. The assumption is made that the various sources of noise are not correlated. Thus σ_n, the standard deviation of the total noise, may be calculated by taking the root mean square of the standard deviations of the individual noise sources.

The standard deviation of the time measurement error, σ_M (in seconds), is of primary concern here.

$$\sigma_M = \sqrt{2}\ \sigma_N / AS = \sqrt{2}\ \sqrt{\sigma_t^2 + A^2 (\sigma_s^2 + \sigma_e^2 + \sigma_a^2)}\ / AS \qquad (8)$$

where S = slope at the amplifier input in volts/second

Examination of equation (8) shows that if the second term under the radical is large, then the increased slope at the zero-crossing will have a relatively small effect on reducing the value of σ_M. However, if the second term under the radical becomes small because the σ's are samll, then σ_M will be approximately inversely proportional to the amplifier gain, A.

σ_a and σ_s can be made small by utilizing narrow electrical bandwidths. σ_l can be made small by driving the rotating analyzer from the crystal time base. It should also be noted that, other things being equal, increasing the speed of rotation will reduce the magnitude of σ_M. As mentioned above, however, the pulse response of the magnetic recording system must be taken into account. Further, for a space mission, increasing the rotation speed means a wider electrical bandwidth, and the effect that this will have on the power consumption must be carefully evaluated.

Circular dichroism in the sample will, in general, cause the light incident on the analyzer to be elliptically polarized. Scattering, which causes depolarization, and nonspecific absorption affect the intensity of the light striking the photoelectric detector, but do not change the phase angle, θ, as shown in equation (9).

$$I^2 = \frac{P}{2} \exp(-Kd) + \frac{Q}{2} \exp(-Md) \cos(2wt + 2\theta), \qquad (9)$$

where $P = B^2 + C^2 + S^2$

$K = k_a c_a$

$M = (k_a c_a + k_s c_s)$

B = the amplitude of the major axis of the ellipse

C = amplitude of the minor axis of the ellipse

$Q = B^2 - C^2$ = ellipticity

S = Scattered, depolarized light which passes through the analyzer

k_a = absorption coefficient of nonoptically active material

k_s = scattering coefficient

C_a = concentration of absorbing material

C_s = concentration of scattering material

d = cell length

B and C are given by equations (10) and (11):

$$B^2 = I^2 \left[\exp(-k_r dc/2) + \exp(-k_l dc/2) \right]^2, \qquad (10)$$

and

$$C^2 = I^2 \left[\exp(-k_r dc/2) - \exp(-k_l dc/2) \right]^2, \qquad (11)$$

where

K_r = absorption coefficient of right circularly polarized light

k_l = absorption coefficient of left circularly polarized light

c = concentration of dichroic substance

The quantities shown in equations (10) and (11) are wavelength dependent. B and C have values of consequence only in the neighborhood of an absorption band.

Examination of equation (9) shows that the effect of the presence of dichroism, depolarization scattering, and nonspecific absorption modifies the first term on the right and affects only the coefficient of the time-dependant second term. As discussed above, the dc term is discarded by passing the signal through a capacitor. Only the amplitude and not the phase angle of the second term is altered. Since the system is relatively insensitive to signal amplitude, the presence of considerable amounts of dichroism, depolarization scattering, and nonspecific absorption should be tolerable. Indeed, by use of neutral density filters and sucrose solutions, it has been possible to obtain measurements of optical rotation in the presence of an optical density of 5.5.

Absorption can have a deleterious effect on the accuracy when the beam illuminating the system contains stray light of wavelengths other than the selected one. This is most likely when the absorption spectrum displays a strong wavelength dependance. In this case, the measured optical rotation (i.e., the apparent optical rotation) may be less than the true optical rotation

produced by the sample at the nominal wavelength. In general, the effect of relatively narrow absorption bands will be to make the apparent optical rotation smaller than the true optical rotation. This is due primarily to the fact that the emission spectrum of most light sources is much more intense at the long-wavelength end of the spectrum than at the short-wavelength end. In any region of the spectrum where this behavior is reversed, however, the apparent optical rotation will be larger than the true optical rotation. The magnitude of this effect depends upon the stray light spectral distribution and the absolute amplitude and shape of the absorption band. The ideal situation is to use a light source which contains no stray light. Because of the premium placed upon spectral purity, lasers come immediately to mind. Where a laser cannot be used, the strong spectral lines produced by an arc discharge may reasonably approximate the ideal situation.

Still another reason for requiring spectral purity can be discerned by examining figure 4. The upper curve shows the optical rotatory dispersion spectrum in the neighborhood of the Cotton region, and the lower curve is the absorption spectrum which is associated with the Cotton region. Optical rotation is an additive phenomenon. If the measuring spectral bandwidth is too broad, or if stray light is present, the apparent rotation may approach zero. In similar fashion, if the measuring spectral bandwidth is too broad, both halves of the optical rotatory dispersion curve are encompassed by it. Since the Cotton region contains both dextrorotation and levorotation, the net optical activity measured will, in general, be less than would be the case if only the dextrorotary or levorotatory portion of the optical rotatory dispersion curve were measured with sufficiently narrow bandwidth. Absolute criteria cannot be applied, as the specific needs depend upon the shape of the optical rotatory dispersion curve under consideration. However, if a line source is utilized, these interferences become nonexistent.

Practically, a line source, such as a mercury arc lamp produces emission in regions of the spectrum other than that of the selected line. Thus, the interference due to stray light may be minimized, but not necessarily eliminated.

A vector representation of the effect of stray light is shown in figure 5. The vectors represent the amplitude and phase of the sinusoidal modulation of the light intensity produced by the rotation of the analyzer prism with respect to the polarizer prism. The sample is between these two prisms. The x-axis coincides with the reference from which optical rotation is measured and represents the spatial position of the plane of polarization in the absence of an optically active sample.

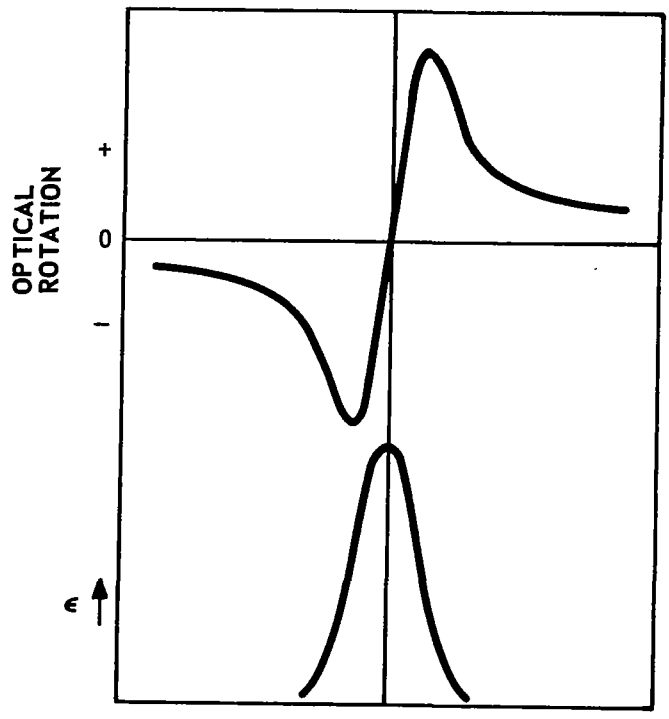

Figure 4. The Cotton Region

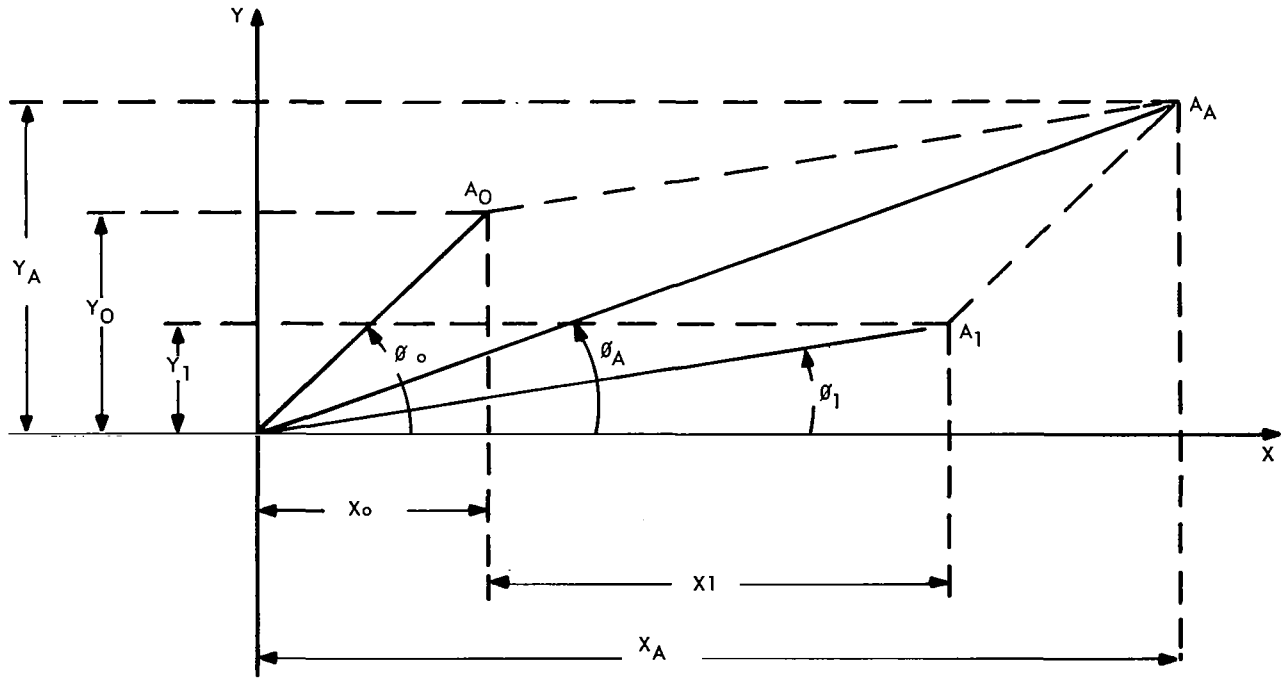

Figure 5. Vector Representation of the Effect of Stray Light

In this figure:

A_o = the amplitude of light at wavelength λ_o

λ_o = wavelength at which the sample has maximum optical activity and strong absorption

ϕ_o = optical rotation of λ_o by the sample

A_1 = the amplitude of light at wavelength λ_1

λ_1 = wavelength at which the sample has optical activity less than maximum and weak absorption

ϕ_1 = optical rotation of λ_1 by the sample

A_A = the vector sum of A_o and A_1

ϕ_A = the apparent optical rotation

Inspection of figure 5 shows that ϕ_A, the apparent optical rotation, is less than ϕ_o, the true optical rotation. The converse could also occur. The diagram shows clearly that when stray light is present, the departure from the true optical rotation is a function of both the absorption spectrum and the optical rotatory dispersion of the material. The conditions for obtaining a true reading are: (1) the absence of stray light (Vector $A_1 = 0$), or, (2) optical rotation that is essentially constant over the spectral range that includes the desired wavelength and the stray light.

Condition (1) can be achieved with such a monochromatic source as a suitable arc discharge lamp and a double pass monochromator. Condition (2) means that it may be desirable to make a measurement close to but not too far into the Cotton region. In the case of the extraterrestrial experiment, the latter is probably preferable. It would maximize the probability of detecting optical rotation even though the magnitude of the rotation measured would not be maximum. Also, it would make the requirements for spectral purity less stringent. A simple light source and filter would thus be feasible. The loss in sensitivity that occurs when the measurement of optical rotation is not made at one of the peaks of the Cotton region may be more or less recovered by utilizing the ability of the system to make measurements in the presence of high optical density, i. e., increased concentration. Again, the absorption spectrum in the region of the spectrum occupied by the stray light should be essentially flat.

4. MATERIALS AND METHODS

Figures 6, 7 and 8 are schematic diagrams of the electronic portions of the breadboard instrument. The circuitry is conventional, but pains have been taken to utilize stable power supplies where required and to minimize or eliminate sources of spurious phase shifts. Not shown is the electronic counter, which includes the crystal oscillator. This is a commercial instrument and, insofar as a breadboard is concerned, the function can be served by any one of a number of available instruments.

Figures 9 and 10 are photographs of the experimental setup utilizing the breadboard instrument. In figure 9, the monochromator which has been added to convert the instrument to a spectropolarimeter can be seen at the left. The electronic counter and some of the power supplies may be seen at the right of the figure. The box in the center is the cover that houses the polarimeter proper. Figure 10 is an inside view of the polarimeter housing showing, on the right, the magnetic track surrounding the rotating analyzer. The polarizing prism is at the extreme left of the figure.

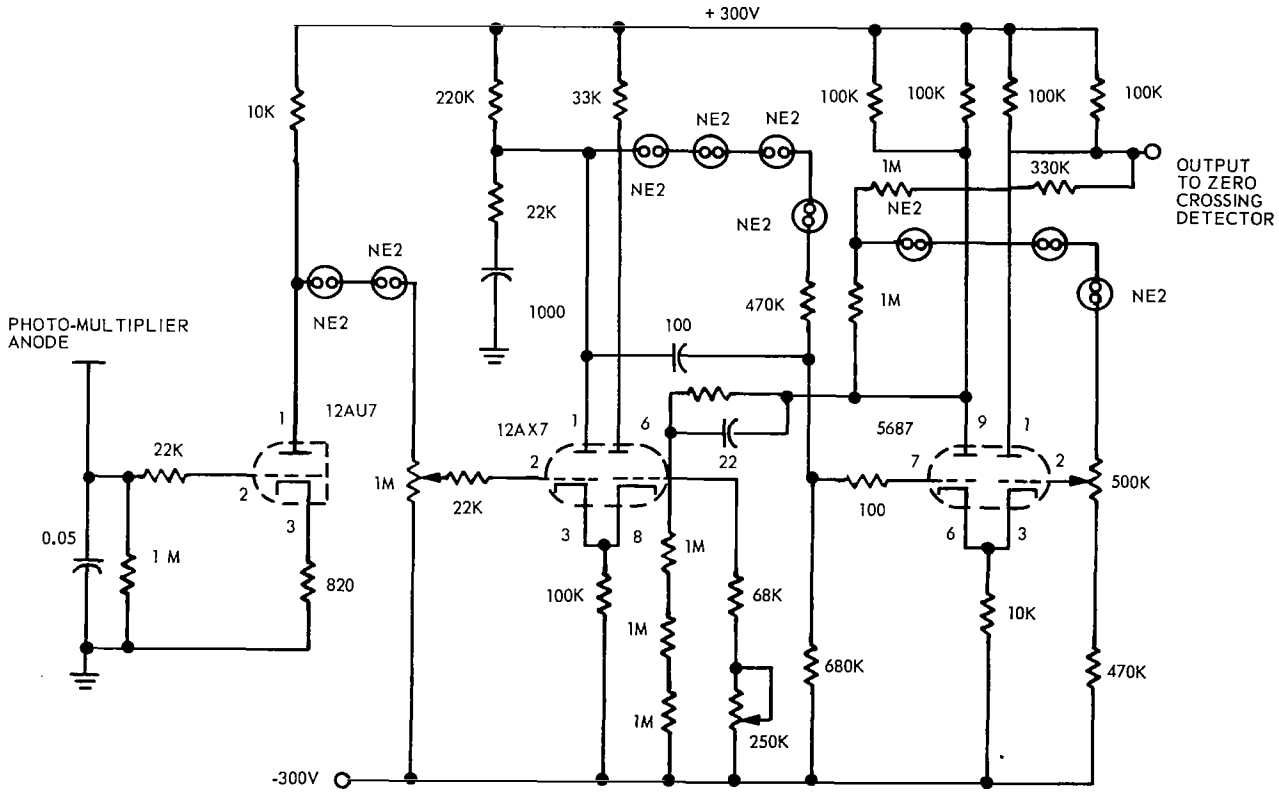

NOTE: ALL CAPACITANCES IN UUF

Figure 6. Preamplifier, Schematic Diagram

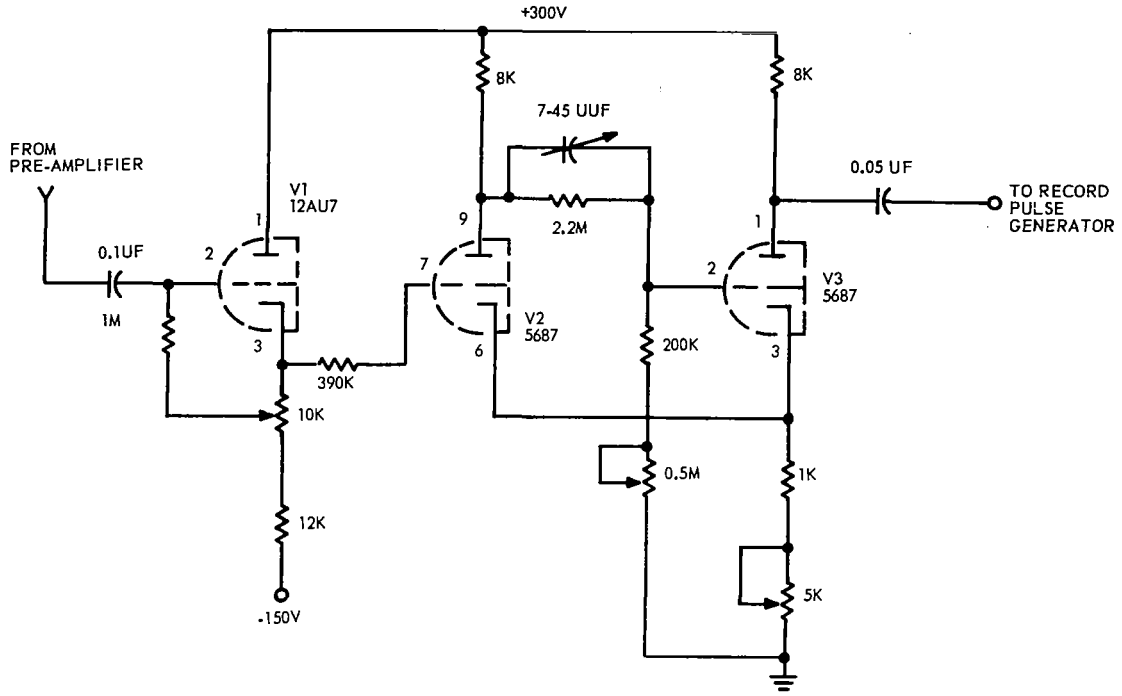

Figure 7. Zero-Crossing Detector, Schematic Diagram

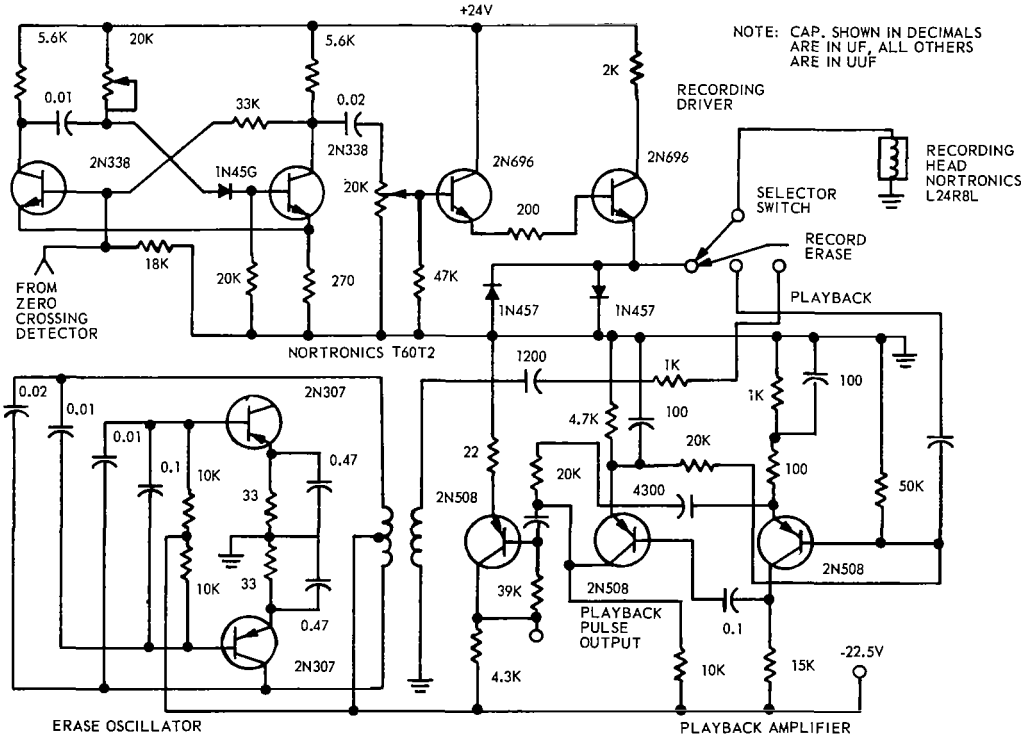

Figure 8. Magnetic Record, Playback and Erase, Schematic Diagram

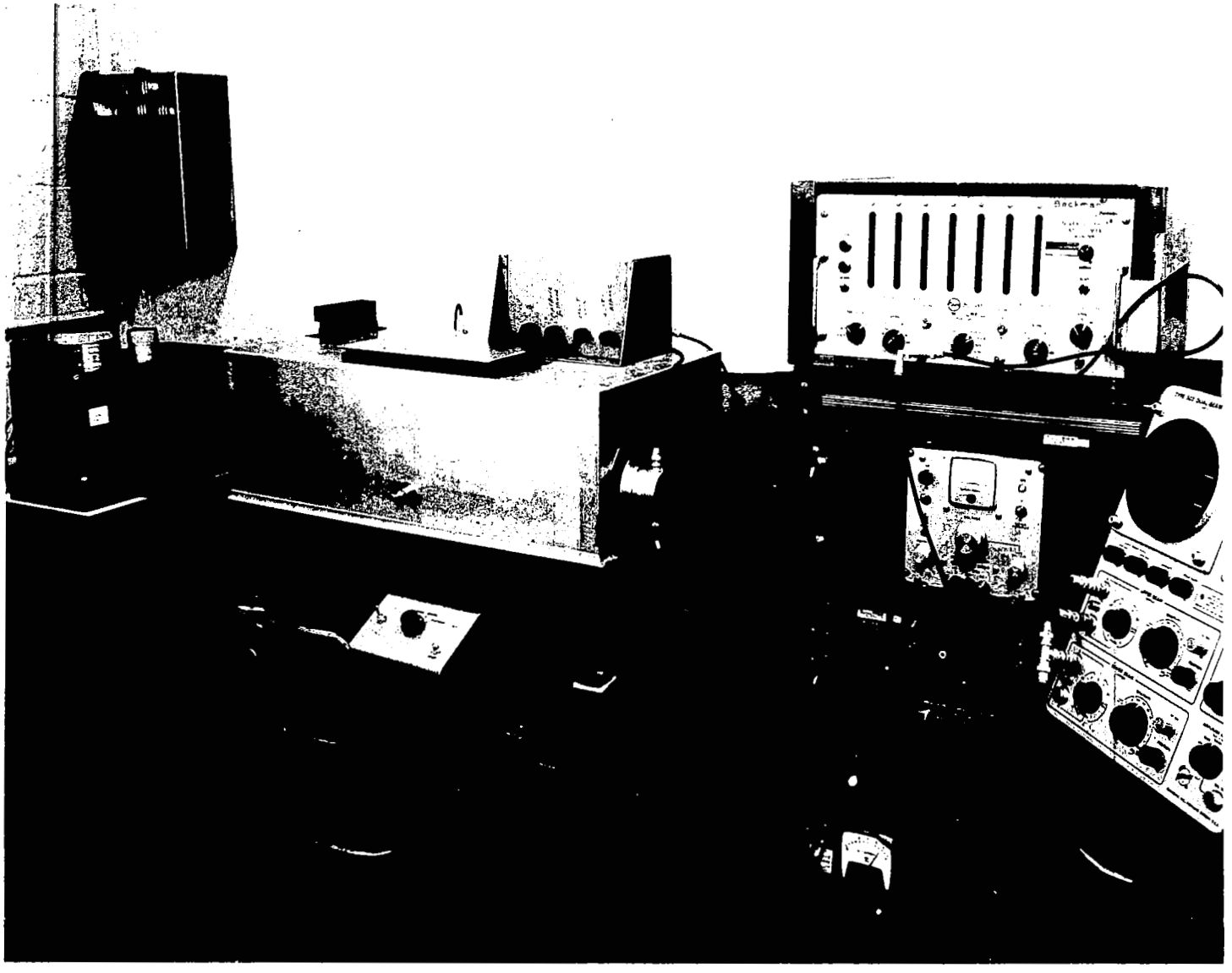

Figure 9. Photograph of Single-Beam Spectropolarimeter Breadboard Experimental Setup

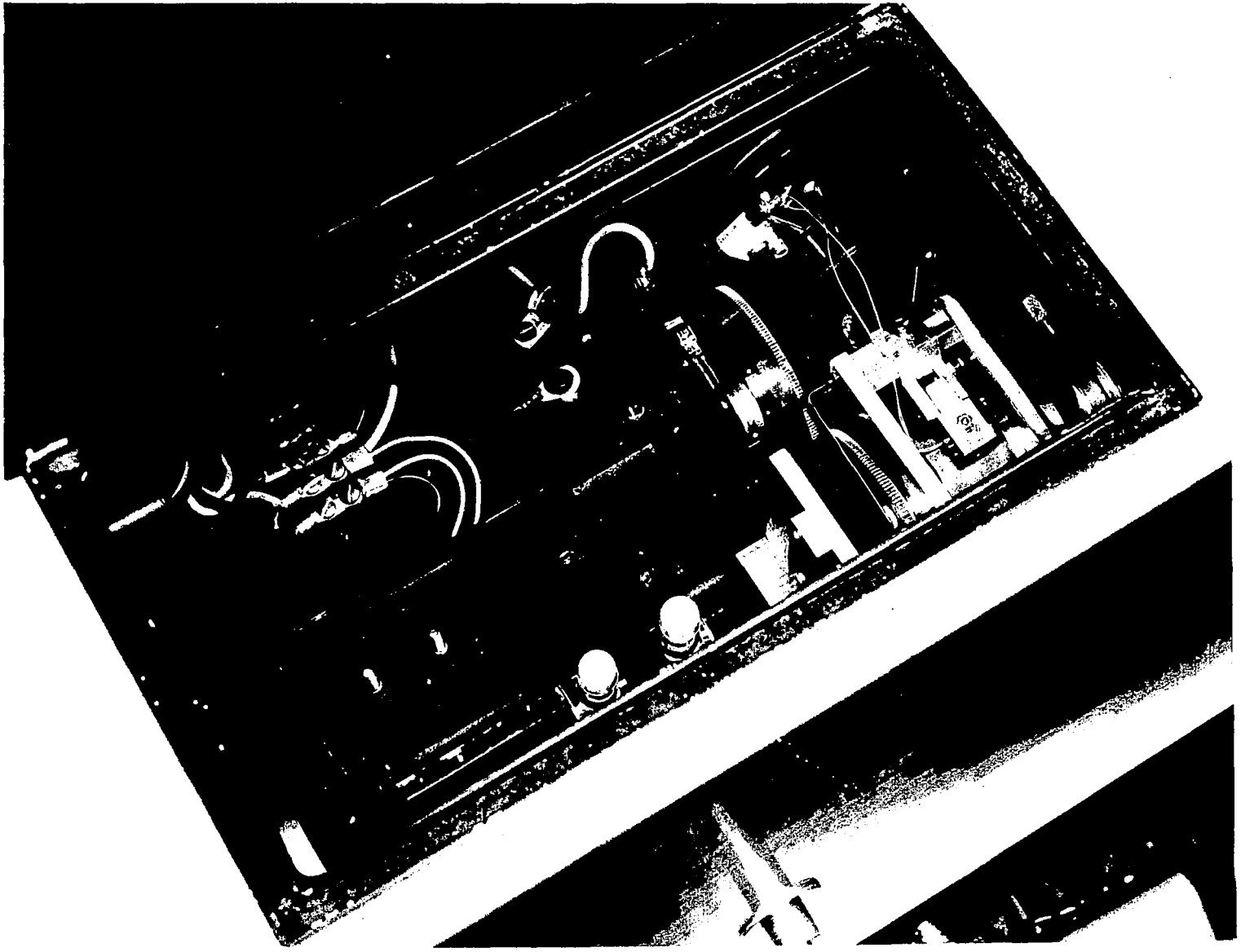

Figure 10. Photograph of Breadboard Single-Beam Polarimeter Showing Rotating Analyzer and Magnetic Recorder

4.1 Measurement of Optical Rotation

Desert soil extracts were prepared as shown elsewhere in this report. Organic extracts and fractionation of ancient sedimentary strata were prepared by Dr. T. Hoering of the Carnegie Institution of Washington.

Measurements were made using 5-cm quartz cells. When small amounts of optical rotation were expected (i.e., the sample pulse would overlap the reference pulse of the magnetic drum), a bias consisting of a 1-cm quartz cell filled with sucrose was placed in tandem with the sample cell. The sucrose bias provided a known amount of optical rotation as its effect, but did not otherwise affect the measurements. The optical rotation produced by the sample was determined by subtracting the observed rotation from the known rotation produced by the sucrose. Observed rotations smaller than the sucrose biasing rotation indicated levorotation. Observed rotations larger than the sucrose biasing rotation indicated dextrorotation.

The monochromator which was added to the breadboard to make it a spectropolarimeter is a Leitz in-line visible and UV instrument, containing both glass and quartz prisms. It is a single-pass instrument and, hence, produces appreciable stray light. The stray light was partically controlled by using glass absorption filters in addition to the monochromator. The light source is a xenon lamp. The filters utilized were as follows:

Wavelength Interval (mμ)	Filter
250-400	Corning 7-54
400-560	Kodak Wratten 44
560-600	Kodak Wratten 24

4.2 Calibration

The functioning of the instrument was checked along with its calibration with a 5 percent sucrose solution (1-cm quartz cell) against distilled water as reference. The wavelength range was 260-600 mμ. Instrument readings were compared with literature values. The sucrose solutions used for calibration and bias were checked with a Rudolph polarimeter at the sodium D line.

This is a direct reading instrument. The counter indication in units of time differs from the angular measurement by a constant. For the present time base (one megacycle) and a rotational speed of one revolution per second, 1 millisecond equalled 0.36 degree of optical rotation.

Data from the measurements of calibrating solutions and model compounds were plotted on log-log paper. The straight line that should result, in regions far from the Cotton region, is a very rapid check of the performance of the instrument.

Measurement procedure consisted of recording a reference pulse (water for aqueous extracts and n-heptane for organic extracts) on the magnetic drum. The pulse due to the reference was then recorded on magnetic track. The pulses were then read off and the time interval between them measured with an electronic counter. This reading was converted to degrees. This procedure was followed at each wavelength at which measurements were made. Wavelength changes were made manually. The rotation produced by the cells themselves was recorded separately and used to correct the readings as needed.

4.3 Extraction Procedures

The desert soils utilized in this study were obtained through the courtesy of Dr. Harold Mazursky of the Geological Survey, U. S. Department of the Interior, and Dr. R. E. Cameron of the Jet Propulsion Laboratory's Soil Science Division. The agricultural soils were local Virginia samples obtained from nearby grassy fields and gardens. All soil samples were sieved to approximately 200 microns particle size and stored in a dessicator over silica gel. The soil chosen for study of extraction and analysis for optical activity was selected because its moisture content is similar to that calculated from spectroscopic data for the Martian surface.[1]

4.3.1 Extraction Procedures

A. Extraction Procedure for Chemical Assay

Accurately weighed portions of the soil were extracted by magnetic stirring for a variety of soil-to-extractant ratios and extraction times and subsequently centrifuged at 10,000 rpm for 10 minutes. The supernatants were utilized for ORD determinations, spectrophotometric measurements, and qualitative and quantitative chemical analysis for carbohydrates, total protein, and nucleic acids. Total organic matter was determined on the dry soil samples.

B. Extraction Efficiency of Phosphate and Borate Buffers for Soil Nucleic Acids Utilizing Tritated Ribonucleic Acid (RNA)

The tritium-labeled RNA used as a tracer had been prepared from *E. coli*. A uracil requiring mutant of *E. coli* (ATCC 9723-g) was grown under standard conditions in a medium containing uracil-H^3. After the washed cells were lysed with sodium lauryl sulfate, the RNA was extracted with water-saturated phenol and subjected to purification on Sephadex G-25. The final solution contained 735 μg RNA/ml with an activity of 2.01×10^6 dpm/ml, equivalent to 2,750 dpm/μg RNA.

1. Air-dried soil samples (5.0 gm each) were agitated for 1 minute with 10.0 ml of 0.1-M phosphate buffer pH 8.0 or 0.1-M borate buffer pH 9.0 and centrifuged for 10 minutes at 3,000 rpm. One series of soil samples was left in contact with buffer for 16 hours before centrifugation. The clear supernatant solutions were withdrawn and undiluted aliquots were used to determine absorption spectra in the near ultraviolet range (220 mμ to 350 mμ).

2. RNA-H^3 (0.1 ml of solution containing 73 μg RNA) was added to 1.0 gm soil samples. After thorough mixing, these soil samples were left to air-dry at room temperatures. Each dried sample was agitated with 2.0 ml of buffer solution for one minute and centrifuged for 10 minutes. Aliquots of the supernatant solutions, withdrawn immediately after centrifugation, were used to determine radioactivity and optical absorption in the near ultraviolet.

C. Extraction of Soil for Optical Activity

In order to determine the optimal soil-to-extractant ratio for extracting maximum amounts of optical activity, accurately weighed portions of JPL 1-2 were extracted with 0.1 M citrate buffer pH 5.0 containing 0.05 M EDTA (ethylenediamine tetracetate) at soil-to-extractant ratios of 1:40, 1:10, and 1:2 (wt:vol). In order to study the effects of time on yield of optical activity, contact times of 10 seconds, 30 seconds, 1 minute, 5 minutes, 15 minutes and 30 minutes were used. Following extraction by rapid magnetic stirring, the solutions were clarified by centrifuging the slurries for 2.5 minutes at 2000 rpm. Four-ml aliquots were removed from the supernatants for chemical assay. The remainder were quick frozen in dry ice-acetone and stored in a deep freeze at -20°C until optical rotatory dispersion (ORD) and absorbance measurements could be performed. After thawing, the soil extracts were clarified of any residual turbidity by centrifugation in the cold at 10,000 rpm for 10 min and subsequently examined by ORD. The absorption spectra of all extracts were recorded in a 1-cm cell with a Bausch and Lomb 505 spectrophotometer from 240 mμ to 500 mμ at the same time as the ORD measurements.

4.3.2 Chemical and Physical Characterization of Soil Extracts

A. Carbohydrate Determination

1. Qualitative. A drop of the soil extract was placed on filter paper and allowed to dry. The dried spot was sprayed with aniline diphenylamine or aniline phthalate (both from Sigma). The development of color after heating for 5 minutes at 100°C was taken to indicate the presence of carbohydrate.

2. Quantitative. Quantitation of carbohydrate extracted was carried out with the α-naphthol procedure.[2]

B. Total Protein Determination

1. Qualitative. A drop of the soil extract was placed on filter paper and allowed to dry in air. The dried spot was sprayed with ninhydrin (Sigma). The development of color after heating for 5 minutes at 100°C was taken to indicate the presence of protein or amino acids.

2. Quantitative. Two methods were utilized for quantitative total protein determinations. One was the biuret reaction,[3] and the other the method of Lowry, et al.[4]

C. Porphyrin Determination

19 m of soil was shaken with 10 ml of ethyl acetate for 15 minutes. The solutions were examined for orange fluorescence when illuminated with an ultraviolet light (Ultraviolet Products UVSL-13). The presence of orange fluorescence was indicative of porphyrin.

D. Organic Matter Determination

Organic matter content was determined on the dry soil by the Walkley-Black dichromate oxidation procedure.[5]

E. Deoxyribonucleic Acid Determination (DNA)

DNA content of soil extracts was determined by a modified diphenylamine method.[6]

F. Organic Extractants

Attempts to extract polar compounds from both Virginia and desert soils were carried out by extraction of 2 gm portions of soil with 50 ml of dimethylsulfoxide (DMSO) or N,N'-dimethylformamide (DMF) for 10 minutes. Aqueous 80% or 50% solutions of DMSO and DMF were also tried by extracting 10 gm Virginia soil with 100 ml of extractant for 30 minutes followed by evaporation of the extractant in vacuo and then redissolving the residue in 10 ml of water.

Phenolic extractions of Virginia soil were also carried out. In this case, 3 gm soil was stirred with 25 ml H_2O saturated phenol for 10 minutes.

G. Sephadex Gel Fractionation

Sephadex G-25, G-75 and G-200 (Pharmacia, Sweden) were washed by repeated suspension and decantation in H_2O or EDTA-citrate buffer. The gels were allowed to swell and then poured into columns measuring from 1.5 x 15 cm to 2.5 x 30 cm, and allowed to settle. After washing each column with 200-300 ml of buffer or H_2O, the void volume of each column was determined with blue dextran, which has a molecular weight of 10^6 and is above the exclusion limit for all three gels. The column void volume determinations were reproducible to 0.5 ml. Following a further washing of the column, 1-2 ml of the soil extracts were carefully layered onto the top of the column and eluted with H_2O or buffer in a reservoir with a head of approximately one meter. A Packard automatic drop-counting fraction collector was employed and fractions of approximately 5 ml collected. The flow rate was about 0.5 ml/min. The fractions were analyzed for carbohydrate, protein, and nucleic acid as described previously.

H. Thin-Layer Chromatrography (TLC)

Several soil extracts were examined by TLC for a qualitative analysis of soil constituents. This technique permits a quantitative analysis as well. Thoroughly clean 20 cm x 20 cm glass plates were spread with silica gel or diethylaminoethyl (DEAE) cellulose (E. Merck A. G., Darmstadt) to a depth of 125μ with a Brinkmann-Desaga apparatus. Model compounds were run in the following systems after activation of the plates at 110°C for 2 hours. The extracts were applied to a line on the plates with a microliter

pipette and dried with a hot air hair dryer. The plates were then developed in the same solvent system as the model compounds.

The Rf values of the model compounds are indicated in parenthesis. The differences between the experimentally determined Rf values and those obtained from the literature were approximately 8-10%.

Amino acids - 10 µl of Dl-serine (0.25) DL-lysine (0.12) L-cystine (0.10) L(-)tyrosine (0.42) and L(+)histidine (0.14), (10^{-3} to 10^{-4} M). chromatographed on silica gel F in butanol-acetic acid - H_2O (60:20:20 v/v). Plates were sprayed with ninhydrin as spot locator.

Carbohydrates- 10 µl each of d-glucose (0.32) and D-ribose (0.63), (5×10^{-3} M). chromatrographed on Silica gel F in the upper phase butanol-acetic acid-H_2O (40:10:50 v/v). Plates were sprayed with aniline phthalate to locate spots.

Nucleotides - 2 µl each of deoxyadenosine (0.65), thymidine (0.71), Cytidine (0.96), uridine (0.51), guanosine-3'-phosphate (0.02), ($3-4 \times 10^{-3}$ M). Chromatographed on DEAE-cellulose in 0.03 N HCl. UV absorbance was used for spot location.

All chemicals stated in this experimental section were commercially available reagent grade salts or spectroscopic grade solvents.

4.4 Laboratory-Flight-Development Instrument

4.4.1 Strategy of Experiment

The general design philosophy was to establish a one-cycle, automated device that would register activity at only one wavelength. This philosophy was based on future possible usage in determining extraterrestrial life on the planet Mars. The general configuration of the analyzer portion of the instrument was constructed in such a manner as to approach a spaceborne assembly; however, no other regard was given to making this device a space-worthy instrument. The only input requirements of this system are power for performing the experiment and the injection of soil sample prior to each measurement.

On the assumption that the flight model would be a "one-shot" instrument, it was decided to construct the developmental unit basically as such an instrument with various modifications that would permit it to be used as a laboratory model. (See figure 11.) For example, the hydraulic section is designed to permit the soil processing to be varied as may be required by changing the sequence or the timing of the motor driven cams that operate the solenoid valves. The tubing, mixing chamber, valves, etc., are assembled in such a manner that they can be easily removed for cleaning or purging. The "one-shot" principle has also been followed, by the use of a pressurized reservoir that supplies only enough fluid for one experiment. Although the analyser and processor could have been designed smaller, it was decided not to sacrifice the ease of maintenance and the versatility that are required in a laboratory model. Repeat experiments could be run on a mission by parallelling the processing portion of the system.

The philosophy used in the electronic portion of the instrument was to prove the capability of the device rather than develop space approved techniques and components. Wherever possible, commercial amplifiers, digital circuitry and power supplies were used in this instrument.(See figure 12.) No full-scale effort toward space qualification was made at this time, but a number of components within the experiment were investigated on the basis of space problems such as sterilization. Items under investigation include such components as photomultiplier tubes, transistors, etc.

4.4.2 Relationship to Breadboard

The same general technique for processing the phase measurements was adapted for the flight development model. The implementation of this technique was modified to be compatible with solid-state circuitry. The major problem encountered was design of a voltage-sensing circuit used in establishing the point at which the sine wave crossed its zero axis.

One pulse is recorded on the storage drum during a measurement cycle. This reference pulse is read from the drum and its leading edge is compared with the leading edge of the zero-crossing signal originating from the

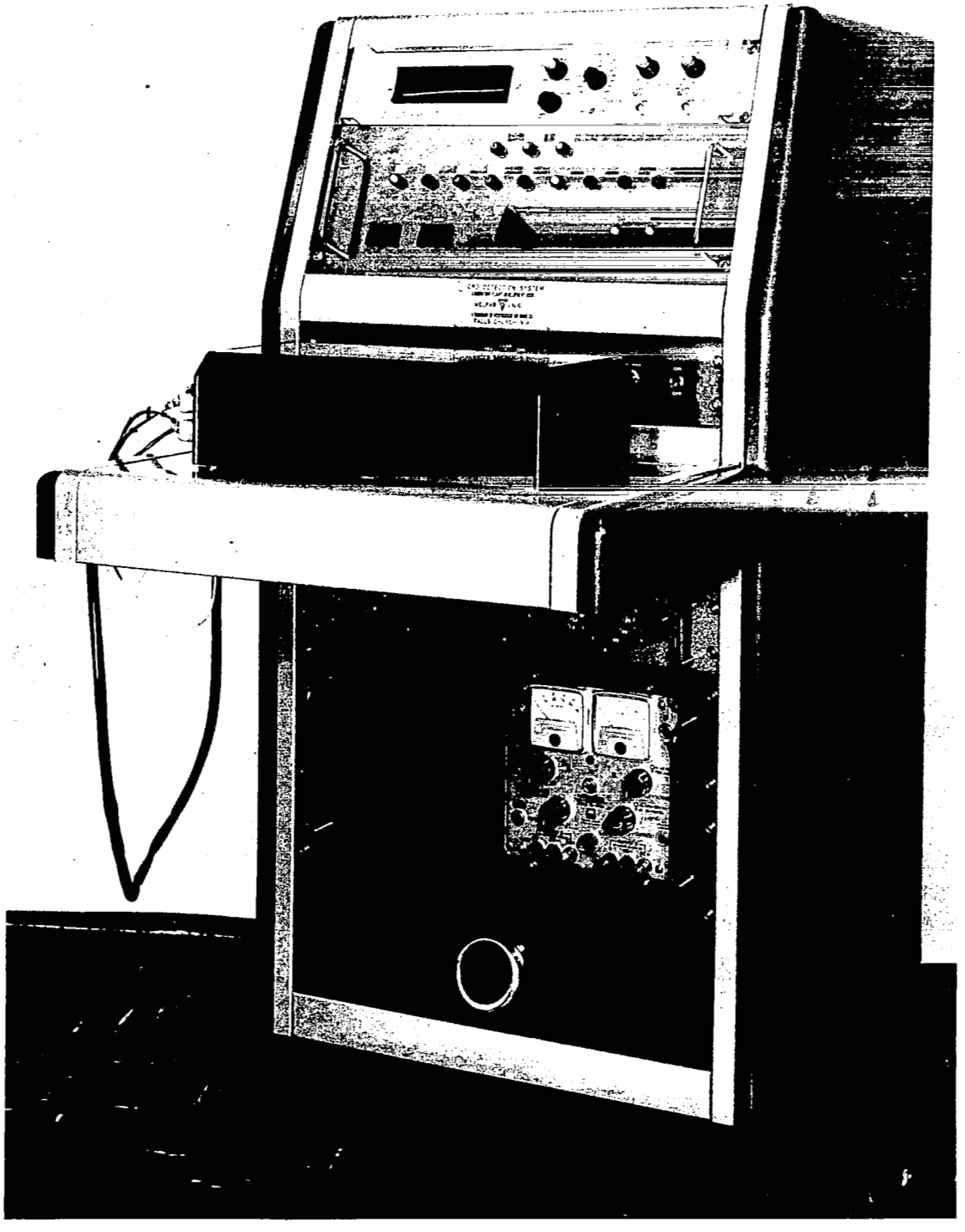

Figure 11. ORD Detection System

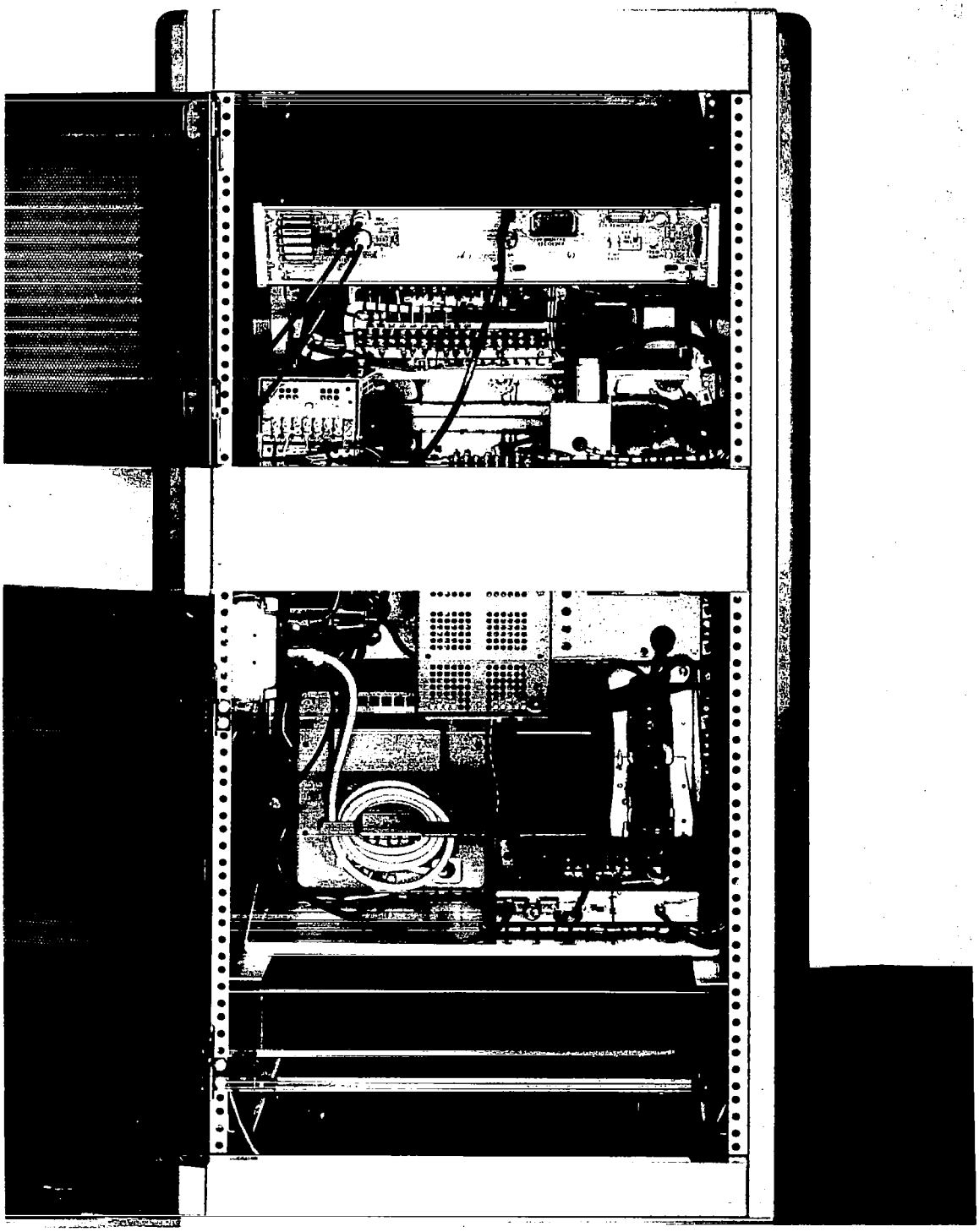

Figure 12. Electronic Console, Rear View

photomultiplier tube with the soil sample mixture in the optical cell. The time difference of these two leading edges is displayed on the counter for each measurement cycle. The "compare" step in the program can be set to a single-cycle measurement or a repeat cycle. The repeat cycle allows a single reference signal on the drum to be compared to the analytic pulse of each rotation of the drum and the counter updated for each time measurement.

The basic principles of the breadboard unit have been incorporated into the processor and optomechanical assembly with several modifications. The Glan prisms were replaced by polarizing filters (Polacoat) that permitted the assembly to be made smaller. All optical elements including the photomultiplier tube and light source have been mounted on a common track to minimize alignment problems. The light source is a small quartz iodine lamp. Although the system was designed for automatic operation, it can also be used for experimental purposes by disconnecting the hydraulics and inserting the standard 5-cm sample cells in the optical path.

4.4.3 Operational Sequence

A motor-driven series of cams operate switches which set the time and sequence of events for the entire system. The timing cam of each switch is adjustable to permit changes in the time interval of each step as may be required.

The sequence of events for one complete measurement is as follows:

With CONTROL SWITCH at -

FILL: Solenoid valves positioned to allow system to be filled with solvent.

LOAD: Solenoid valves positioned to allow soil sample to be loaded in the mixing chamber.

OPERATE: Timing motor is started by pushing START button to begin processing cycle as follows:

Step 1: Erases drum and permits system to stabilize.

Step 2: Records reference mark on drum.

Step 3: Starts mixer motor to mix soil sample with solvent.

Step 4: Positions solenoid valves to permit mixed sample to flow to the sample cell.

Step 5: Compares the reference mark on the magnetic drum with the signal being generated with the soil in the sample cell and displays the time difference on the counter.

Step 6: Permits the display cycle to be repeated and the display updated after each reading.

Step 7: Completes cycle and returns timer to its starting position.

4.5 Detailed Description of Polarimeters

4.5.1 Processor

The hydraulic system is mounted on the same base plate as the opto-mechanical assembly. (Refer to figure 13.) It consists of four electrically operated solenoid valves, a solvent reservoir, mixing chamber and motor, filter and its connecting tubing and fittings. Three manually operated stopcocks are used to facilitate filling the system. All materials in contact with the solvent are made of stainless steel or Teflon to minimize the possibility of contaminating the solvent.

To eliminate the need for a pump or compressed air supply, it was decided to store the solvent in a reservoir under pressure by means of a spring-actuated piston as shown in figure 14. To load the system, it is necessary to connect an external supply of solvent under a pressure of 120 psi to V5. V5, V6 and V7 are opened and the control switch on the console is set to FILL, opening V1, V2, V3, and V4. When all the air is vented through V6 and only clear solvent appears, V6 is closed. The pressure of the external supply is increased until a maximum of 120 psi is reached or until solvent flows from V7. V5 and V7 are closed and the external supply is disconnected. The system is now loaded and pressurized. The control switch is turned to LOAD; this closes valves V1, V2, V3, and V4 and permits the cap to be removed from the soil inlet to the mixing chamber without loss of solvent or pressure. The soil sample (and solvent if necessary) is inserted to prevent entrapping any air under the cap when it is reinstalled. The system is now ready for automatic operation.

The system must be cleaned and a new filter installed after each automatic cycle. (For cleansing procedure, refer to the Instruction Booklet.)

It may be desirable at times to fill the reservoir without disturbing the sample in the mixing chamber or sample cell. To do this, external charging supply is connected to V6 (figure 15). The control switch on the console is turned to LOAD and V6 and V7 are opened. The pressure of the external supply is increased to 120 psig or until clear solvent flows from

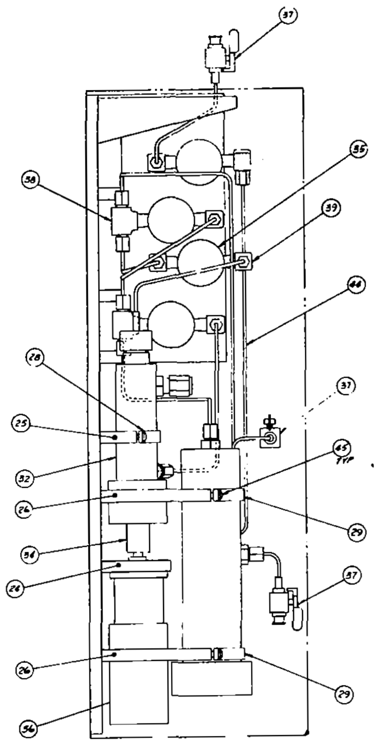

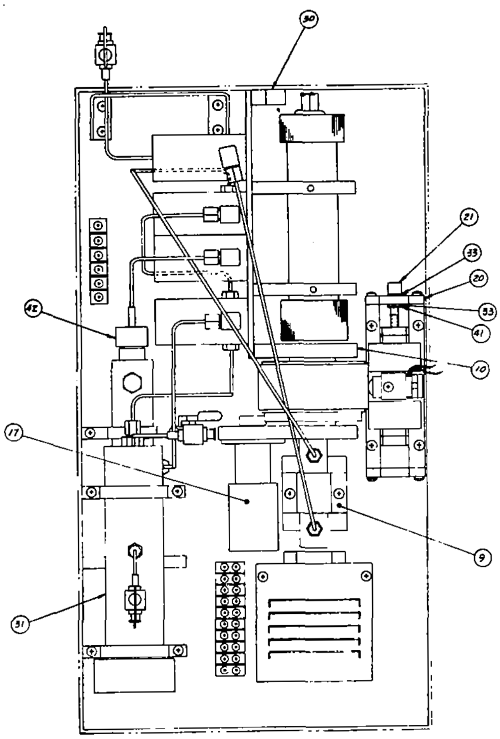

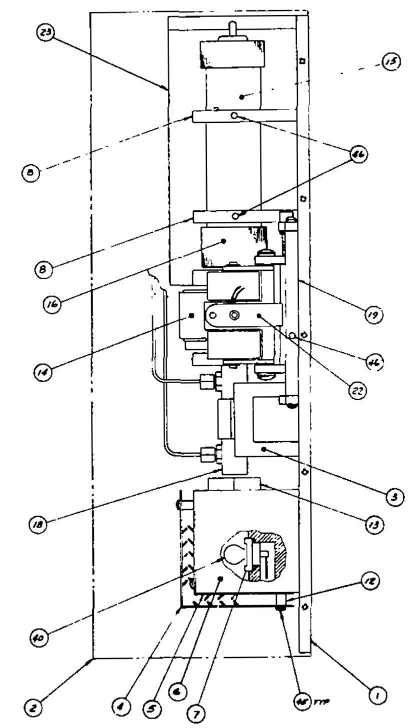

		49				
		48				
		47				
5		46		COML	SETSCREW NO 4-40	
AR	3	45		—	NO. 4-40 HARDWARE	
AR		44		—	TUBING, .065OD.,.010 WALL	CRES
		43				
1		42	83071	XX30 012 40	FILTER HOLDER	
1		41	97464	1001-14	RING, RETAINING	
1		40	08806	1962 QUARTZLINE	LAMP	
3		39	02570	100-2-1-3/16	ELBOW	
2		38	02570	100-3TTM-3/16	TEE	
5		37	06651	MS 01	STOPCOCK	
1		36	25130	C-6A-531-11	MOTOR	
4		35	81978	2DA9175	VALVE SOLENOID	
1		34		R256091	COUPLER	
2		33		R256118	WASHER	
1		32		R356514	MIXER	
1		31		R256250	RESERVOIR ASSY	
1		30		R256179	BRACKET MTG VALVE PLATE	
2		29		R256178-5	BRACKET	
1		28		R256178-2	BRACKET	
		27				
2		26		R256176	PLATE RESERVOIR	
1		25		R256177-2	PLATE MTG MOTOR & MIXER	
1		24		R256768	MOTOR MOUNT	
1		23		R256175	PLATE VALVE MTG.	
1		22		R365785	MAGNETIC HD ASSY	
1		21		R256104	SCREW ADJ	
2		20		R256102	PLATE END	
2		19		R256101	GUIDE	
1		18		R255813	SAMPLE CELL ASSY	
1		17		R256050	MOTOR ASSY	
1		16		R255876	FILTER ASSY	
1		15		R255878	PHOTO TUBE ASSY	
1		14		R255873	DRUM ASSY	
1		13		R255874	LENS ASSY	
4		12		R256393	SPACER	
1		11		R256872	MOTOR MTG PLATE ASSY	
1		10		R255871	DRUM PLATE ASSY	
1		9		R255816	RETAINER	
2		8		R255830	PLATE MTG, PHOTO TUBE	
1		7		R256392	PLUG	
1		6		R356257	LAMP HOLDER	
1		5		R256394	BAFFLE, BOTTOM	
1		4		R256395	BAFFLE, TOP	
1		3		R355319	BASE, SPECIMEN	
1		2		R450563	HOUSING	
1		1		R450564	PLATE, BASE	

SYM:
1. SHOP PRACTICES, MELPAR STD 130-005 APPLIES.
2. CUT & ROUTE ITEM 44 TO MEET READ CONNECTIONS PICTORIAL FOR POINT TO POINT HOOKUP ONLY
3. MELPAR STD 130-009

Figure 13. Analyzer, Assembly Drawing

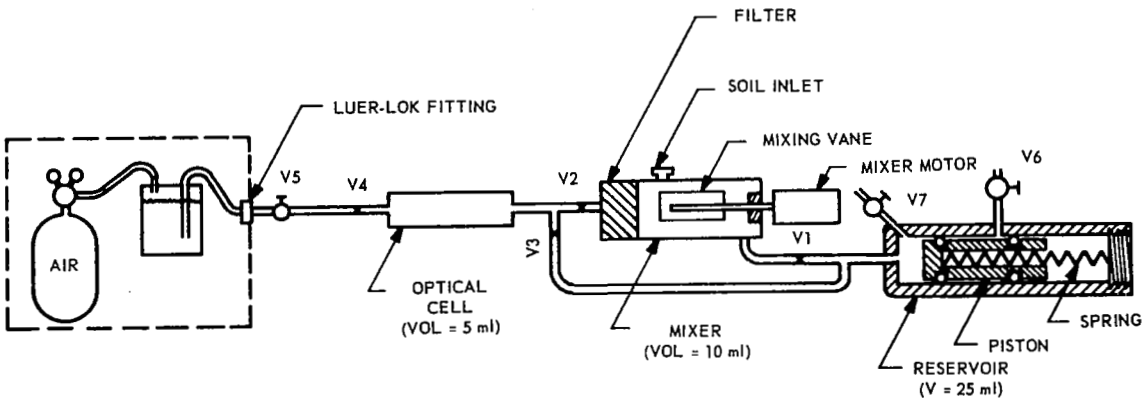

Figure 14. Processor, Charging Schematic (System)

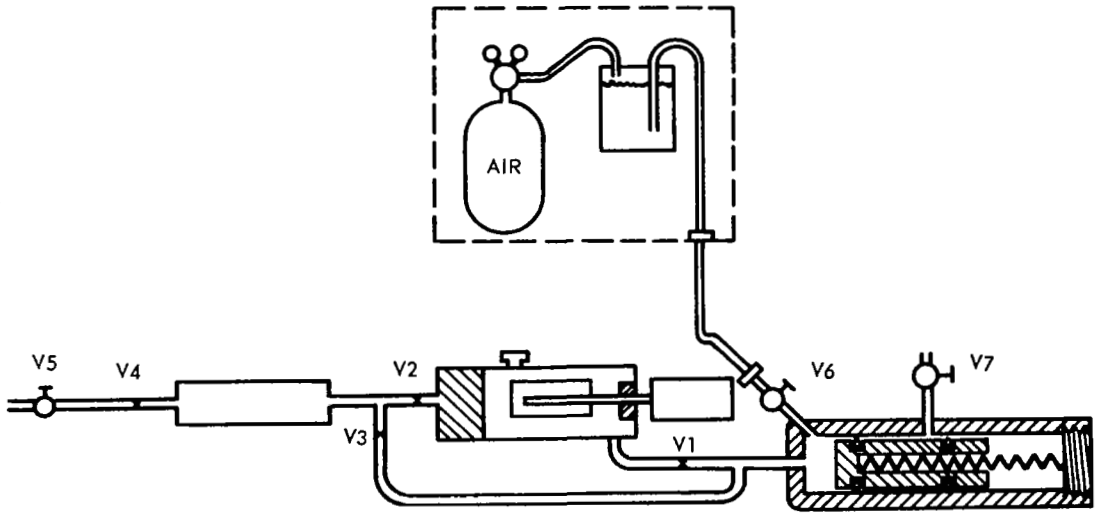

Figure 15. Processor, Charging Schematic (Reservoir)

V7. V6 and V7 are closed and the external supply removed. The reservoir will now be loaded with solvent which can be used to further dilute the sample.

The volumes of the major flow components of the system are: reservoir, 25 ml; mixer, 10 ml; and optical cell, 5 ml. Tubing used for all connections is 1/32 inch I.D. (volume = 0.15 ml per foot of length), miniature valves were used to minimize their dead volume so that the volumes of the three major components listed above is essentially the total system volume.

Nominally, the system will be filled with solvent and a 1.0-gm soil sample will be deposited in the mixer and mixed with the 10 ml of solvent. For the delivery of maximum concentration of soil solubles to the optical cell, the bypass line will remain off during the delivery stroke of the reservoir piston while the solvent in the mixer is transported to the optical cell. Since the ratio of mixer volume to cell volume is 2:1, there is sufficient sample to flush out the "blank" solvent in the cell and the interface volume where sample and blank solvent are mixed and still provide sufficient sample to completely refill the optical cell. By metering solvent from the reservoir into the line between the mixer and the optical cell, any concentration of soil solubles from mixer concentrations down to zero can be attained.

Although every attempt was made to minimize the size of the processor using commercially available components, it is felt that its present size can be decreased with a small development effort on the part of the solenoid manufacturers. Additional space can be saved by eliminating the mixing chamber motor. If it is found that mixing is required, it would be possible to drive the mixer via gears by means of the drum drive motor. The reservoir could be made smaller by using a shorter piston. It is estimated that the size of the processor could be reduced by approximately 20%.

Stainless steel was used for all components of the hydraulic system because of its availability. The reservoir and mixer were fabricated with thick wall sections to prevent damage when the instrument is subjected to laboratory use. These parts could be fabricated of titanium with minimum wall thickness. The elimination of the mixer motor would save approximately 5 ounces. A 25% reduction in the weight of the processor could be achieved if these ideas were used.

Since the entire system is pressure tight, outgassing of other materials or nearby components will have no effect on the solvent. All materials used in the processor are compatible with all space environments and should present no problems. Reliability of the electrically operated solenoids have been proven through many years of testing. To prevent cold welding of the solenoid armature in the hard vacuum of outer space, it is planned to coat its surface with one of the solid lubricants that have proved highly successful in this type of environment.

The power consumption could be reduced by a redesign of the solenoid coils. The solenoid valves now in use require approximately 7 watts each. By judicious redesign to fit the application, it is estimated that 2 watts could be saved for each valve used. Of course, the elimination of the mixer motor would save an additional 8 watts.

4.5.2 Flow Rates

The major restrictor in the system is the filter at the mixer outlet. Its flow rate is 5 ml/min for 1 atmosphere pressure differential across the filter holder. The initial flow rate, when the reservoir spring is fully compressed, (system pressure 120 psig) is $\frac{120}{14.7} \times 5 \simeq 40$ ml/min, and will fill the 5-ml optical cell in less than 8 seconds with no by-pass flow. Near the end of the reservoir piston stroke, the system pressure will be $\frac{40}{14.7} \times 5 = 13.6$ ml/min, and require 22 seconds to fill the optical cell with no bypass dilution flow. With dilution flow to decrease the sample concentration, the above rates will be reduced, while clogging of the filter will increase the time required to transport sample from the mixer to the optical cell. The solution filter which filters the solvent-dirt mixture as it is transported from the mixer chamber to the optical cell is housed in a modified standard 13-mm diameter holder. The filter elements are arranged as shown in figure 16. The diatomaceous silica filter is formed in place in the filter holder using a slurry of Johns Mansville Cellite 503 and drawing a vacuum on the filter holder. Quantity of slurry used is sufficient to provide a final filter thickness of approximately 3 mm. A Millipore 0.45-micron HAWP filter is used for the membrane filter and standard Millipore 13-mm support screens are used. The flow direction must be as shown in figure 16, so that any material that may flake off from the diatomaceous silica filter will be trapped by the membrane filter. A diatomaceous silica filter provides filter-bed action to decrease the clogging tendency of the membrane filter without increasing the cross-sectional area.

The water flow rate of this filter assembly is approximately 5 ml/cm^2/min when the filters are clean.

4.5.3 Optomechanical Assembly

The optical and mechanical assembly was designed to provide the flexibility and accessibility required for laboratory testing and evaluation with the fact in mind that the flight model must withstand the severe environments of launch, long space flight and crash landing on Mars.

In view of this, several changes were made in the design of the preflight instrument. One of these changes was the substitution of film polarizers for the Glan polarizing prisms. A recent application of Polacoat film polarizers to measuring polarized fluorescence[6] was the major consideration in the use of these polarizers in the instrument. McDermott and Novick[7] have found these polarizers to be stable and generally satisfactory. An inquiry to the Polacoat Company revealed that the coating had been found to be stable at 300°F for 1 hour, but that the upper temperature limit for the coating had not been determined.[8] A temperature of 300°F is well within the spacecraft sterilization temperature range as well as that of its ultimate environment. The wider acceptance angle of the film polarizer is considered an advantage over the Glan prisms used previously; in addition, the special

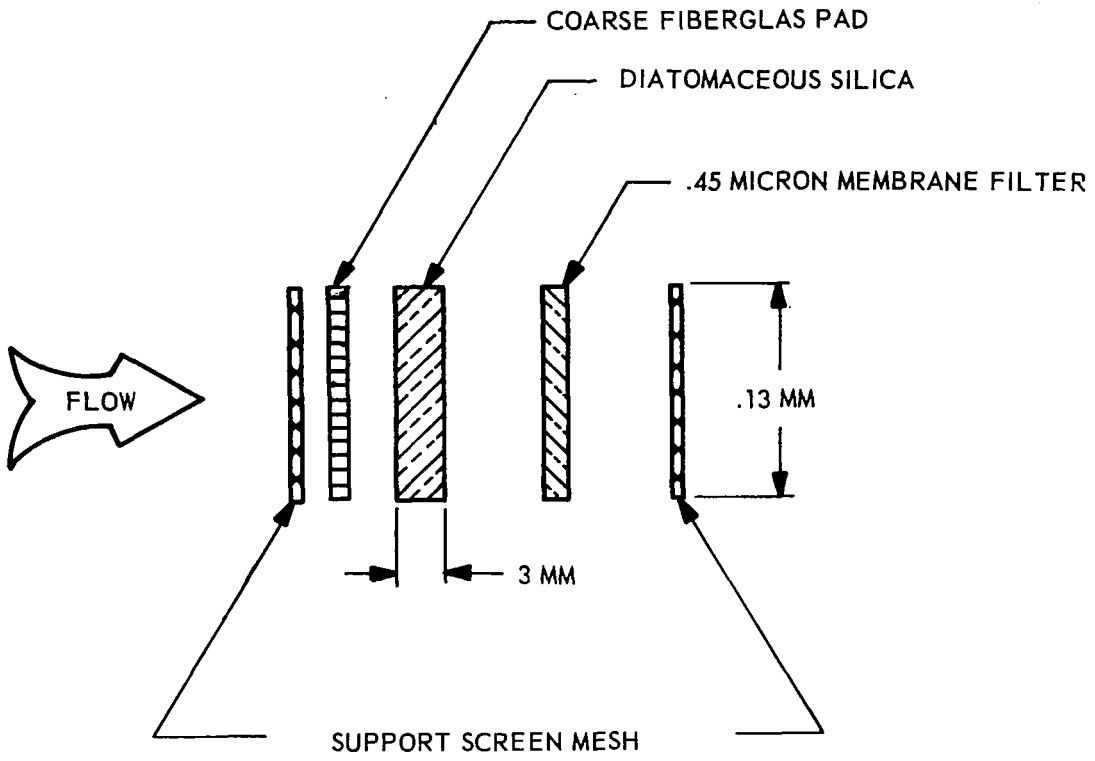

Figure 16. Filter Arrangement

ultraviolet polarizing formula (PL-40) from Polacoat transmitted more light than the Glan polarizers throughout the UV spectrum. It was also felt that the film polarizers would provide less weight and greater mechanical stability than the compound prism assembly.

Transmission spectra of the PL-40 Polacoat films (see figure 17) on quartz windows measured on a Gary 15 spectrometer indicated approximately twice the unpolarized light was transmitted through the crossed films as was indicated for typical crossed film in the manufacturer literature; however, in the optical rotation analyzer under discussion, unpolarized light appears at the photomultiplier as a high unmodulated "dark current" and is therefore blocked from the ac signal amplifiers. It was decided that this amount of unpolarized light could be tolerated. Another sample of Polacoat film, 105-UV, was found to have very little unpolarized light, a maximum of 0.35% at 370 $m\mu$, but had essentially no transmission below 300 $m\mu$.

A mercury gas discharge lamp was originally chosen as the irradiating source for the preflight instrument because of its high intensity and narrow spectral lines. However, this lamp exhibited a broad-band plasma oscillation. This oscillation was so prevalant that the overall sensitivity of the system was highly degraded. A filament lamp was substituted. The filament source has approximately the same energy as the arc discharge lamp used previously.

A quartz-iodine lamp was chosen (General Electric "Quartzline" model 1962). This lamp is compact, rugged, and very efficient. The quartz case provides good ultraviolet transmission while the iodine vapor provides a self-cleansing action that maintains the high transmission of the quartz envelope. The filament is operated at a brightness temperature of 3100°K. The lamp emission spectrum is essentially black body so that peak spectral radiance is approximately 1.2×10^{6} watts cm^{-2} $ster^{-1}$. The relative radiance at 3600 Å is 4.3×10^{-2} so that the radiance in a 100-Å interval centered at 3600 Å is 5.1×10^{-2} watts $cm^{-2}ster^{-1}$. A schematic diagram of the optical system is shown in figure 18. The relative emission of the G. E. Quartzline lamp is shown in figure 19 for the unfiltered case and for the case of filtering with a Corning 7-37 ultraviolet filter.

The following estimate of energy assumes that the condensing lens is the only aperture in the system. It considers the attenuating effects of the lens, primary filter, and two polarizing filters.

The needed parameters are:

T_1 = transmission of primary filter (Corning 7-37 filter) data measured

T_2 = transmission of formula PL-40 Polacoat filter, from manufacturer data, 2 layers

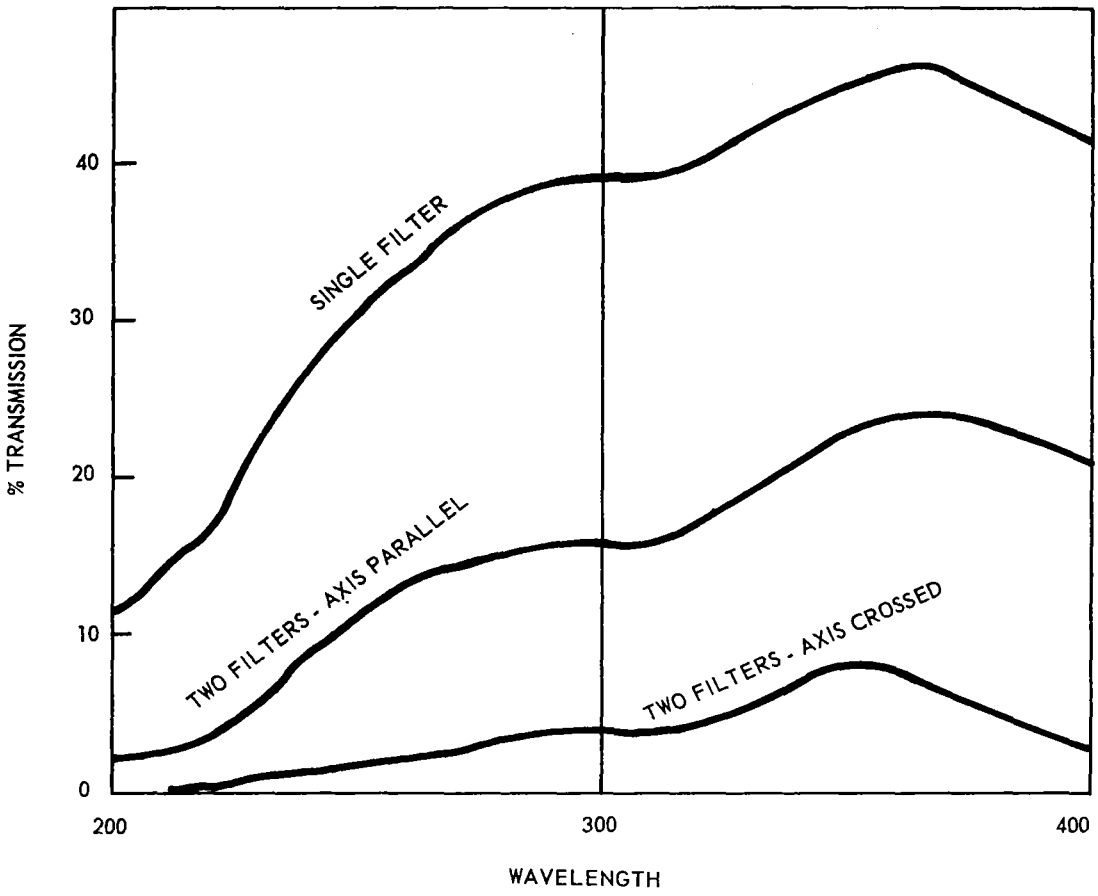

Figure 17. Transmission of Polacoat PL-40 Filters

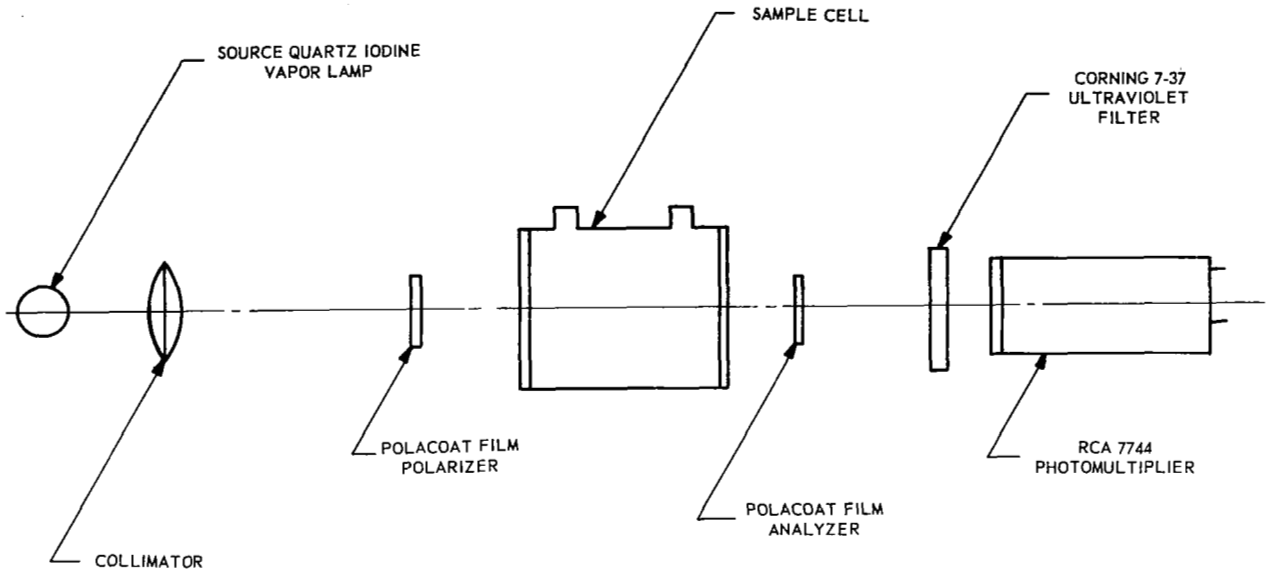

Figure 18. Optical System, Schematic Diagram

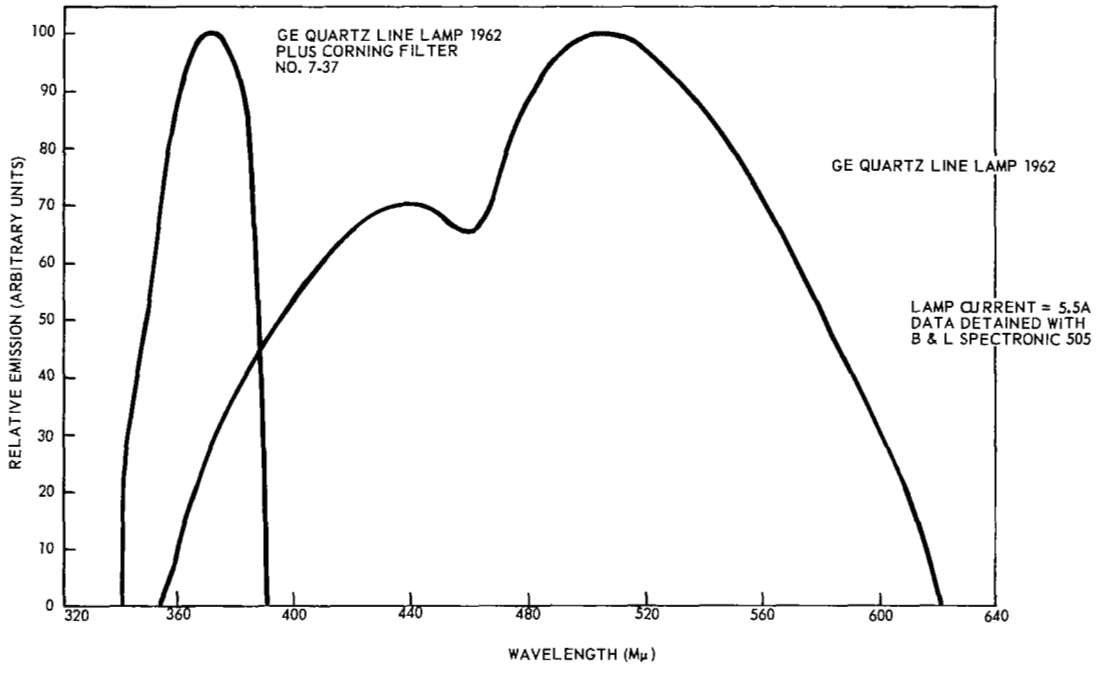

Figure 19. Emission Spectra - GE Quartzline Lamp 1962 and GE Quartzline Lamp plus Corning 7-37 Filter

T_3 = transmission of quartz lens, estimated

R_λ = relative radiance of G.E. Quartzline iodine vapor lamp model 1962, from manufacturer data

N_λ max = maximum spectral radiance (watts cm^{-2} $ster^{-1}$)

P = radiant power (watts)

ds = area of source 1 mm x 0.284 in.

L = distance from the center of the filament to the center of the lens = 25/16 in.

θ = total angle subtended by lens as seen by the filament

D = lens diameter = 0.5 in.

λ = wavelength (millimicrons)

The power emerging from the final polarizing filter is:

$$P = \int_{\lambda_1}^{\lambda_2} P_\lambda \, d\lambda,$$

where $P_\lambda = \pi N_{\lambda\ max} R_\lambda T_1 T_2 T_3 \sin^2 \theta \, ds.$

The angle θ is calculated as follows:

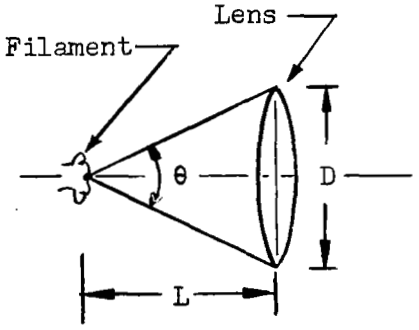

$$\tan \frac{\theta}{2} = \frac{D}{2L} = \frac{4}{25} \qquad \theta = 18.16^\circ$$

$$\therefore \sin \theta = 0.312$$

The parameters $N_{\lambda max}$, π, $\sin^2 \theta$, and ds are constant:

$N_{\lambda max} = 1.18 \times 10^{6}$ watts cm^{-2} $ster^{-1}$ cm^{-1}

$ds = 0.725 \times 0.1\ cm^2 = 0.0725\ cm^2$

$T_3 \simeq 0.9$ across the entire spectrum of interest

From these parameters we calculate:

$$P_\lambda = \pi \times 1.18 \times 10^{6} \times 0.9 \times 0.0974 \times 0.0725\ R_\lambda T_1 T_2$$
$$= 2.36 \times 10^{4}\ R_\lambda T_1 T_2$$
$$= 2.36 \times 10^{4} \phi_\lambda$$

[In the following table, we write $(a \times 10^{-n})$ as (a-n).]

λ (mμ)	320	330	340	350	360	370	380	390	400	420
T_1	1.0-3	1.9-2	1.1-1	2.3-1	3.2-1	2.8-1	9.2-2	2.0-3	3.7-4	1.0-5
T_2	2.2-1	2.4-1	2.6-1	2.7-1	2.8-1	2.8-1	2.8-1	2.7-1	2.7-1	2.7-1
R_λ	1.6-2	2.0-2	2.7-2	3.4-2	4.2-2	5.3-2	6.5-2	7.8-2	9.0-2	1.25-1
ϕ_λ	3.5-6	9.1-5	7.7-4	2.1-3	3.7-3	4.2-3	1.7-3	4.2-5	9.2-6	3.4-7
$P_\lambda \Delta_\lambda$	8.4-8	2.2-0	1.86-5	5.1-5	8.8-5	1.0-4	4.0-5	1.0-4	2.2-7	8.2-9

(In the last row, $P_\lambda \Delta\lambda$ is just the power in any 100-Å interval centered at the appropriate wavelength.)

The total power P is:

$P = \Sigma P_\lambda \Delta\lambda = 300$ microwatts

When the two polarizing filters are crossed, the power is attenuated by approximately 10^{-2}; thus,

P (attenuated) $\simeq$ 3.0 microwatts

4.5.4 Magnetic Recording System

Previous tests on the breadboard instrument had shown that it would be highly desirable to be able to adjust the pressure of the magnetic head against the drum to obtain minimum wear and best signal. It was also necessary to be able to select a new track on the drum if wear occurred because of prolonged laboratory testing. To accomplish this and maintain good mechanical stability, a somewhat complex head mechanism was required. Figure 20 is a drawing of the assembly. As shown, a screw is provided to adjust the pressure of the magnetic head against the drum via a small compression spring. Two nylon rollers are used to hold the assembly against the drum. One or both rollers will at all times ride on the drum, depending upon the axial portion of the head. The pressure that the rollers exert against the drum can be varied in a manner similar to that used for the head pressure adjustment.

To minimize head wear, the spring rates of both springs were selected so that at no time could the head exert more pressure on the drum than the rollers. To position the head axially on the drum, adjustment screws are provided to slide the entire assembly to a new drum track via precision guide rails and a slotted track in the base plate. When the axial position adjustment screws are tightened, the assembly is once again mechanically stable.

The silicon rubber magnetic tape was found eccentric by 0.010 to 0.015 inches after installation. This was corrected by grinding the tape after assembly. This procedure provided a perfectly concentric drum with no adverse effects to the magnetic properties of the tape.

A small hysteresis-synchronous motor is used to drive the magnetic drum at 60 rpm. The small pole-to-pole speed variations inherent in a synchronous motor are reduced to an insignificant value by the large speed reduction and the inertia of the gearing and drum. Variations in the angular velocity of the drum due to gearing eccentricities have been minimized by the use of a large-diameter drum gear.

4.5.5 Electronic System

A discussion of each block in the system block diagram of figure 21 will be presented; then, the relationship of one block to another, with respect to signal flow and processing, will be given. The lamp, lenses and photomultiplier tube were dealt with in conjunction with figure 18 and will not be repeated here.

The preamplifier is an operational amplifier P2A purchased from Philbrick Research, Inc. It was chosen because of its low noise and high input impedance ($Z_{in} = 10^{10}$ ohms). In the ORD unit, the P2A is contained

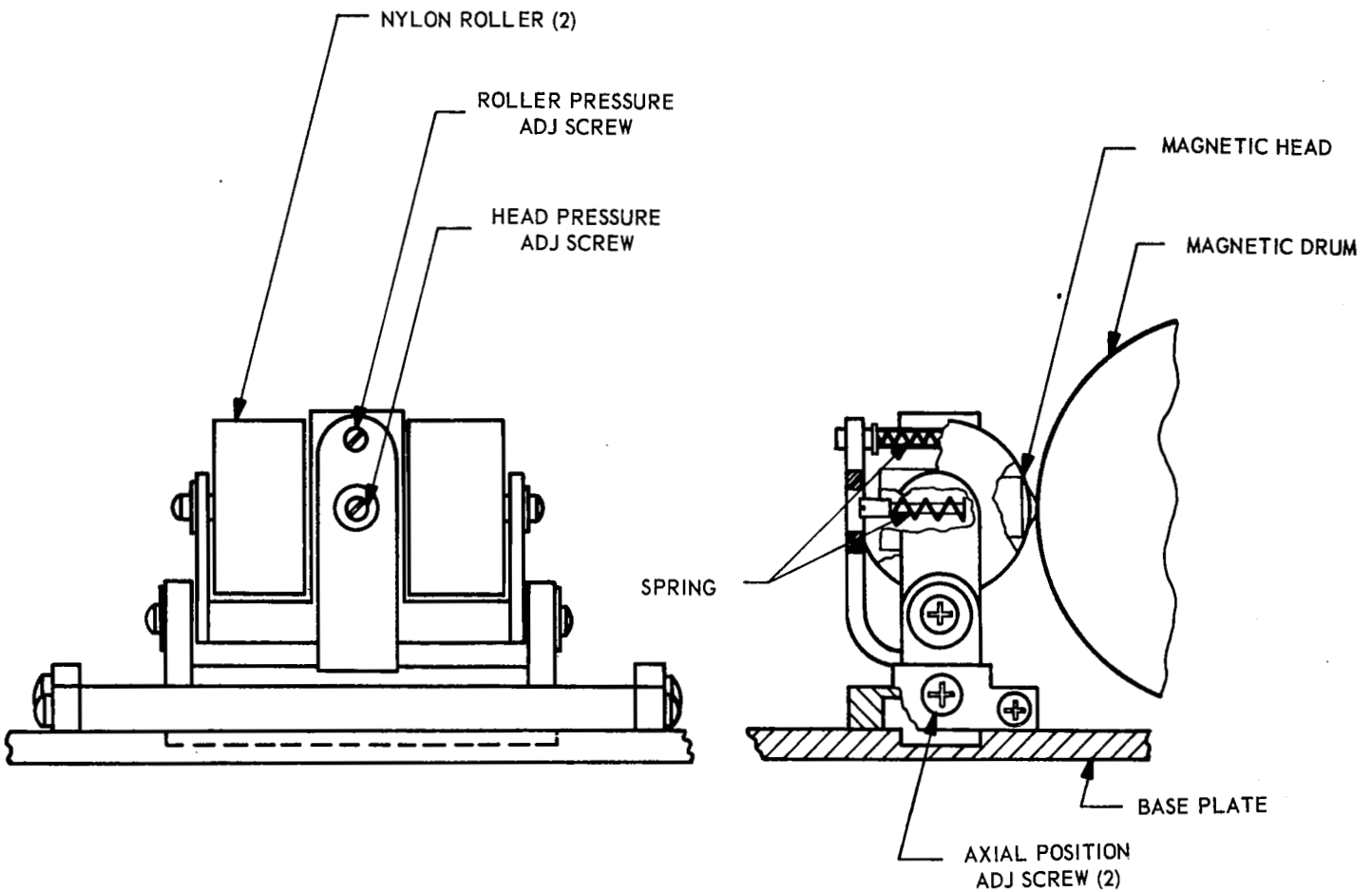

Figure 20. Magnetic Head Assembly

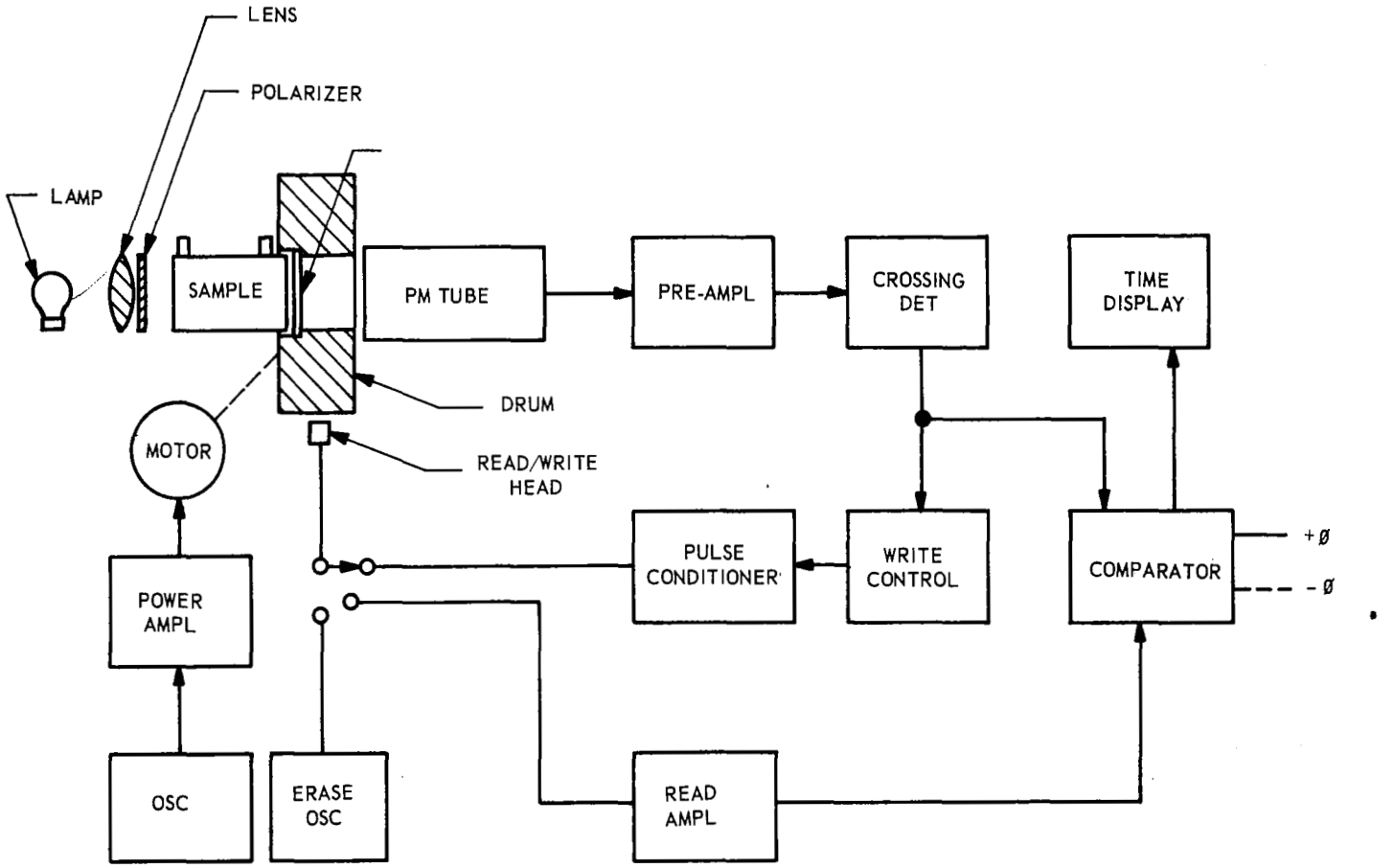

Figure 21. System Block Diagram

in a negative feedback loop which adjusts the overall preamplifier gain to 77 db and makes the gain stability-dependent on the precision resistors of the feedback loop instead of amplifier parameters.

The signal is coupled to the zero-crossing detector (figure 22). The zero-crossing detector is made up of two identical cascaded amplifier sections and a blocking oscillator.

Each amplifier is contained in a nonlinear negative feedback loop that permits three separate voltage-gain regions of the amplifier. First, for low-level signals, the diodes in the amplifier feedback loop do not conduct and the gain of each section is 80 - 90 db. When the signal at the output of the amplifier is large enough to cause the zener diode (figure 22) to conduct, the gain of the amplifier becomes zero and no further change in the output occurs, regardless of the input. Since zener diodes have a larger breakdown voltage when reversed biased than when forward biased, the amplifier output voltage range is -5 volts to +1 volt, approximately.

This type of nonlinear feedback permits the amplifier to have a very large gain without saturating the final stages on high-level signals. Driving a solid-state amplifier beyond its linear range causes propagation delays of the signal and results in errors in time measurement.

The output of the second amplifier stage of the zero-crossing detector is fed to a blocking oscillator, also shown in figure 22. The blocking oscillator is triggered into conduction and generates a 9-volt positive pulse of 2-μs width when the amplifier output voltage goes from +1 volt to -5 volts.

The signal from the zero-crossing detector is fed into two logic blocks, as shown in figure 21, the comparator (figure 23) and the write control, figure 24. Assume now that the sample cell is empty and that it is desired to record a reference signal on the magnetic drum. In this case, the read enable (figure 24) would be energized and the record reset would be deenergized.

The positive zero-crossing signal passes through the read enable gate, causing the record flip-flop to change state. The leading edge of the record flip-flop is differentiated in the "pulse conditioner", amplified, and fed to the recording head. This pulse, now recorded on the drum, is the reference signal from which time is measured.

The record flip-flop remains in the set state and blocks any later zero-crossing signals from being recorded on the drum. The output of the record flip-flop also actuates, via a drive amplifier, the record-ready light on the indicator panel.

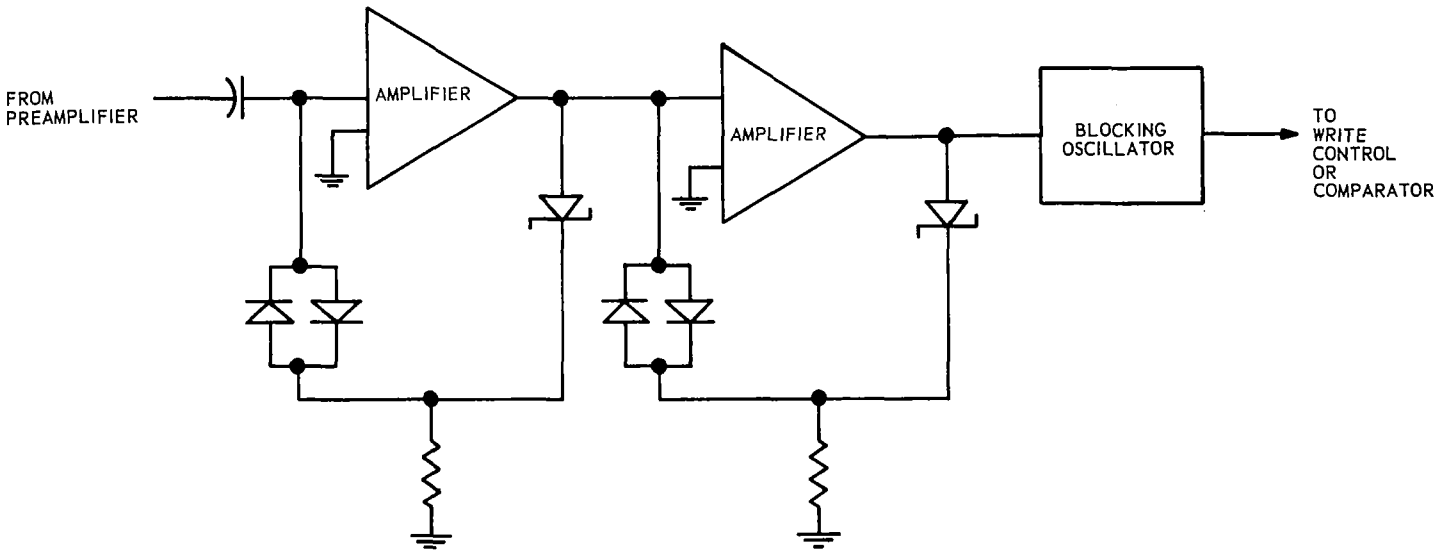

Figure 22. Zero Crossing Detector

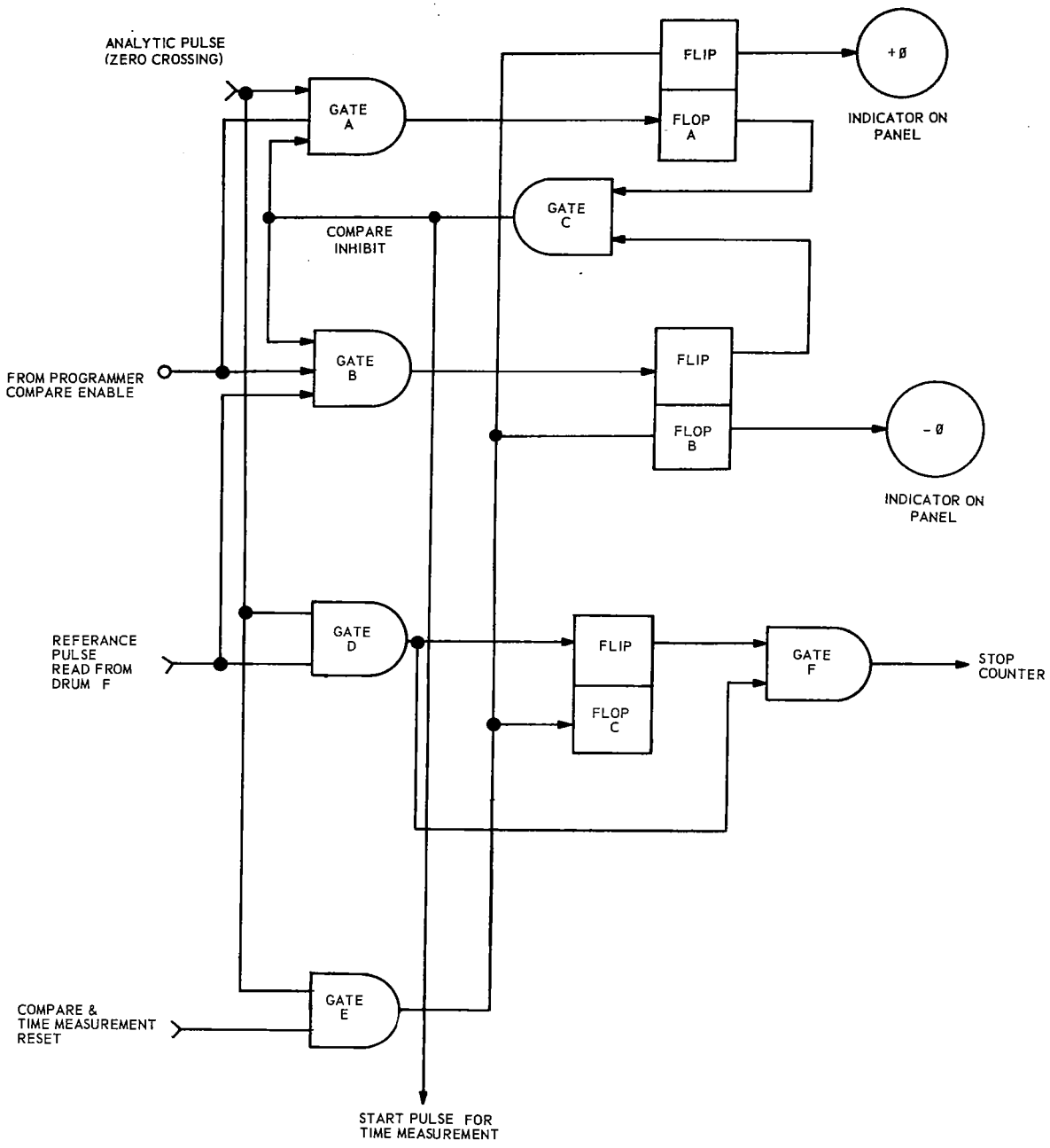

Figure 23. Comparator

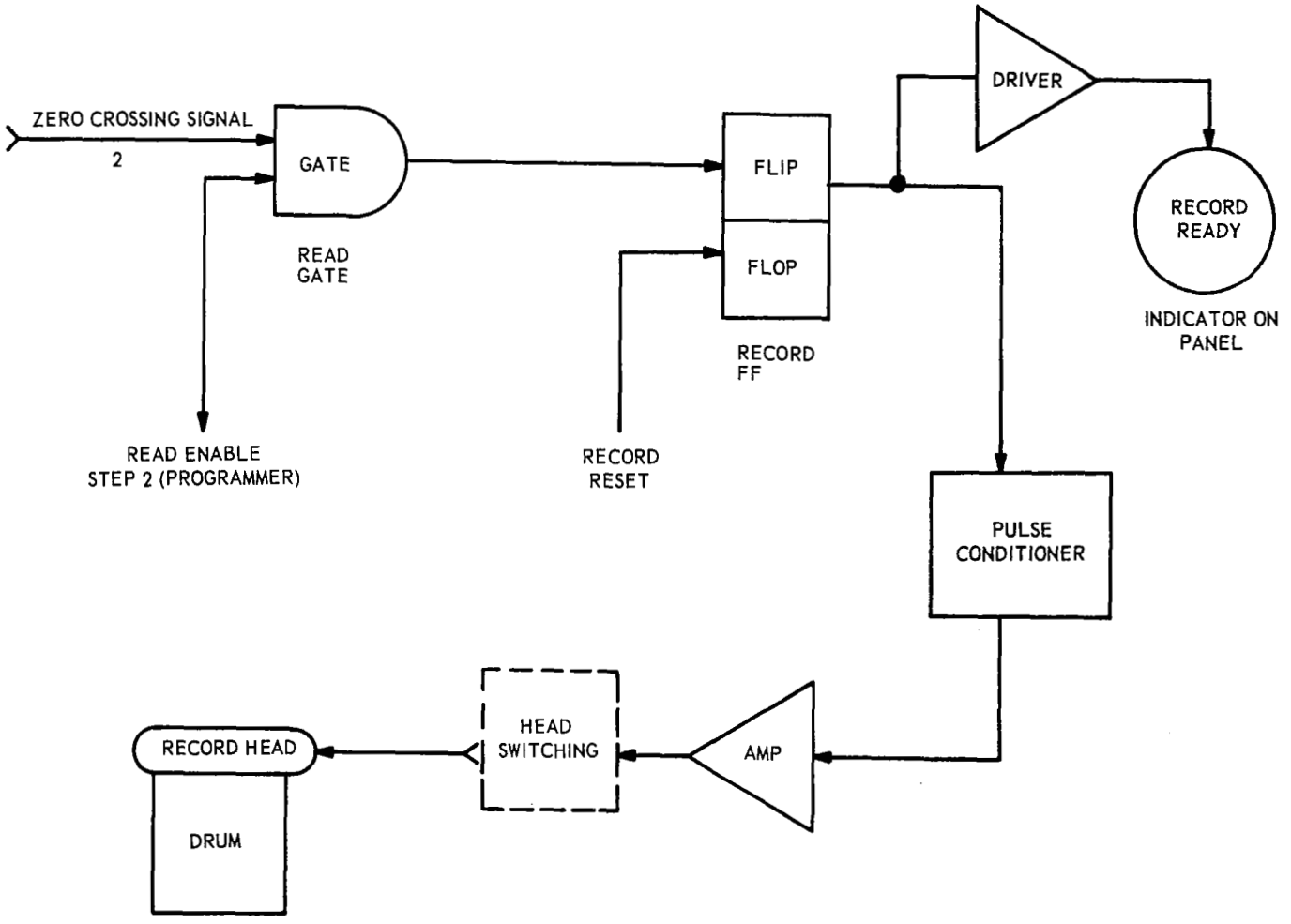

Figure 24. Write Control

It should also be pointed out that the same head is used to write on the drum was well as to read information from the drum. This reduces the number of magnetic heads, but it also requires additional switching circuits. This switching, as indicated in both figure 21 and figure 24, is actually performed by a relay that is controlled by the programer.

4.5.6 Comparator

The comparator logic (shown in figure 23) has three primary functions:

(a) Provide a start-stop pulse for the counter.

(b) Control the phase indicator lights on the front panel, which show positive or negative phase relation of the polarized light.

(c) Generate a recycle signal that resets the comparator circuit, thereby permitting a continuous recount of the phase angle.

How these functions are carried out will now be discussed.

It is assumed that the "Compare Enable" level from the programer is picked up (figure 23). This opens gates A and B and permits either the reference pulse read from the drum, or the analytic pulse from the sample, whichever is first, to pass to respective flip-flop A or B. The output of this flip-flop through gate C generates the counter-start pulse and closes gates A and B.

It will be noticed that flip-flops A and B, in addition to controlling the phase relation lights on the front panel, also conditions flip-flop C to pass the next pulse in gate D. Either the reference pulse or the analytic pulse has already appeared on the input to gate D. The second of these two pulses will now pass to gate F and thereby represent the counter-stop pulse. "The compare-time measurement," by holding gate E open, permits the comparator to be recycled and elapsed time recounted.

4.5.7 Programer

The programer, shown in figure 25, establishes the operational sequence and time for the occurrence of each event necessary for a complete optical rotation measurement. The programer is a motor-driven series of cam-operated switches that are adjustable to permit changes in the time interval of each step as may be required.

The measurement is started by depressing the operate switch located on the front panel. This starts the programer. The sequence of events for one complete measurement cycle is as follows:

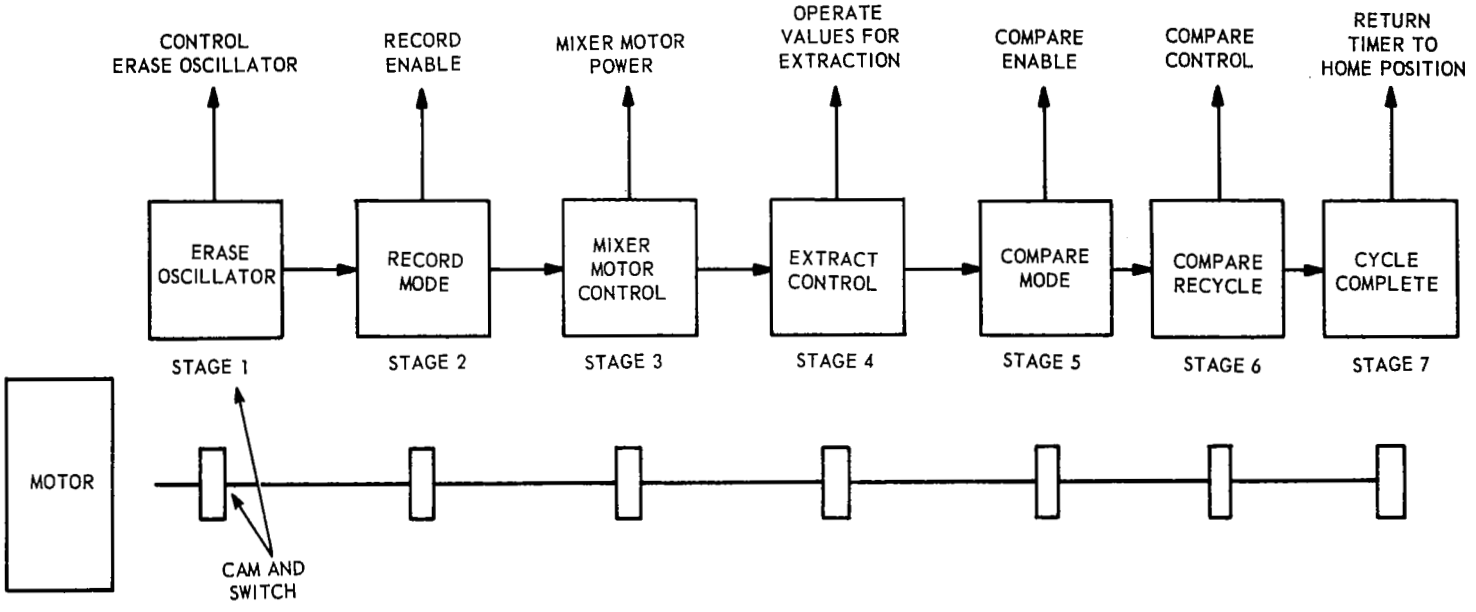

Figure 25. Programer

Step 1 - The erase oscillator is rendered operative and functions for at least two complete rotations of the magnetic drum.

Step 2 - The record control logic is reset and enabled for recording. One pulse is recorded on the magnetic drum.

Step 3 - Power is applied to the mixer motor and the soil sample is mixed with solvent in the mixing chamber.

Step 4 - Power is applied to control the solenoid valves to permit sample extraction.

Step 5 - The comparison logic is enabled and the leading edge of the analytic pulse is compared with the reference pulse read from the drum.

Step 6 - The compare enable level on the comparison logic is retained and the comparison for every other analytic zero-crossing signal is recycled until the normal cycle is restored. This permits the display and ± 0 indications to be updated for each cycle.

Step 7 - The measurement is complete and the timer is repositioned to its starting point in preparation for the next measurement cycle.

4.5.8 Drive-Motor Power

A tuning fork oscillator is used as the frequency standard for the drive-motor power, shown in figure 26. This oscillator has a frequency stability of 0.01% from 0° to 50° C. Assuming the frequency error is reasonably linear and the laboratory temperature varies only 1/10 of this excursion during its operation, the error introduced in the system would be 1 ppm. In terms of angle, this represents an error of approximately 0.003°C. However, the technique of rotating the magnetic storage and the polar analyzer in one assembly will offset a large percentage of this error.

A closed-loop timing control was investigated and found to have the least amount of positional or measurement error between the rotating storage medium and the time measurement counter. This type of timing control would require a countdown counter to divide the basic clock rate (1×10^6 HZ) of the time measurement counter, to 400 HZ to provide the frequency rate for the drive motor. This digital signal would then have to be filtered to remove all excess harmonics and furnished to the motor supply as a sine wave.

Further investigation into the absolute synchronism characteristics of hystereses-synchronous motors will be required to conclude the improvement in time measurement using a closed-loop technique.

4.5.9 Electronic Packaging

Digitally integrated logic was used in the digital portion of the system, first to show the compatability of integrated solid-state circuitry

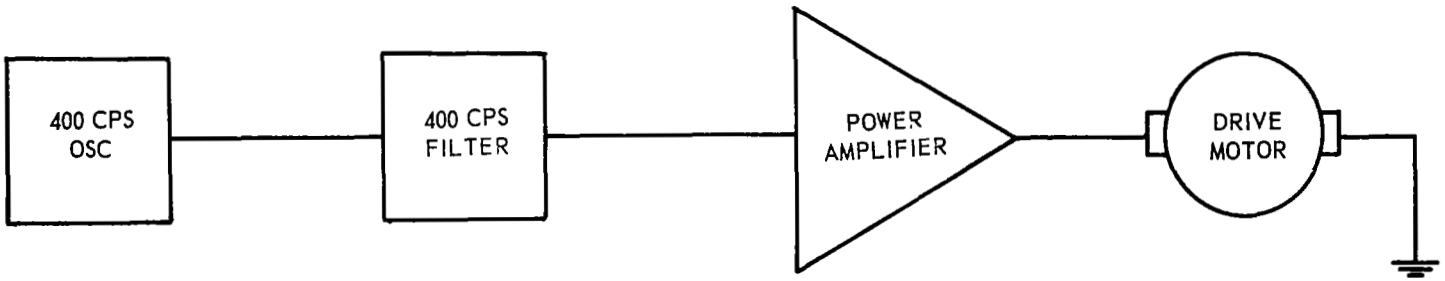

Figure 26. Motor Drive, Block Diagram

with the experiment, and second, to show what can be done in electronic packaging for a possible space module. The entire electronic section can be developed on the basis of integrated circuitry and packaged in a module many times smaller than that presently existing. As an example, the programer or timer in the present system is a mechanical motor-driven cam device that allows for changes in both the programer event cycle and the time for each event to occur. This program, once fully established, can be converted directly to digitally integrated circuit logics and lend itself readily to this type of packaging.

5. RESULTS

The accuracy of the polarimeter was checked by measuring serial dilutions of sucrose solutions as a function of pathlength at 365 mμ. The optical rotation of each of the solutions was measured at the sodium D line with a Rudolph Visual Polarimeter. The amount of rotation to be expected at 365 mμ was calculated from these measurements. The rotations measured agreed with the calculated values. The results are shown in figure 27. The curves show that the instrument is linear over at least 80° of optical rotation. This is not considered to be either a practical or theoretical limit. The displacement between curves is proportional to concentration. The concentration dependance may be determined by taking ratios of the slopes. This is shown in table 1. The agreement between theoretical and experimental results is excellent.

Figure 28 shows the optical rotatory dispersion of sucrose and starch solutions as measured with the single-beam polarimeter. The optical rotatory dispersion of both of these materials obeys a one-term Drude equation which plots as straight lines on log-log paper. Note the excellent agreement between the literature values and the experimental values for sucrose. Also, the experimental values for both sucrose and starch fit a straight line within the limits of experimental error.

Figures 29 and 30 are similar plots of the optical rotatory dispersion of human serum albumin and trypsin respectively. Again note the excellent fit to a straight line and the close agreement with literature values.

Figures 31 through 35 consist of optical rotatory dispersion curves and absorption spectra obtained from aqueous extracts of a variety of soils. The absorption spectra are, in general, featureless. The optical rotatory dispersion curves do show what appear to be Cotton regions. The details of the curves vary from sample to sample and as a function of the extraction condition; however, in all instances, appreciable amounts of optical activity were obtained from rather small quantities of soil.

Figures 36 and 37 show the alterations of the optical rotatory dispersion curves as a function of extraction time and soil-to-extractant ratio. Note that the directions of alteration of the optical rotatory dispersion curves are the converse of each other as in the two figures shown.

Figures 38 and 39 show the alterations and the absorption spectra as a function of extraction time and soil-to-extractant ratio. Note the rapid increase in absorbance at wavelengths shorter than approximately 380 mμ.

Figures 40 through 42 represent organic extracts from ancient sediments. The details are shown on the figures. The absorption spectra for these extracts do show definite peaks. The optical rotatory dispersion curves show Cotton regions associated with these peaks. Note, particularly, the peak at about 400 mμ and the peak in the neighborhood of 530 mμ.

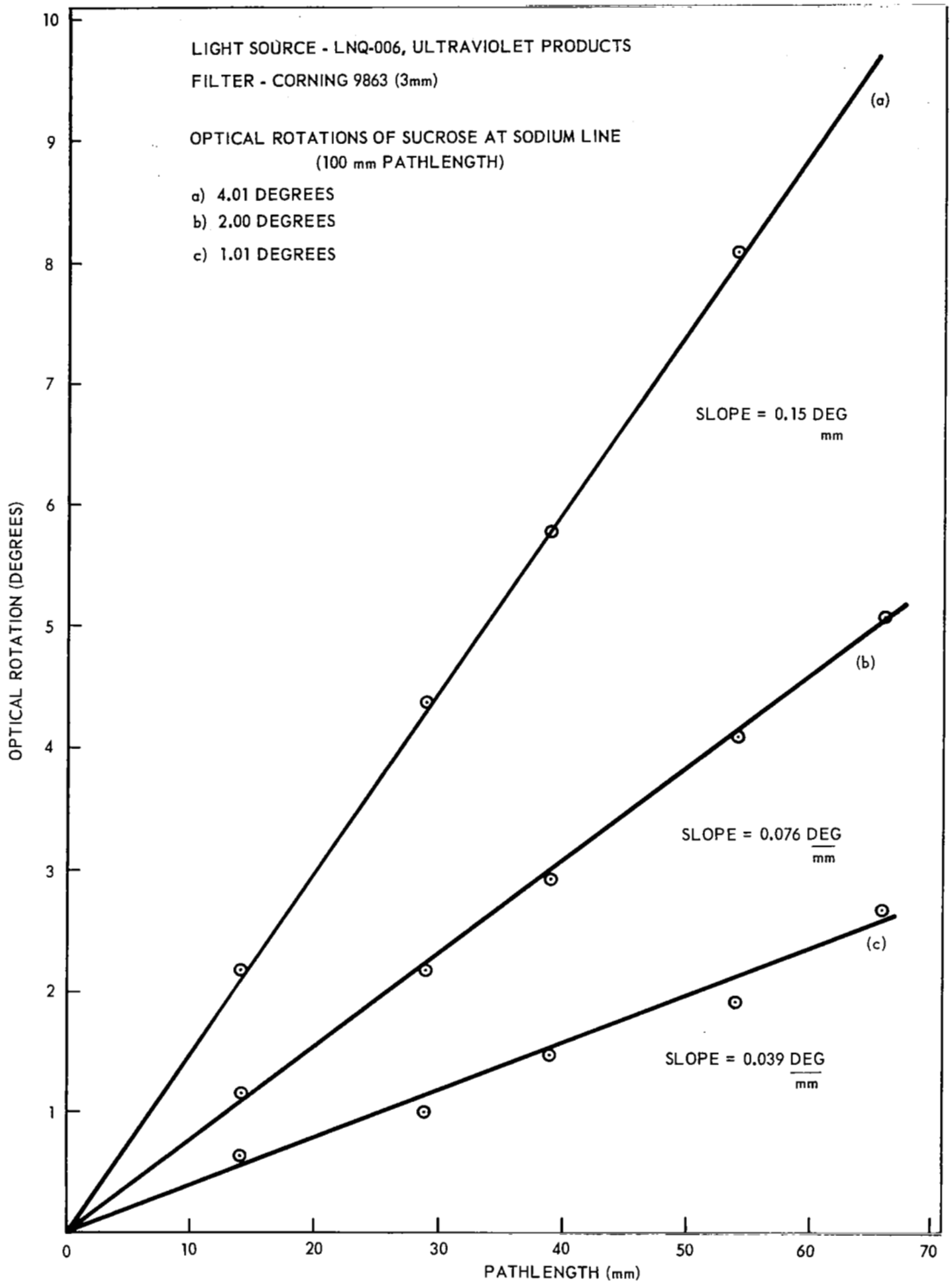

Figure 27. Optical Activity of Sucrose Solutions as a Function of Pathlength

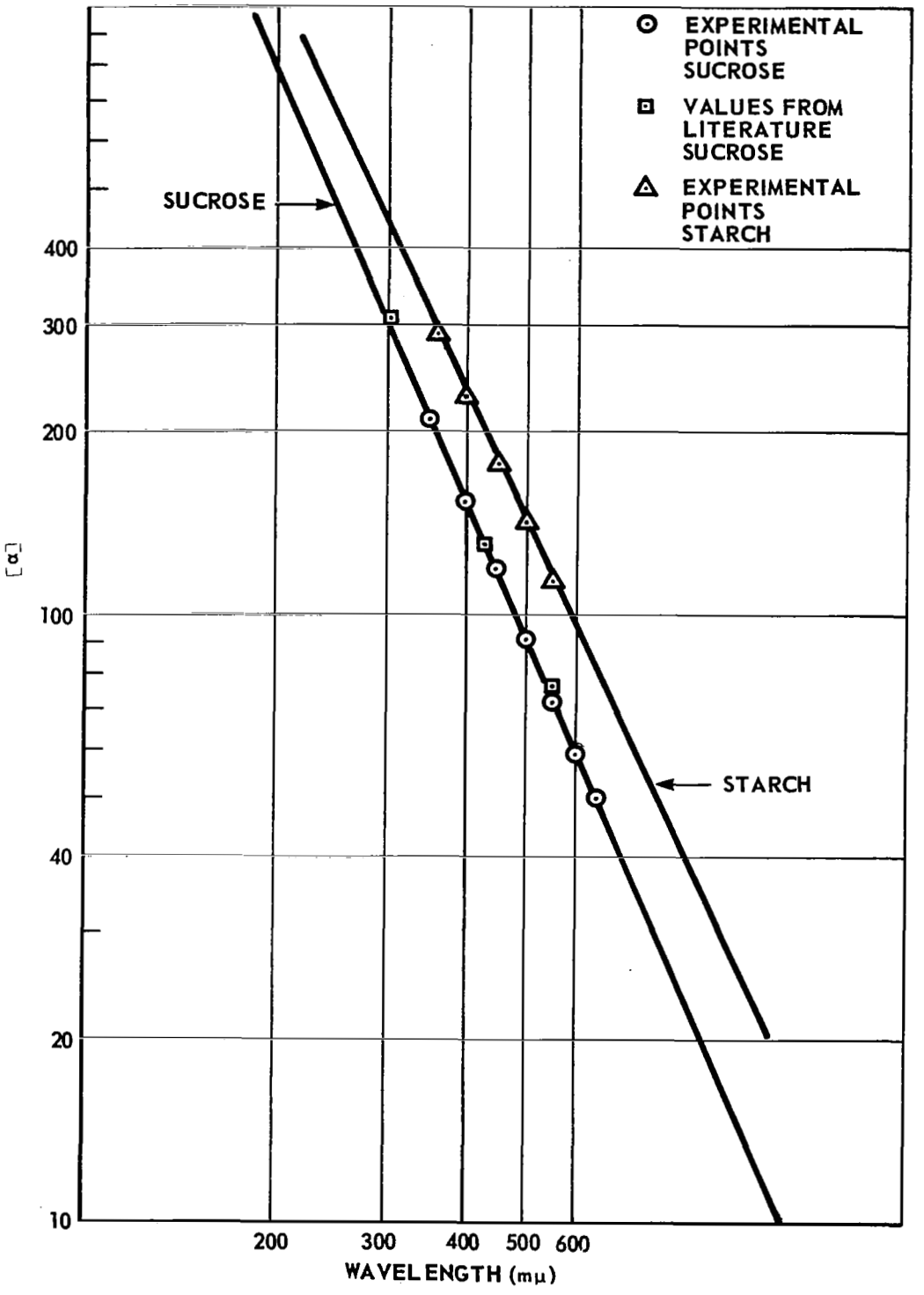

Figure 28. Optical Rotatory Dispersion of Starch and Sucrose

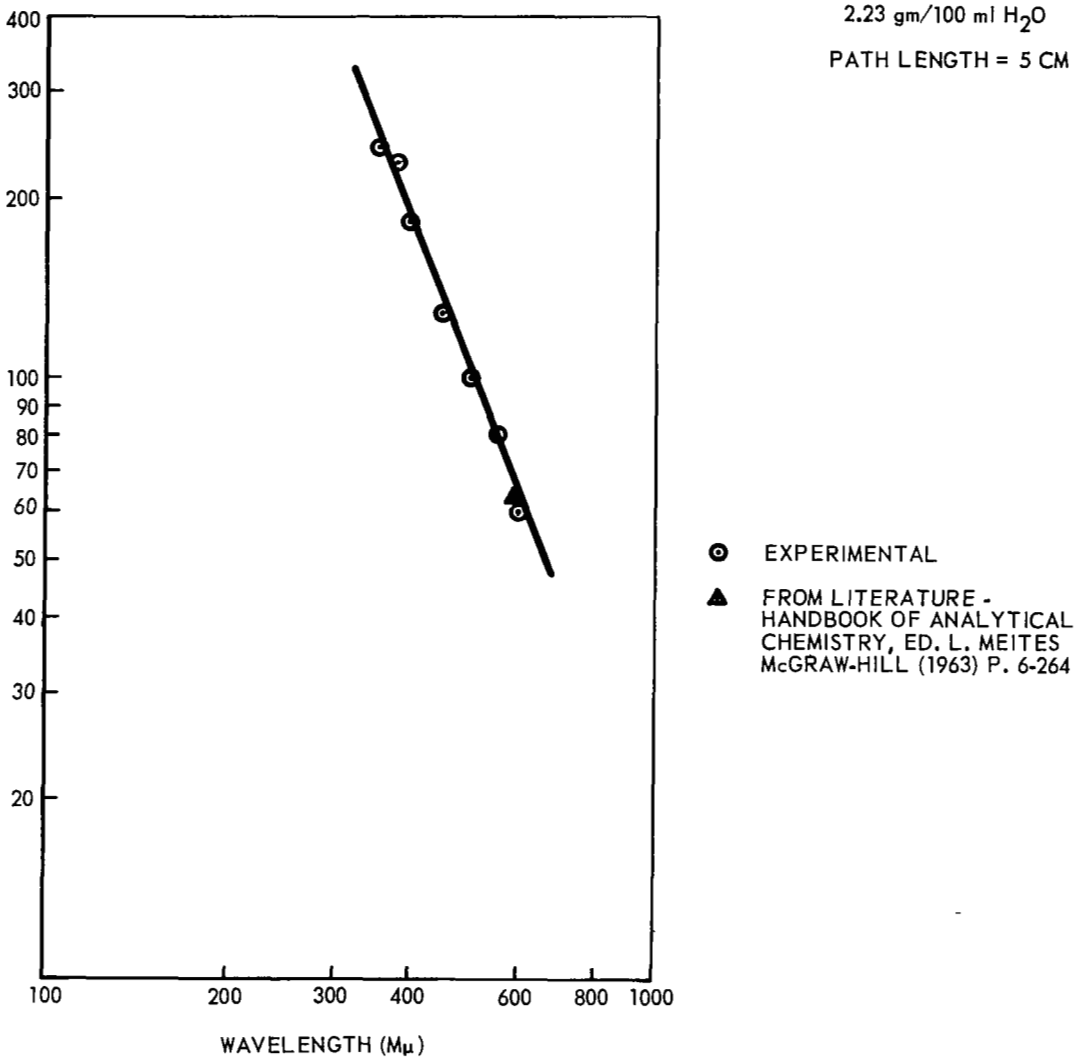

Figure 29. Optical Rotatory Dispersion of Human Serum Albumin

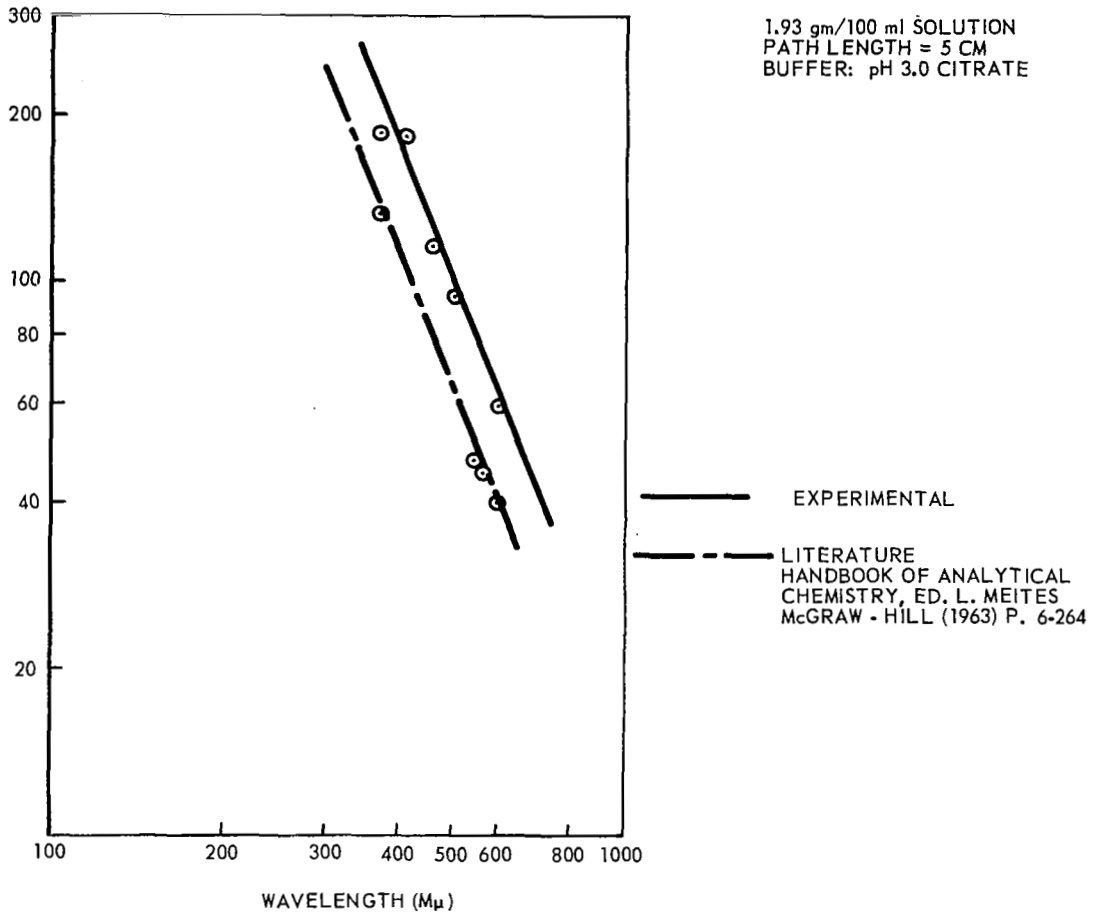

Figure 30. Optical Rotatory Dispersion of Trypsin

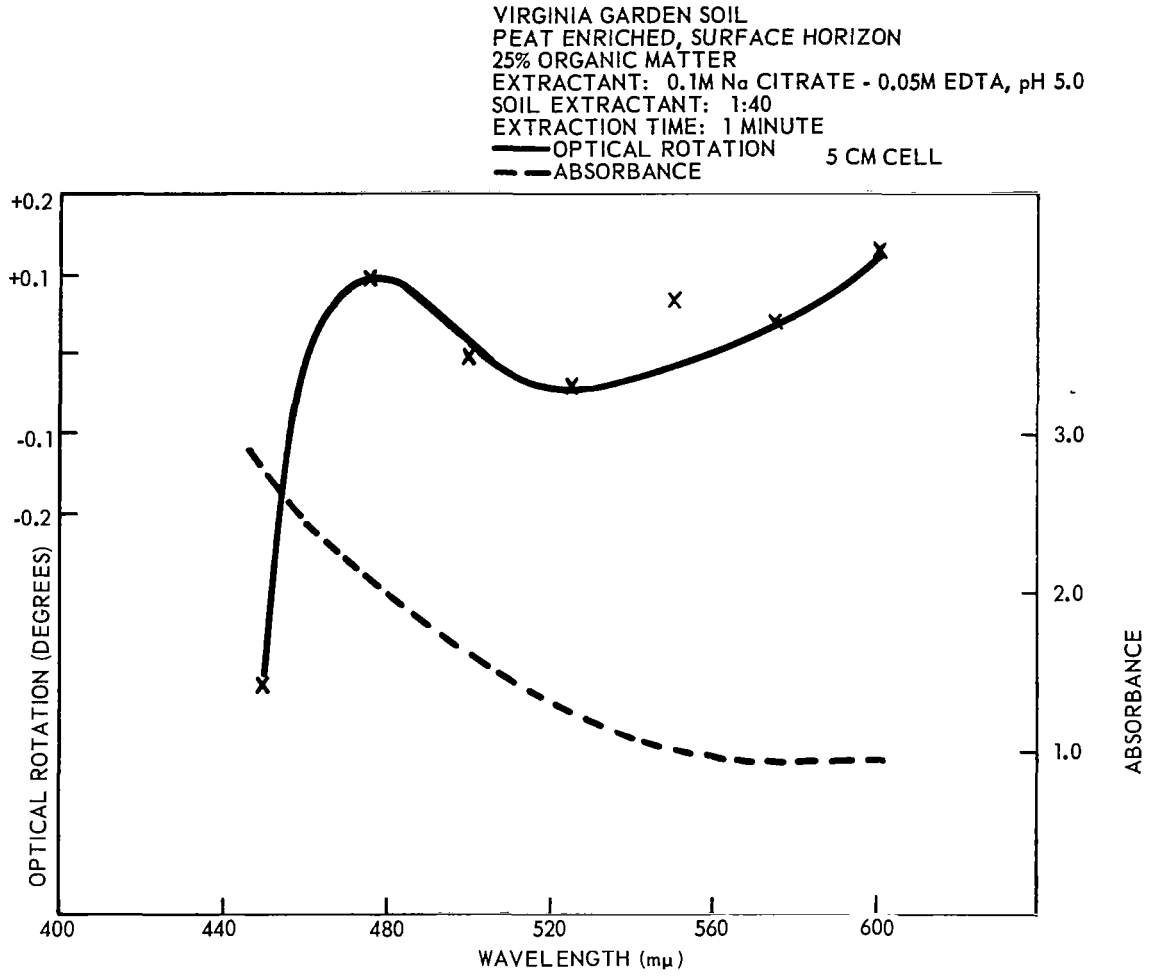

Figure 31. Virginia Garden Soil, ORD and Absorption Spectrum (Aqueous Extract)

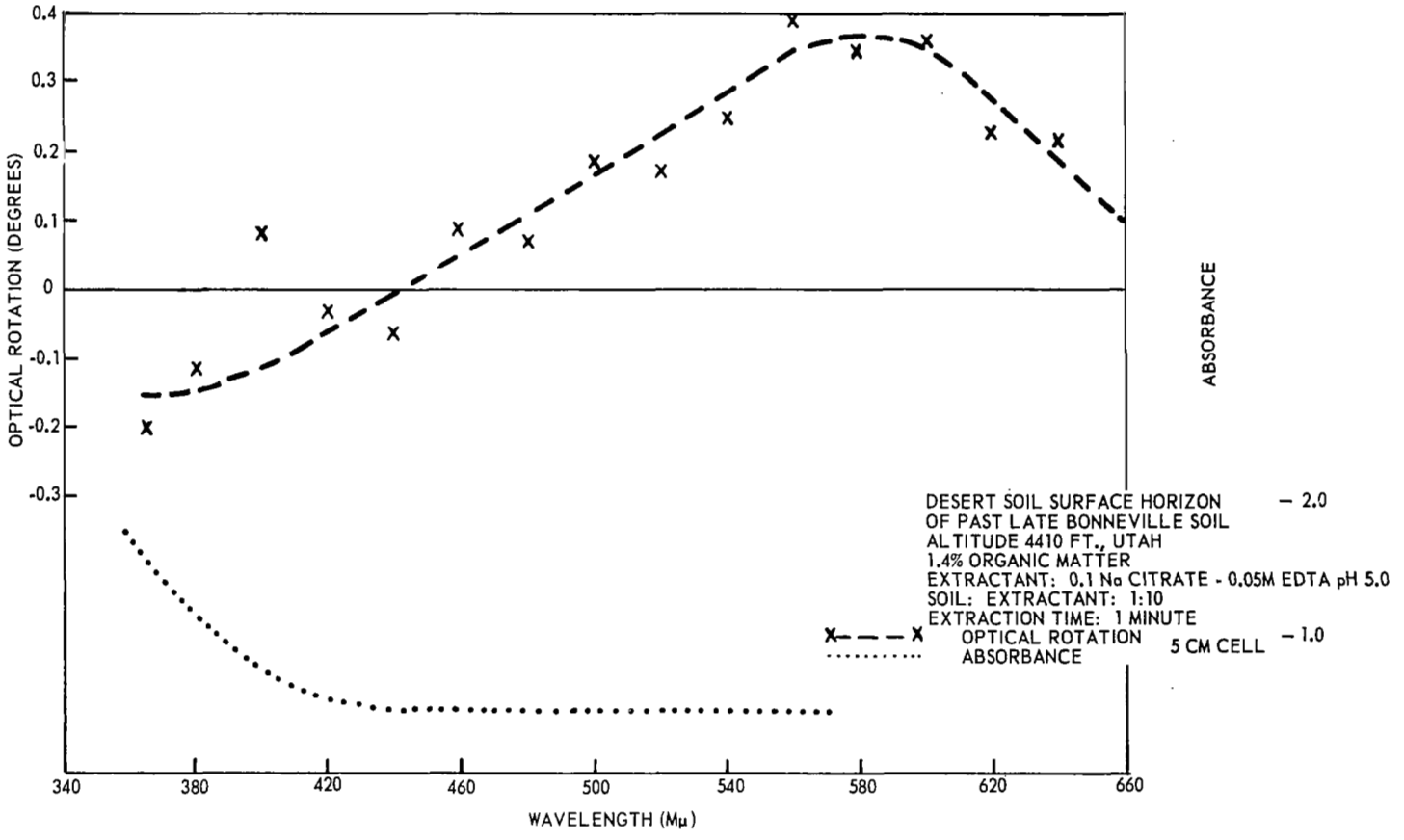

Figure 32. Utah Desert Soil, ORD and Absorption Spectrum (Aqueous Extract)

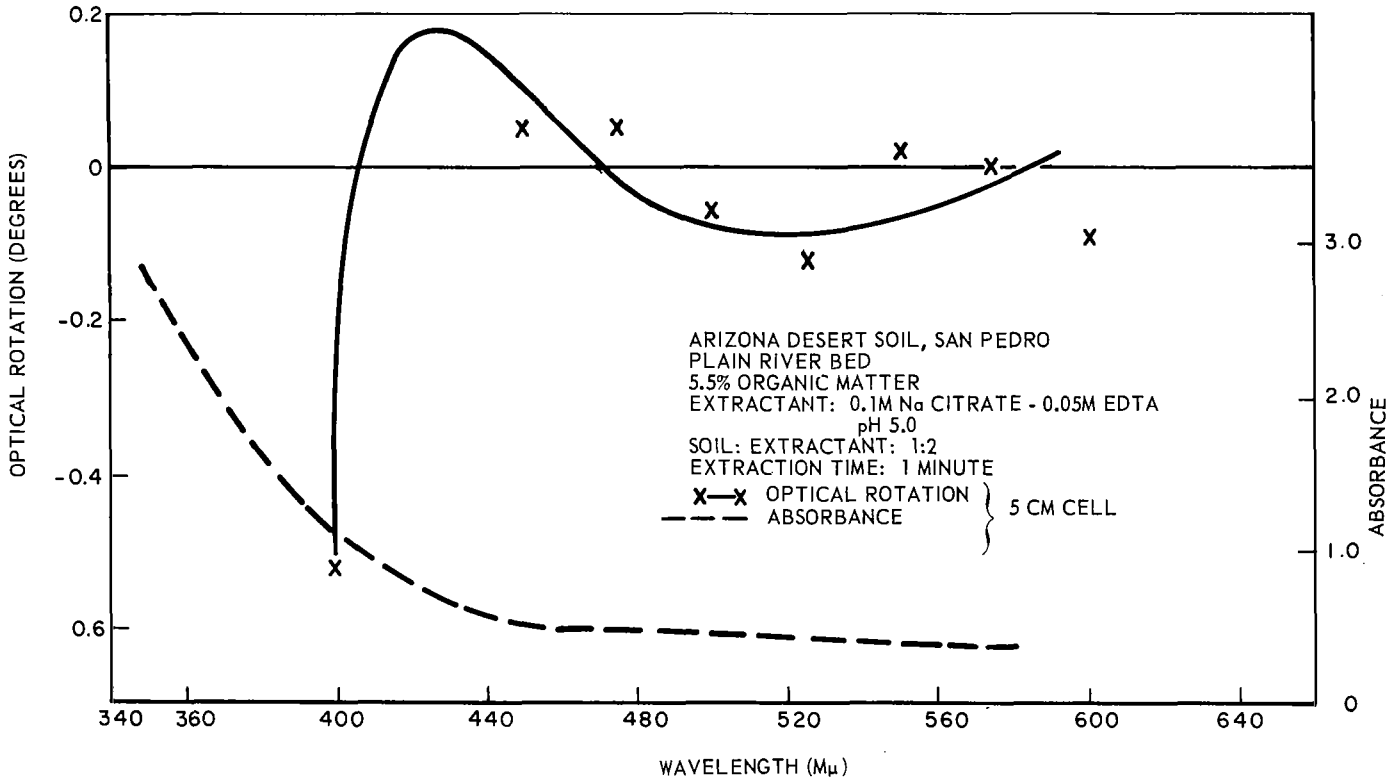

Figure 33. Arizona Desert Soil, ORD and Absorption Spectrum (Aqueous Extract)

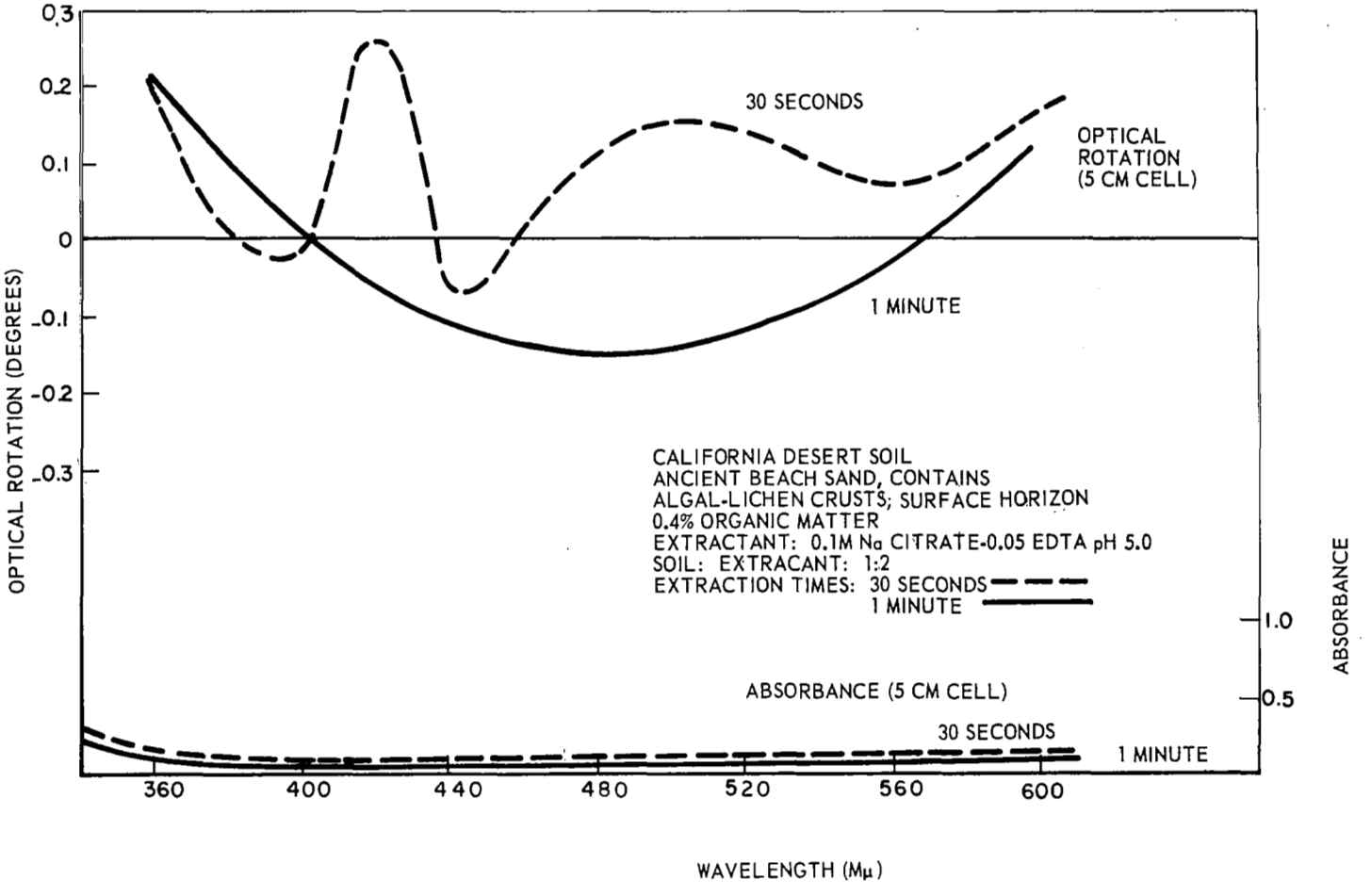

Figure 34. California Desert Soil, ORD Absorption Spectrum (Aqueous Extract, 1:2, 30 sec. and 1 min.)

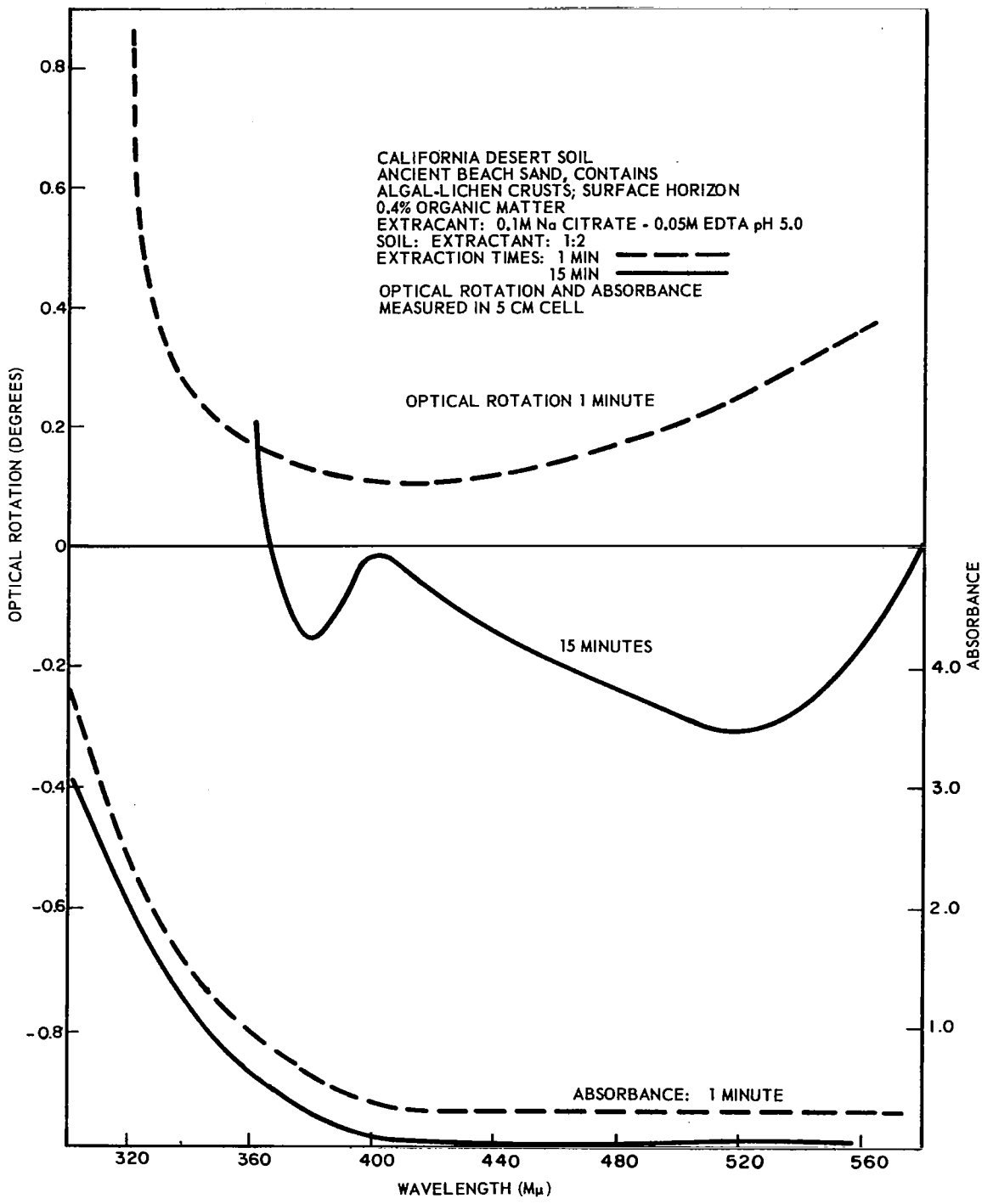

Figure 35. Calfornia Desert Soil, ORD and Absorption Spectrum Aqueous Extract, 1:2, 1 min. and 15 min.)

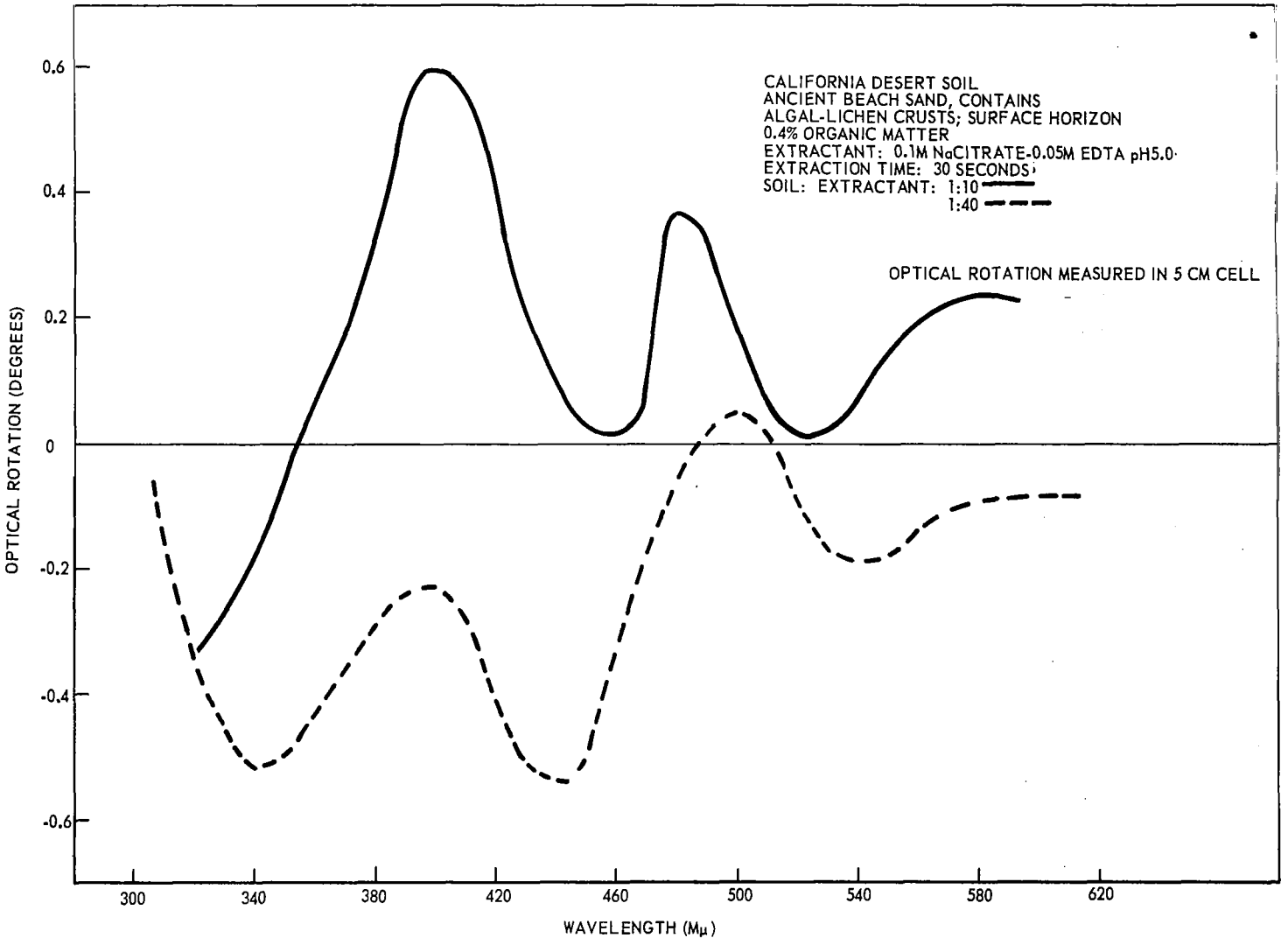

Figure 36. Calfornia Desert Soil, ORD and Absorption Spectrum (Aqueous Extract, 1:10, 1:40, 30 sec.)

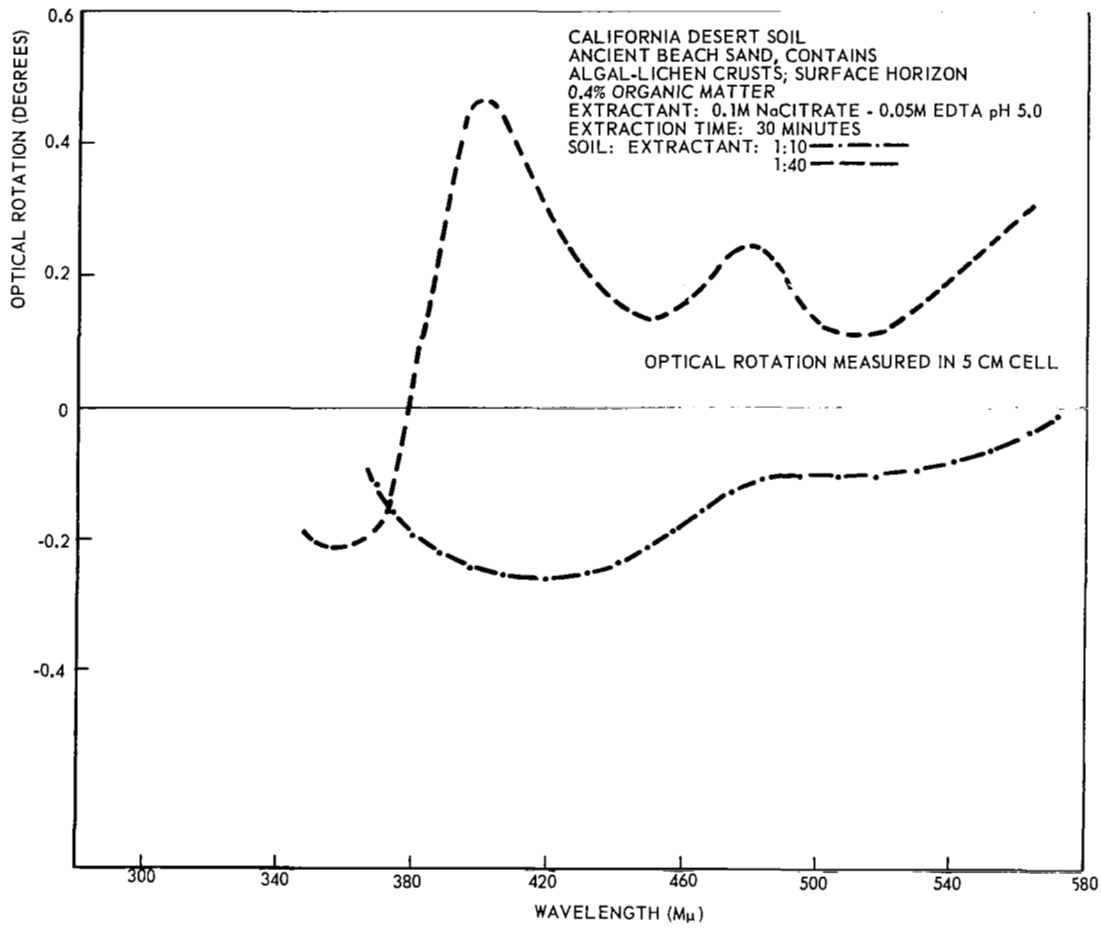

Figure 37. California Desert Soil, ORD and Absorption Spectrum (Aqueous Extract, 1:10, 1:40, 30 min.)

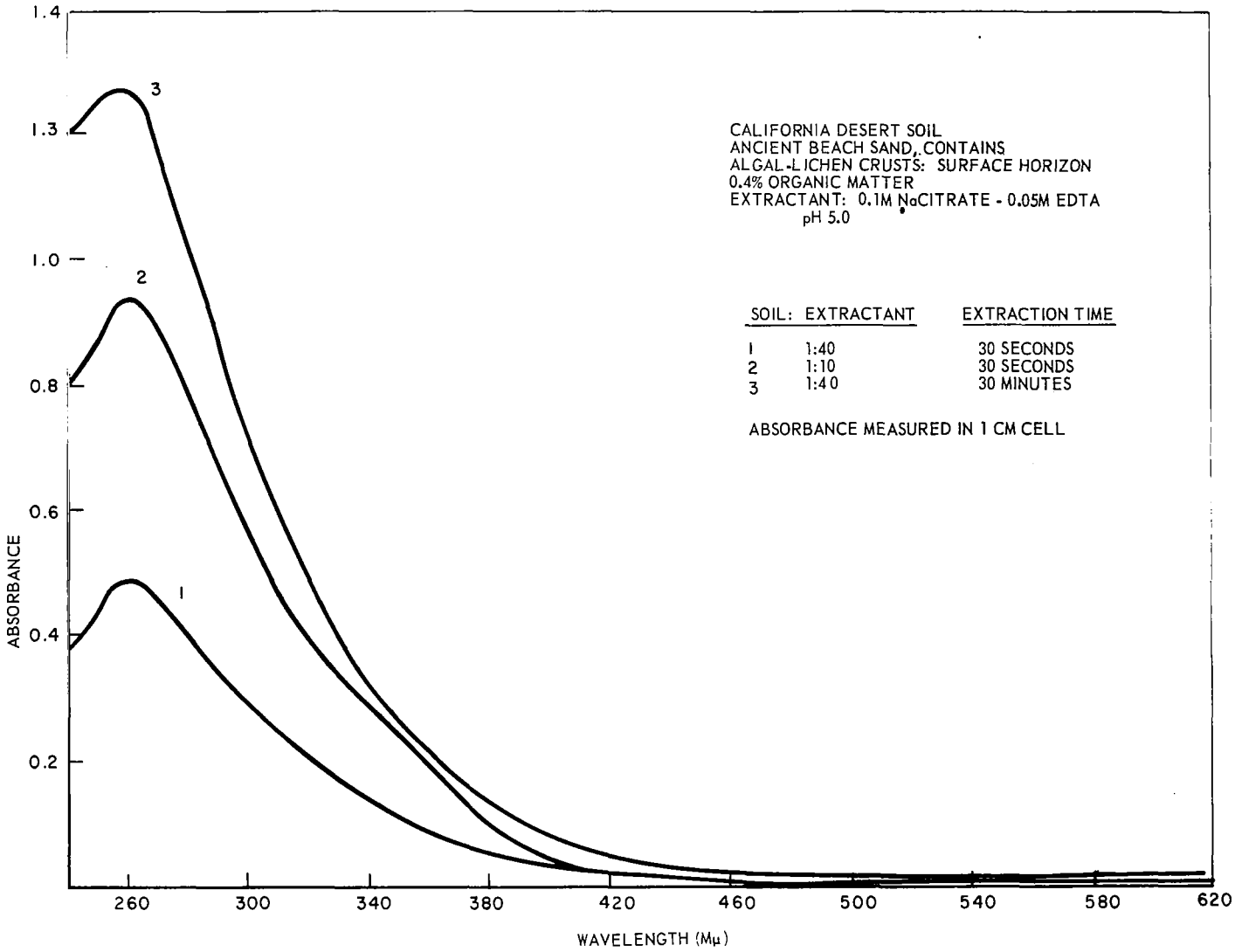

Figure 38. California Desert Soil, Absorption Spectra for Various Soil to Aqueous Solvent Ratios and Extraction Times.

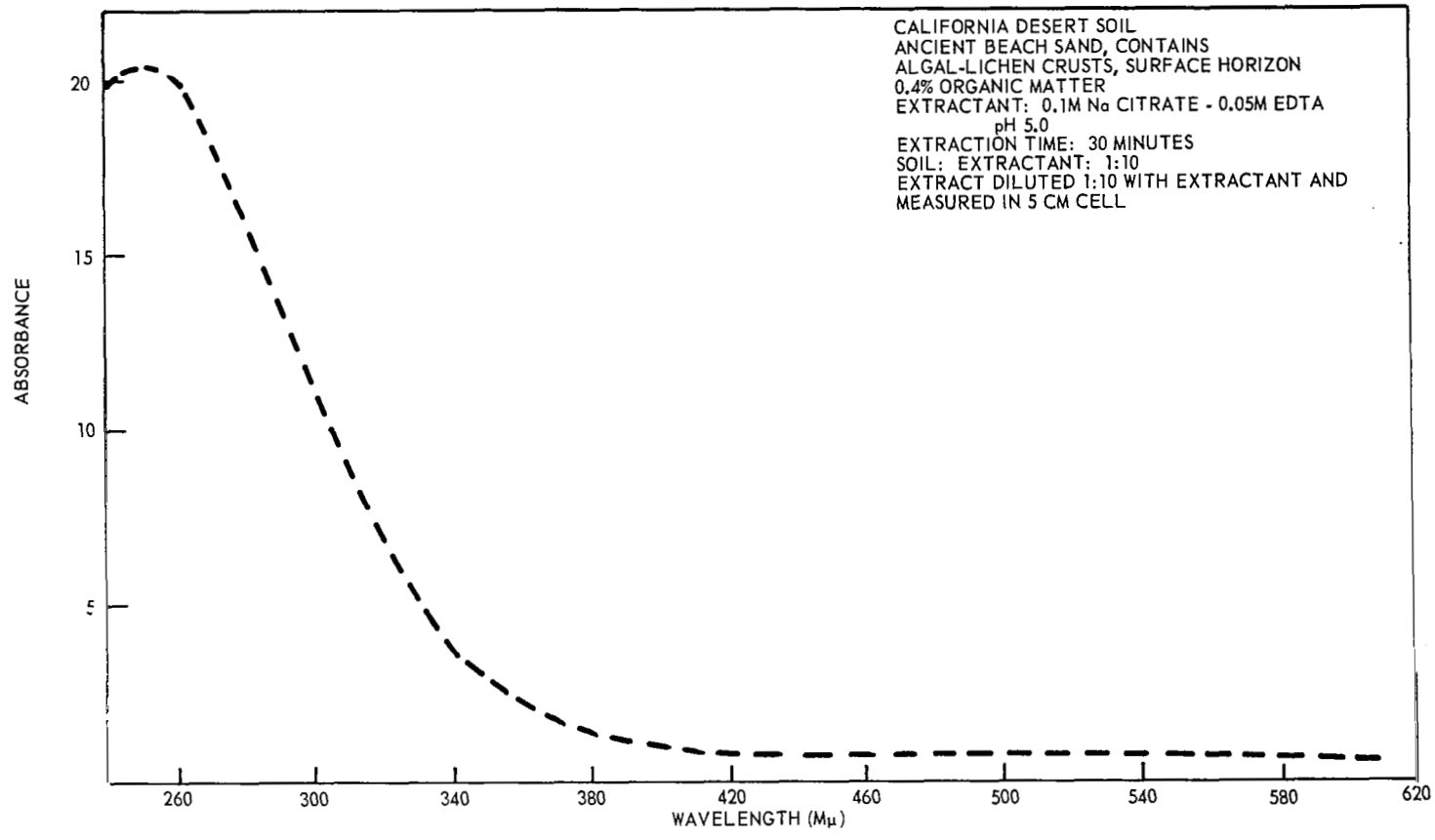

Figure 39. California Desert Soil, Absorption Spectrum (Aqueous Extract, 1:10, 30 min.)

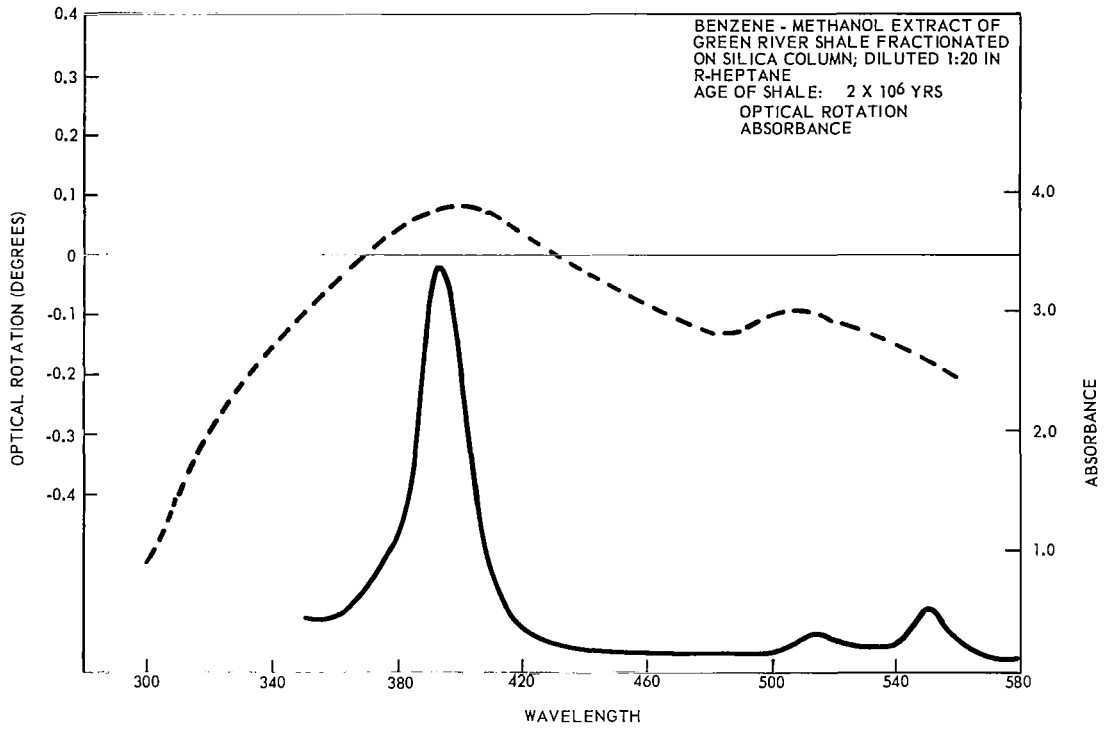

Figure 40. Green River Shale, ORD and Absorption Spectrum (Organic Extract)

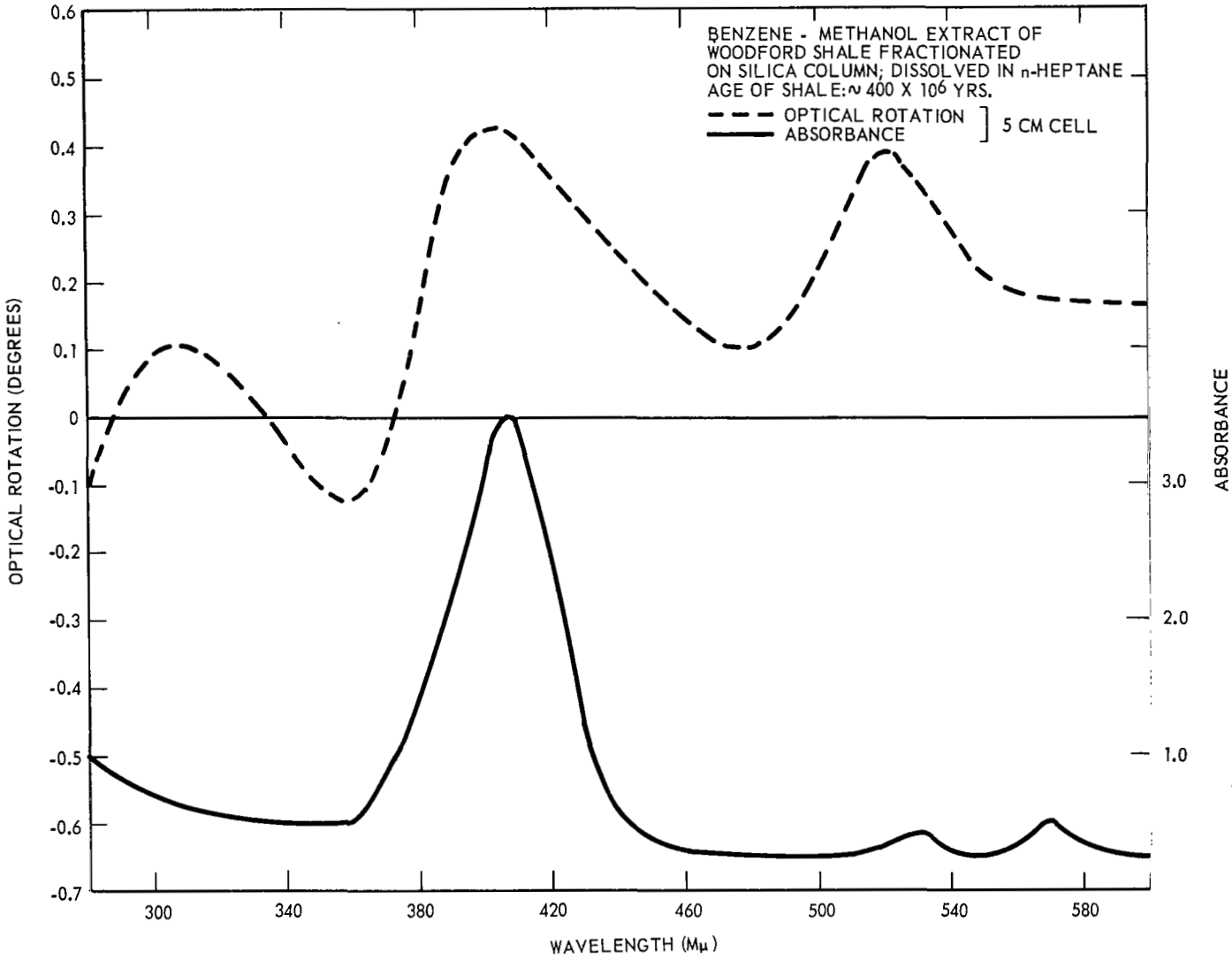

Figure 41. Woodoford Shale, ORD and Absorption Spectrum (Organic Extract)

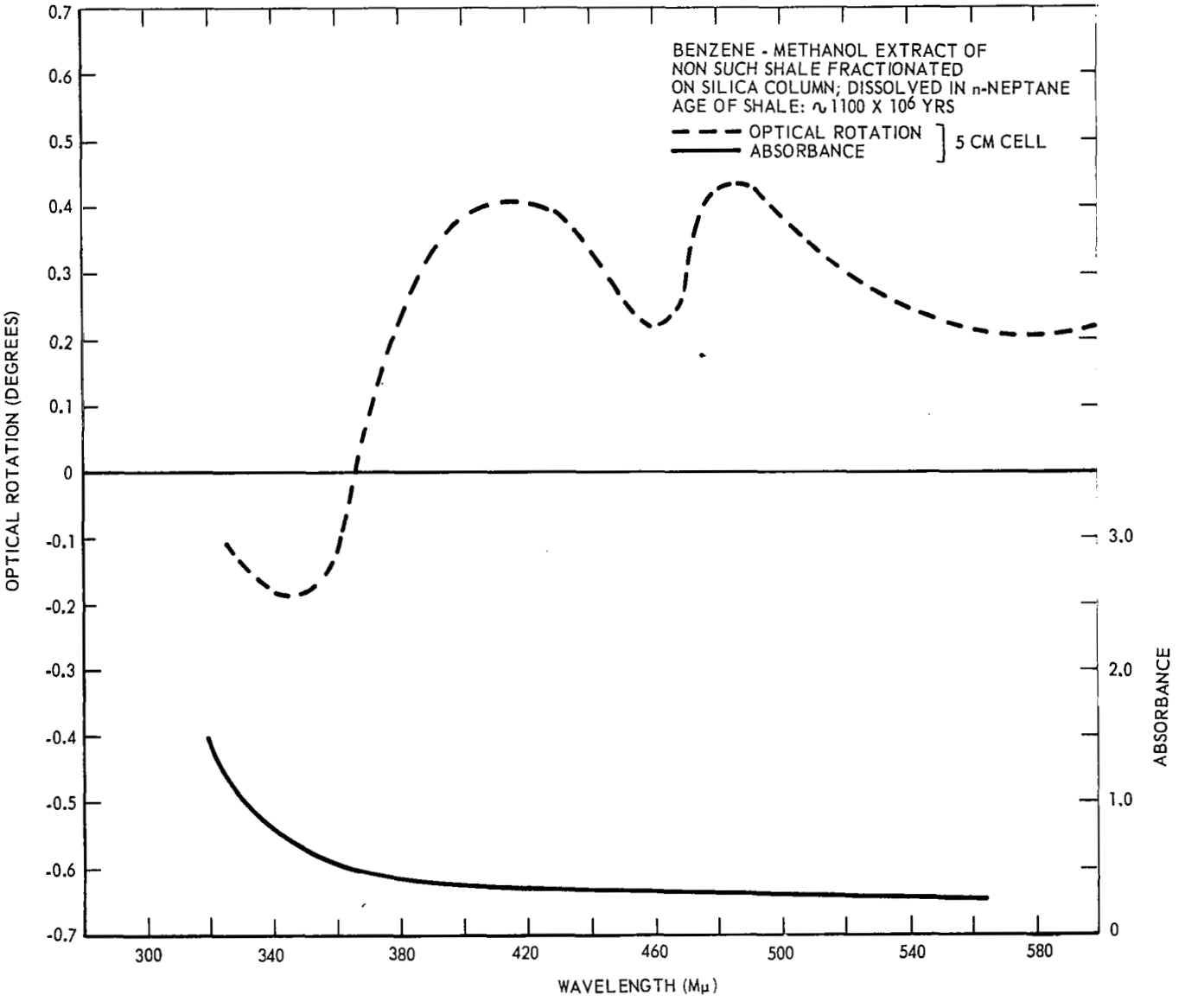

Figure 42. Non Such Shale, ORD and Absorption Spectrum

TABLE 1

CONCENTRATION DEPENDENCE OF OPTICAL ACTIVITY MEASUREMENTS

1 Measured Slopes (deg/mm)	2 Theoretical Ratio of Slopes	3 Measured Ratio of Slopes	4 Difference (3-2) (deg/mm)
(a) 0.15 deg/mm	1	1	0
(b) 0.076 deg/mm	0.498	0.508	0.01
(c) 0.039 deg/mm	0.252	0.260	0.008

5.1 Selection of Soil Extractant

5.1.1 Aqueous Extractants

The efficacy of various aqueous salt systems as extractants for proteins and nucleic acids from Virginia soil (VS-I) is shown in table 2. The various soils utilized in this study are listed in tables 3 and 4 together with their characterizations.

The EDTA-citrate extract of VS-1 gave a strong ninhydrin reaction and a faintly positive test for sugars. The α-naphthol method was negative for the same extract. Both local and desert soils extracted with ethyl acetate showed no orange fluorescence under UV light; therefore, no porphyrins were present (or could not be extracted) or were not in sufficient quantities to be detected by this method.

5.1.2 Organic Extractants

In attempts to extract more optical activity from Virginia soil, the organic solvents N, N'-dimethylformamide (DMF) and dimethysulfoxide (DMSO) were utilized. Extracts of VS-1 with 100% DMF or DMSO exhibited a light amber color. Spot tests for protein or carbohydrate were unsuccessful, possibly due to solvent interference.

Absorption of the phenolic extract of VS-II at 365 mμ was 0.2 and was extremely high in the ultraviolet region of the spectrum. No qualitative tests for proteins or sugars were successful due to solvent interference. The switch to aqueous DMF improved the extraction somewhat.

TABLE 2

EXTRACTION EFFICIENCY OF SEVERAL AQUEOUS AND ORGANIC SOLVENTS

VS-I (2 gm soil + 50 ml extractant stirred for 50 minutes)		
Extractant	µg/ml Nucleic Acid[1] (as DNA)	µg/ml Protein[2] (as Serum Albumin)
0.1 M EDTA pH 5.0	< 2	340
0.2 M acetate pH 5.0	< 2	---
0.1 M EDTA-acetate pH 5.0	< 2	350
0.1 M citrate pH 5.0	5	8
0.1 M EDTA-citrate pH 5.0	< 1	> 400
0.2 M borate-10% urea	---	---
EDTA-citrate + ETOH ppt.	8	---
EDTA-citrate + ETOH supn't	---	---
Dimethylsulfoxide	---	---
N,N'-Dimethylformamide	---	---

[1]Nucleic acid determined by method of Dische[6]

[2]Protein determined by method of Lowry et al.[4]

TABLE 3

CHARACTERIZATION OF AGRICULTURAL AND DESERT SOILS

Soil	Depth	Location	Texture	% Organic Matter	Carbo-Hydrates[1]	Protein[2]	Comments
VS-I	Surface	Northern Virginia	Silty Clay	8.2	+	+	
VS-II	Surface	Northern Virginia	Clay Loam	43.8	++	-	Peat enriched
VS-II	Surface	Northern Virginia	Clay Loam	11.0	+ -		1100°F/24 hrs.
VS-III	Surface 0-1'	Northern Virginia	Sandy Clay	20.5	-		
VS-IV	Surface 0-1'	Northern Virginia	Clay	11.0	-		
VS-V	Surface 0-1'	Northern Virginia	Sandy Clay	19.3	+ -		
DS-I	Surface 0-0.4'	1 mile west of Sandy, Utah	Sandy Loam	1.4	-	+	
DS-II	3.0-3.6'	Desert Bonneville, Utah	Sand	1.4	-	-	
DS-III	80' below Surface	Nevada Desert	Sandy Loam	13.7	+		Playa sediment early pleistocene
DS-IV	Vesicular Horizon	Nevada Desert	Sandy Loam	16.5	-	-	Nevada Post Lake Bed.
DS-V	Surface 0.25-0.7'	New Mexico Desert	Sandy Loam	21.2	+		

TABLE 3 (Cont.)

Soil	Depth	Location	Texture	% Organic Matter	Carbo-Hydrates[1]	Protein[2]	Comments
DS-VI	Surface	California Searles Valley	Silt	13.8	-		Pleistocene Lake Bed
DS-IX	Surface	California Searles Lake	Silty Sand	16.5	-	-	Lake Deposited Silt, Saline
A-1	Surface	Arizona Desert	Sand	5.5			Ridgecrest
A-2	Surface	Arizona Desert	Sand	8.3	-	-	Recent Creek Bed
A-3	Surface	Arizona Desert	Sandy Loam	9.7			High-level Knace
A-4	Surface	Arizona Desert	Sand	1.4	-		San Pedro Plain River Bed
Acetone ppt. of VS-II				100.0	+	++	White ppt.

1 As determined by ninhydrin spray reagent

2 As determined by aniline-phthalate spray reagent

\+ Positive reaction

++ Strongly positive

\- Negative

TABLE 4

CHARACTERIZATION OF DESERT SOILS USED FOR OPTICAL ROTATION MEASUREMENTS

JPL Soil	Depth	Location	Texture	% Organic Matter	µg/ml Carbo-Hydrate[1]	µg/ml Pro-tein[1]	% Moist-ure	Flora[2] GM. Soil	Comments
1-2	Surface 1/16-1/8"	Colorado Desert	Sand	0.29	4	50	0.28	6×10^5	Ancient Beach Sand contains Algal-Lichen Crusts.
34	Surface 1/2"	Kau Desert Hawaii	Sandy Loam	0.058	4	10	6.3	1×10^5	Volcanic Soil
6-1	Surface 1/2"	Mecca Hills Calif.	Clay	0.82	10	27	3.3	2×10^6	Barren, Eroded Clay Hills
35	1/2 -2" Below Surface	Kau Desert Hawaii	Sandy	0.24	10	40	7.9	1×10^5	Volcanic Soil

1. Determination made on extract: values represent those of 30-min extraction times.

2. Represents total microbes, fungi and algae per gram soil (from R. E. Cameron).

VS-I extracted with 80% DMF yielded a dark solution which gave faintly positive ninhydrin and aniline-phthalate reactions. The spectrum of this solution was featureless except for a gradually decreasing absorbance (A_{240} = 1.6 to A_{400} = 0.05). No precipitate formed when ice cold ethanol or acetone was added.

Similar results were obtained when the extraction of Arizona soil A-3 with 50% aqueous DMF was observed as a function of time. In this experiment the extraction of 2 gm of soil with 50 ml of DMF was observed spectrally from 365 to 600 mμ at extraction times of 1, 5, 15 and 30 minutes. The greatest change in optical density was observed at 365 mμ and can be seen in figure 43. All solutions possessed a light amber color. All samples showed a faint positive reaction with ninhydrin and a negative reaction for reducing sugars. ORD measurements on the 1-min and 30-min extracts showed no significant differences at 375 mμ.

5.2 H^3-RNA Extractions

Recovery data for tritium-labeled RNA added to dry soils are shown in table 5. With phosphate and borate buffers, extraction was more efficient at higher than at lower pH values, although none of the four conditions used gave high efficiency. Nondegraded RNA appears to be firmly bound by the powdered soil sample.

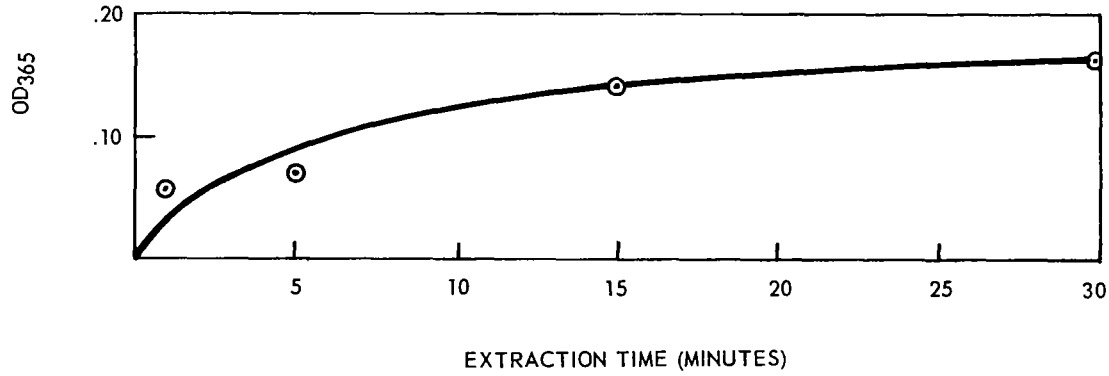

Figure 43. Absorption Spectrum of Arizona Desert Soil Extracted With Dimethylformamide Versus Time

TABLE 5

EXTRACTION EFFICIENCIES OF PHOSPHATE AND BORATE BUFFERS
(H^3-RNA RECOVERY)

Sample	cpm	Counting Efficiency	dpm/0.1 ml Extract	RNA Recovered
		Phosphate Buffers		
5 λ Standard	11,000	13.5%		
0.1 ml pH 5.8 extract + 5 λ standard	10,900	12.6%		
0.1 ml pH 5.8 extract	525		4160	4.1%
0.1 ml pH 8.0 extract + 5 λ standard	8,500	9.3%		
0.1 ml pH 8.0 extract	905		9750	9.7%
		Borate Buffers		
5 λ Standard	12,000	13.5%		
0.1 ml pH 7.4 extract 5 λ standard	10,700	11.9%		
0.1 ml pH 7.4 extract	218		1830	1.8%
0.1 ml pH 9.0 extract + 5 λ standard	8,700	9.2%		
0.1 ml pH 9.0 extract	555		6040	6.0%

5.3 Extraction for Optical Activity

Figure 44 illustrates a typical absorption spectrum for JPL 1-2 desert soil extract at 1:40 soil-extractant ratio for the various extraction times employed. Higher soil-extractant ratios did not alter the shape of the curve but simply elevated the absorbance values considerably at the shorter wavelengths. Figure 45 shows the relative changes in absorbancy between ultraviolet and visible regions of the spectrum. The spectra show no distinctive features other than an absorption peak at 260 mμ. All absorption spectra were corrected to a 5-cm cell so that both absorbance and ORD data would be comparable. This was accomplished merely by multiplying the absorbance readings taken in a 1-cm cell by 5.

5.3.1 Sephadex Gel Fractionation

(a) Virginia soil

In attempts to separate color from the optically active compounds in soil extracts and to approximate the molecular weight of the components, fractionation on Sephadex gels G-25 (molecular weight exclusion limit 5000), G-75 (exclusion limit 50,000), and G-200 (exclusion limit 200,000) were carried out at room temperature. Figure 46 shows the fractionation profile of 1 ml of a 0.1-N NaOH extract (1 gm of Virginia soil ground for 1 minute with 2 ml of 0.1-N NaOH) eluted with distilled water from G-25.

Two yellow bands were initially observed toward the top of the column (these bands descended fairly rapidly) and were off in 1 hour. It can be seen that one major peak is resolved; the brown color is associated with this peak. It may be concluded that the molecular weight of the peak is greater than approximately 5,000 since its position in the fractionation profile is within the void volume for this size column. All fractions were faintly positive with ninhydrin reagent.

In order to determine the upper limit of the molecular weight for this extract, gel fractionation on G-200 was carried out. Ten ml of the aforementioned extract was placed on a 1.5 x 18 cm column and eluted with 1.0% NaCl. The elution profile is shown in figure 47. Two distinct peaks are observed. The resolution is not good due to the large sample size, but the small, broad peak comes off within the void volume for this column, while the larger narrow band is somewhat retarded by the gel.

(b) Arizona desert soil (A-3)

Similar attempts to fractionate desert soil were interesting. One ml of an 0.05-M EDTA-citrate pH 5.0 extract of A-3 was placed into a 2.0 x 15 cm G-25 column and eluted with distilled H_2O. Two definite bands were observed 10-15 minutes after charging the column. Both bands were off the column in about 1 hour (similar observation with Virginia

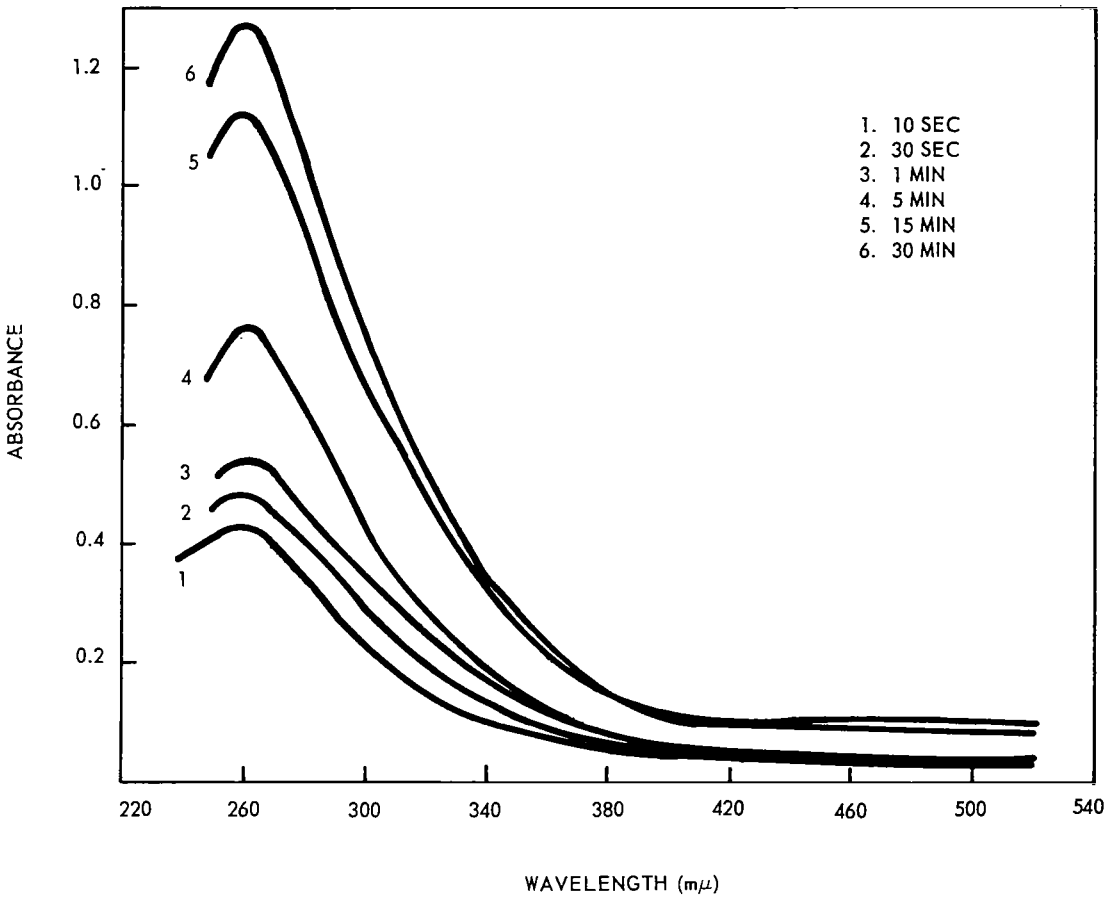

Figure 44. California Desert Soil Absorption Spectra for Various Extraction Times, Aqueous Extract, 1:40

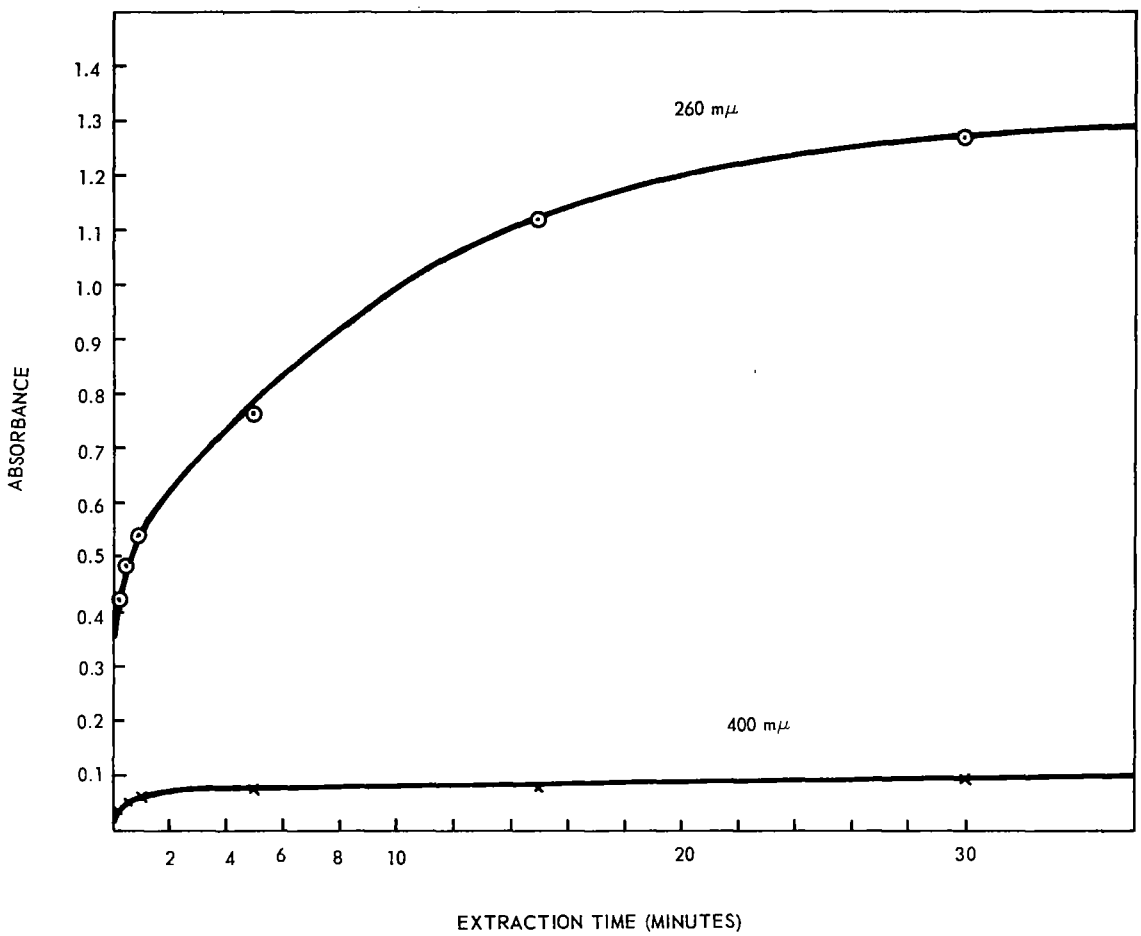

Figure 45. California Desert Soil, Comparison of Absorbancies in the Ultraviolet and Visible Regions of the Spectrum

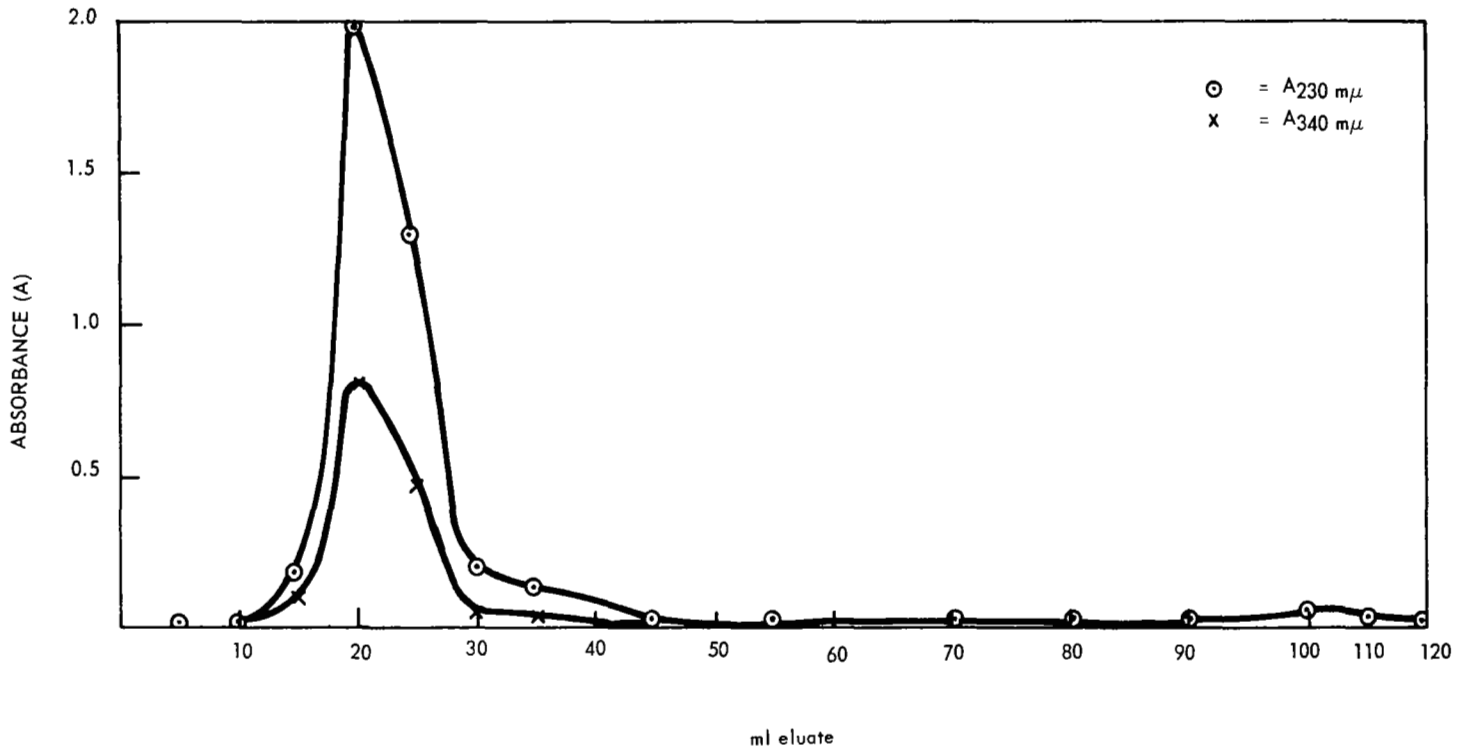

Figure 46. Virginia Soil, 0.1 N NaOH, Sephadex G-25 Fractionation

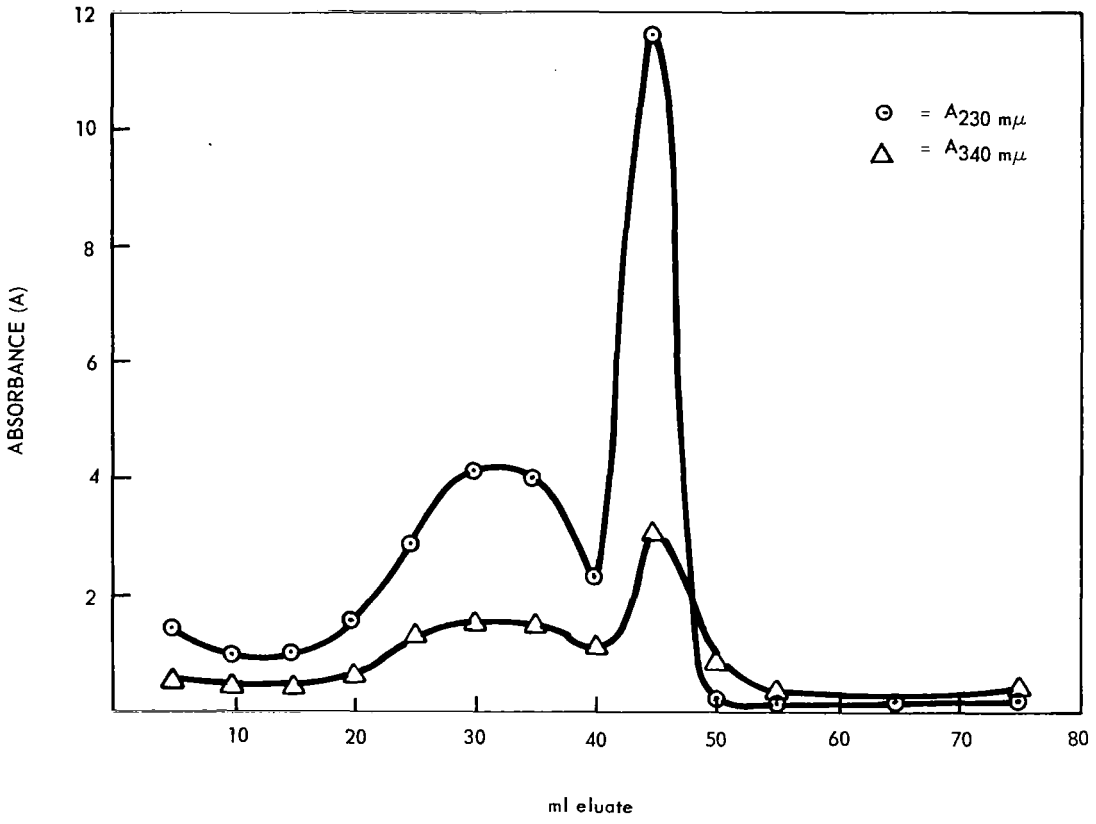

Figure 47. Virginia Soil, 0.1 N NaOH, Sephadex G-200 Fractionation

soil extract). The recovery was 97%. The fractionation profile is illustrated in figure 48. Three separate bands are resolved, most of the color moving with the first band. It is of interest that even though all fractions were faintly positive for protein (ninhydrin spray), only the second and third bands were faintly positive for reducing sugars. A shift in the UV absorption maximum from 260 mμ to 280 mμ was observed after 25 ml of eluate had come off (trailing edge of first peak). This shift reversed itself 3.5 ml later (at start of second peak). The second and third peaks were somewhat retarded by the gel, indicating the presence of low molecular weight compounds. The narrowness of the bands suggests a considerable degree of monodispersity. The fact that the first peak falls within the void volume (30 ml) implies that the molecular weight is greater than 5,000, while the slower two peaks are less than 5,000.

Biuret analysis showed the first peak to contain 60 μg/ml protein although all fractions gave some lesser positive reaction. No sugars could be detected with aniline phthalate. Even though the absorbance was quite large at 260 mμ, very little color was visible to the eye.

5.3.2 Thin-Layer Chromatography (TLC)

Several soil extracts were examined by TLC for a qualitative analysis of soil constitutents.

Chromatography of Virginia soil extracted with formic acid, Virginia soil extracted with 0.1 M EDTA-citrate buffer and desert soil (DS-I) extracted with 0.1 M EDTA-citrate buffer was carried out in the systems described. The results are given in table 6. The formate extract exhibited a well-defined absorption peak at 260 mμ. $A_{280}/A_{260} = 0.76$ suggests the presence of nucleic acids as well as large amounts of protein. Spectra of VS EDTA and DS citrate - EDTA extracts showed well-resolved peaks between 260 mμ and 280 mμ after removal of the spots from the silica gel chromatoplate and elution with 0.06 N HCL.

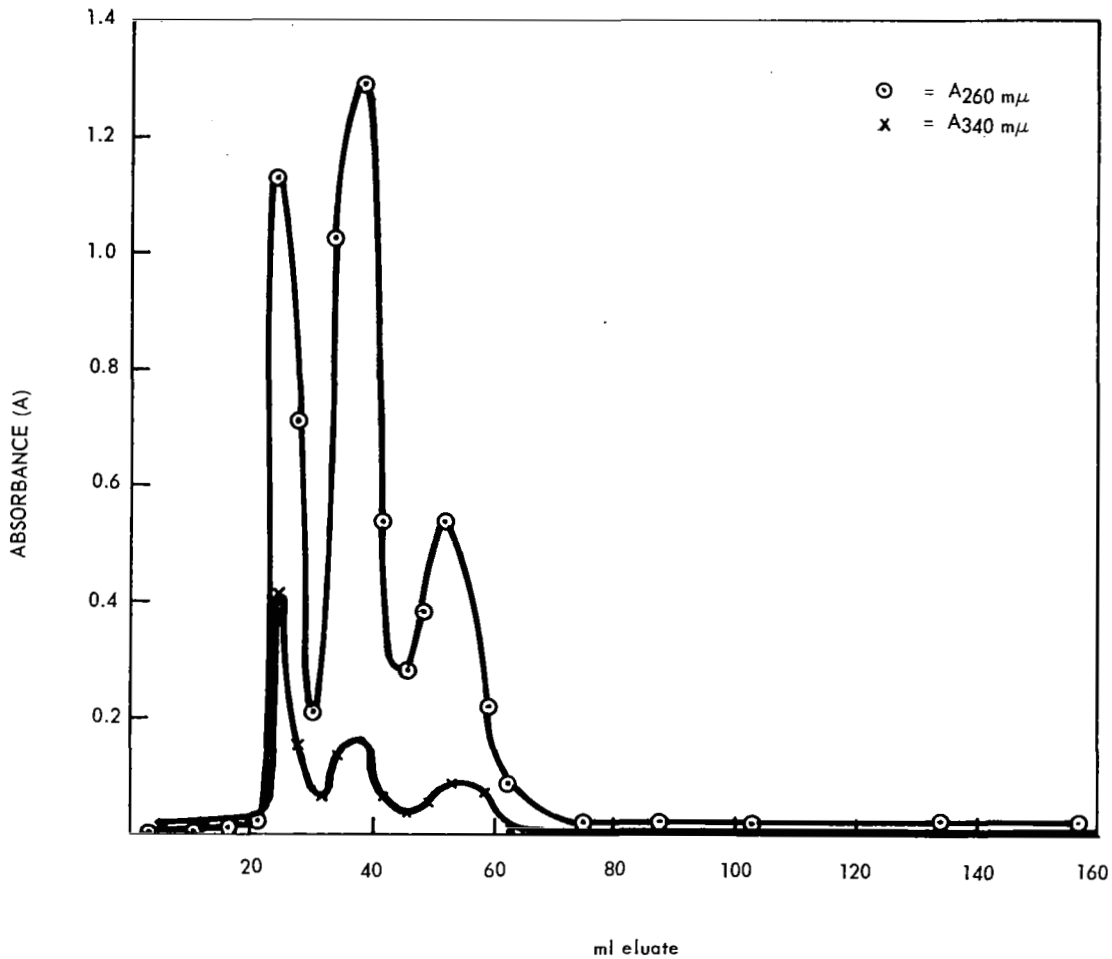

Figure 48. Arizona Desert Soil, 0.1 M Na Citrate - 0.05 M EDTA, pH 5, Sephadex G-25 Fractionation

TABLE 6. THIN-LAYER CHROMATOGRAPHY OF SOIL EXTRACTS

TLC OF SOIL EXTRACTS FOR AMINO ACIDS
(Silca Gel F - Butanol-acetic acid - H_2O/60:20:20)

Sample (10 µl)	R_f	Ninhydrin	Aniline Phthalate	Fluorescence	UV
VS formate	0	-			
VS EDTA-citrate	0.01	+			
	0.08			Blue	
	0.23	+		Blue	
DS EDTA-citrate	0.01	+			
	0.08			Blue	

TLC OF SOIL EXTRACTS FOR CARBOHYDRATES
(Silica Gel F - Upper Phase, butanol-acetic acid- H_2O/40:10:50)

Sample (10 µl)	R_f	Ninhydrin	Aniline Phthalate	Fluorescence	UV
VS formate	0		-		
VS EDTA-citrate	0.13		±	yellow	
DS EDTA-citrate	0.12		-	yellow	

TLC OF SOIL EXTRACTS FOR NUCLEIC ACIDS
(DEAE-cellulose-0.03 HCl)

Sample (50 µl)	
VS formate	Large UV absorbing band from origin to end of migration (15 cm) observed. Large ninhydrin positive spot in formate extract; R_f = 0.13
VS EDTA-citrate	
DS EDTA-citrate	Large UV absorbing band; yellow fluorescent band

5.4 Analysis of Extracts for Optical Activity

As can be seen from figures 38, 44, and 45, the absorption at wave lengths greater than 350 mμ does not change appreciably relative to changes at 260 mμ for any given soil:extractant ratio. Since our observation of optical activity has been confined mainly to wavelengths greater than 300 mμ and since at high soil:extractant ratios the magnitude of the absorbance was also high relative to the magnitude of optical rotation, it seemed of interest to compare the optical activity with respect to absorbance and to quantitate the relationship, if any.

To gain insight as to the absorbancies involved at high soil extractant ratio, the absorbance of a 30-min extract was 29.0 at 260 mμ and 3.0 at 369 mμ. For a 30-second extract, A = 14.0 at 260 mμ and 1.5 at 360 mμ.

Figures 49, 50, and 51 compare the optical rotation obtained at 3 different wavelengths for various soil: extractant ratios at different extraction times with the absorbance of the same solutions. The fact that the absorbances are linear on a semilog plot indicate that absorbance is an exponential function of the extraction time.

The optical rotation data, on the other hand, presents a complex picture. The direction of rotation that is obtained at any particular extraction time appears to be a function of the soil: extractant ratio and the absorbance.

Figure 19 shows the spectral distribution in the beam of light produced by a General Electric Quartzline Lamp (1962) after passing through a Corning No. 7-37 glass filter. Comparison with the previous figures shows that this is a useful spectral band for detecting optical activity in aqueous extracts.

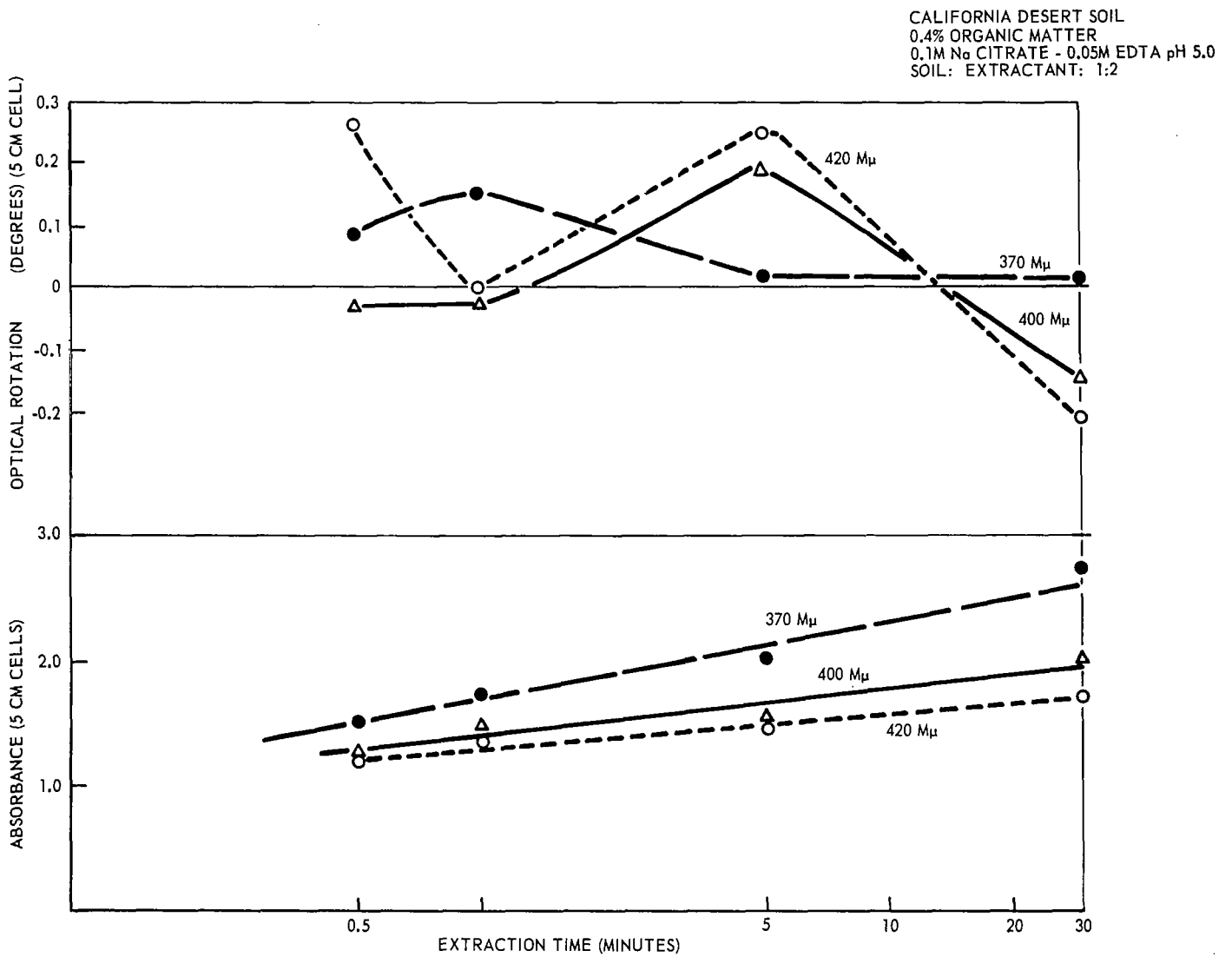

Figure 49. California Desert Soil, ORD and Absorbance Versus Extraction Time (Aqueous Extract, 1:2)

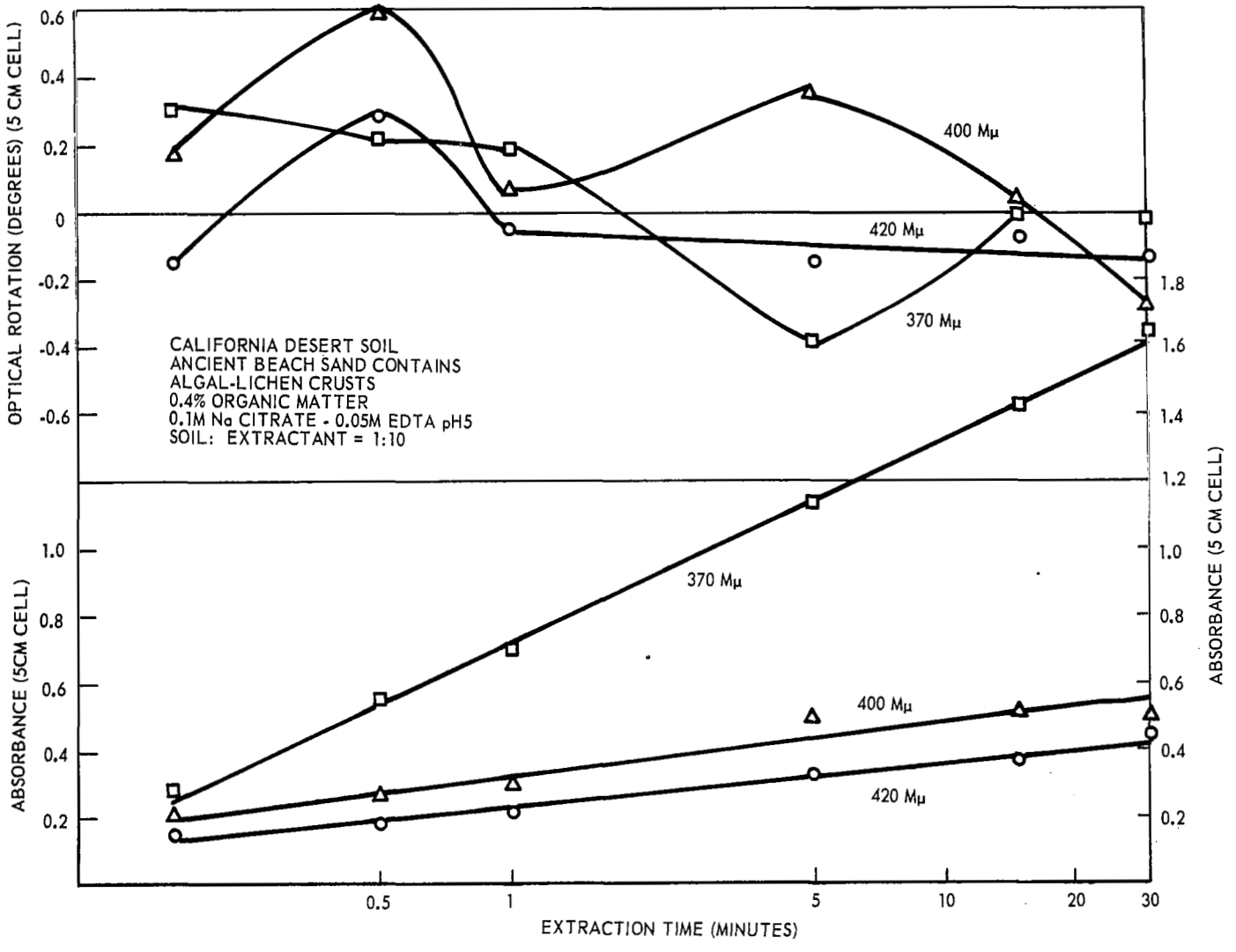

Figure 50. California Desert Soil, ORD and Absorbance Versus Extraction Time (Aqueous Extract, 1:10)

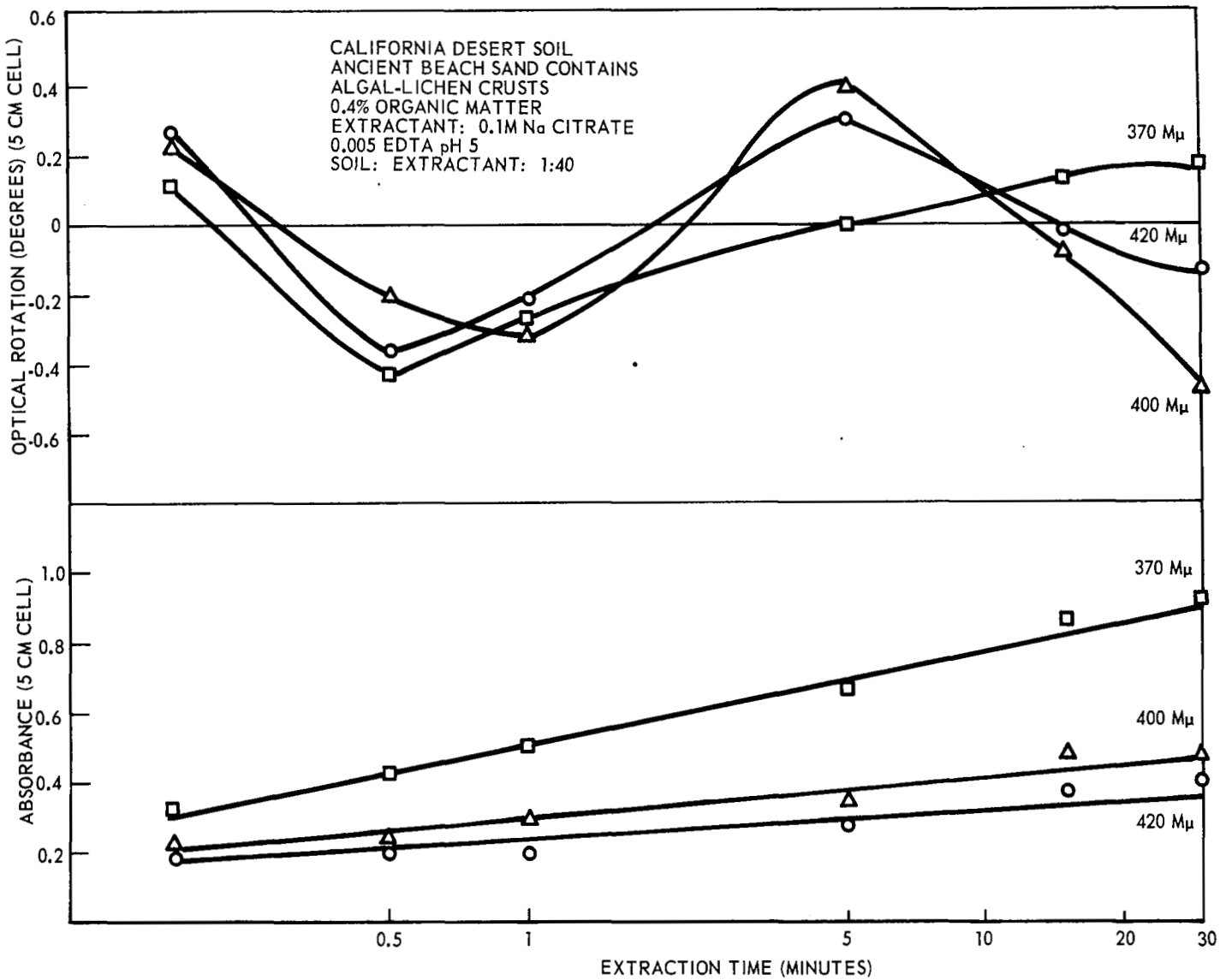

Figure 51. California Desert Soil, ORD and Absorbance Versus Extraction Time (Aqueous Extract, 1:40)

6. DISCUSSION OF RESULTS

The results shown in the previous section clearly indicate that the performance of thenew polarimeter is satisfactory. The limitations on its performance are, in great measure, due to the poor monochromation produced by the single-pass monochromator and filter combination. This severely limited operations in the UV with strongly absorbing solutions, and with solutions having pronounced absorption bands.

In the visible portion of the spectrum, these limitations are not nearly so severe due to the decreased absorption of the solutions and the characteristics of the light source. For all solutions measured, optical rotation was obtained in the visible (deep samples of desert soil showed no optical activity), particularly in the neighborhood of 400 mμ. Also, the instrument itself is capable of measuring optical rotation in the presence of an optical density of approximately 5. But to utilize such high optical density requires commensurate spectral purity, a problem which is not insoluble. The spectral purity required, in turn, depends upon the absorption spectrum of the material being measured.

In any event, the instrument has demonstrated its ability to operate in the presence of high optical density. This results in a concommitant relaxation of the requirement for great rotational sensitivity as higher concentrations can now be accommodated. This is salutary for the space problem: an instrument which is more rugged than the conventional instruments can be expected; yet, in chemical terms, it would have approximately the same sensitivity. Thus, sensitivity of the present instrument is approximately 0.05 degrees. Conventional instrumentation is approximately 0.005 to 0.01 degrees or less for an optical density of 2. If an optical density of 3 is utilized in the new polarimeter, this would be equivalent to a sensitivity of 0.005 with conventional instrumentation since ten times the material would be present in the optical path.

The optical rotatory dispersion curves show what is already well known, namely, that soil is a very complex material of highly variable composition. Nevertheless, common features do exist which could be utilized to make a simple, single-wavelength instrument that would detect the simple presence of optical activity with a high order of probability.

The results also show that there is a wealth of information to be obtained by optical rotatory dispersion and that further work is required to elucidate the observed rotations.

The results also show that macromolecular components and their degradation products, common to both organically enriched and desert soils, may be identified in terms of their chemical and/or molecular properties. The optical density associated with soil extracts has been attributed to the presence of polyaromatic residues which constitute humic material. These

humin complexes and their association with minerals and organic nitrogen and phosphate compounds impart a brownish color to aqueous extracts. The colored compounds also appear to be intimately associated with soil polysaccharides although the nature of this association is not known, and these polysaccharides form the major organic constituent of soil.[10] This point is borne out by the fact that the colored peaks in the Sephadex fractionation profiles showed positive tests for carbohydrates, while those peaks possessing considerably less color yet high absorbance at 260 mu were negative for the same test.

The particular choice of extractant was dictated by the studies enumerated in tables 1 and 4. That system which extracted, from an organically rich soil, the greatest amount of optically active compounds, such as proteins, carbohydrates, etc., was chosen for extraction of a desert soil for subsequent analysis by ORD. The rationale behind the use of chelating agents such as citrate and EDTA is based on their complexing of Ca^{++}, Fe^{++} and Mg^{++} ions which are known to be associated with soil organic matter. In our hands, this combination of sequestering agents seemed to work best. Currently available standard assays for the determination of organic matter content could not be utilized for the soil extracts since the extractant itself is organic and would give erroneous values; therefore, there is still some doubt as to the absolute amount of organic material in the extract.

The studies with the tritiated RNA indicated that anionic macromolecular components were difficult or impossible to extract with gentle phosphate or borate buffer treatment, regardless of pH. It is quite apparent, however, that some nucleic acid has been extracted with the citrate-EDTA buffer as evidenced by Table 1 and by TLC (Table 2). Furthermore, it is known that Mg^{++} ions can be tenaciously bound to nucleic acids and that EDTA is an excellent chelating agent for Mg^{++} ions.

The Sephadex chromatographic separations enabled us to determine the molecular weight limits of the macromolecular components of the soils under study and to compare the characteristics of the components of organically enriched soils with desert soils. Usually two or three major fractions were separated with both fertile and desert soils. These fractions ranged in molecular weight from approximately 5,000 to greater than 50,000. Since the areas under the peaks of the fractionation profiles were quite large, one may assume that large amounts of organic material were extracted with the citrate-EDTA buffer system. The detection of amino acids, sugars and nucleic acid components by thin-layer chromatography supports this conclusion.

Correlation of the amount of each of the organic constitutents (proteins, carbohydrates, etc.) with optical rotation was not possible due to the intrinsic heterogeneity of the soil samples themselves. Also, no strong correlation of percent organic matter with optical activity was

found. This is probably due to lack of knowledge about the organic content of the extract.

The differential extraction efficiency with different extractants may be due to varying solubilities of organic matter having different physicochemical properties. Autooxidation alters many of the properties of extracted organic matter. Production of humin-like substances may occur during the extraction process.[11] Metals are known to catalyze oxidation and polymerization reactions.[12] Photochemical oxidations may also occur to some extent. One major difficulty with all extractants is that the crude extracts of organic matter are contaminated with salts, clays, and metals such as aluminum, iron and magnesium.[13]

Thus, it can be seen that without extensive purification procedures specific for a particular component under examination, crude soil extracts will present a complex picture when analyzed by sophisticated instrumentation and thus cannot be subjected to the same critical level of analysis as purified compounds.

The results also show that absorption curves of crude extracts, by themselves, are not a sensitive index of extraction efficiency due to the complex mixture of ultraviolet absorbing compounds present in soils. The results do show convincingly that organic material possessing an easily detectable quantity of optically active constitutents can be extracted from desert soil depleted in organic matter content using a simple, non-optically active organic salt extractant at optimum soil:extractant ratios and extraction times.

7. CONCLUSIONS AND FUTURE STUDIES

1. Optical rotation does exist in soil extracts made by simple procedures.

2. Relatively simple instrumentation can be developed to meet the space mission requirements.

3. Optical rotation is generally found in soil samples (of those examined).

4. The experiment is ready for development into a flight package, but much more scientific work should be carried on to reinforce the present results and provide a scientific background for interpreting the results of a space mission.

5. There are also improvements possible in the instrumentation that should be investigated. Some of these improvements, such as better monochromation may result in much better scientific information in addition to improved instrument performance.

6. Conclusions related to the chemistry with requirements for future work are given below.

Conclusions

It has been shown that under controlled experimental conditions, valid data may be accumulated from a soil which is extremely heterogeneous in composition and virtually devoid of soluble organic material (compared with agriculturally enriched soils). The possibility that a large part of the organic matter that is present in the desert soils does not possess optical activity, reduces the chances of observing activity at presently achieved polarimeter sensitivities. Therefore, quantitative methods of analysis that are too rigorous will not yield consistent results. The current experiments were designed bearing in mind the parameters of an extra-terrestrial exploration program; i.e., a small quantity of sample to be processed, as short an extraction time as possible to yield a maximum of optical activity detectable within the sensitivity limits of the instrumentation, compatibility with the assigned power requirements, and the preferential use of an efficient, stable and non-corrosive extractant.

Examination of the desert soil studied so far, has shown definite trends. The data do suggest that the following rules for operation of a soil optical activity detection program may prove to yield the most information in a minimum of time and with a minimum of ambiguity.

1. Extraction of soil at 25° C or higher with 0.1-M sodium citrate - 0.05-M disodium EDTA, pH 5.0.

2. Extraction times should not exceed 5 minutes.

3. The ratio of soil to extractant should not exceed 1:10; on a weight-volume basis.

4. Observation wavelength region should be between 350 and 450 mμ, preferably 350-420 mμ.

Future Studies

Further experiments on the other soils listed in table 5 should be similarly examined as for the JPL 1-2 soil above. Study of a soil that possesses one fifth of the organic matter content of the soil reported here (JPL 34) would be the next logical step for correlation of optical activity and soil organic matter extraction.

Investigations are also necessary to further characterize the components of desert soil. It may prove desirable to perform some preliminary fractionation of the extraterrestrial soil before examination for optically active compounds. Certainly, the removal of interfering substances would enhance the response of the instrumentation possibly to a level approaching that obtained with model compounds (sucrose, albumin, starch). It would be possible also to investigate other extractants not heretofore considered within the framework of the present study, which would selectively extract particular soil organic components of interest to a mission such as this. Such extracts might lend themselves readily to simple separation methods without deleteriously affecting the gross properties of the solubilized components.

Further study is also suggested for determination of the efficiency of aqueous extracts at varying pressures, and at temperatures approaching the freezing point.

8. REFERENCES

1. Anon., Proposed Biological Exploration of Mars Between 1969 and 1973, Nature, 206 (4988):974-80 (1965). - Materials and Methods

2. Dische, Z., New Color Reactions for the Determination of Sugars in Polysaccharides, Methods of Biochemical Analysis, D. Glick, Editor, Interscience Publishers, Inc., N.Y., 2:319 (1955).

3. Henry, R.J., Sobel, C. and Beckman, S., Interferences with Biuret Methods for Serum Proteins, Use of Benedict's Qualitative Glucose Reagent as a Biuret Reagent, Anal. Chem., 29:1491 (1957).

4. Lowry, O.H., Rosebrough, N.J., Farr, A.L., and Randall, R.J., J. Biol. Chem., 193; 265 (1951).

5. Walkley, A., Standard Methods of Chemical Analysis, F. J. Welcher, Editor, D. van Nostrand Co., Princeton, 6th Ed. 2:2315 (1963).

6. Dische, Z., Color Reactions of Nucleic Acid Components in the Nucleic Acids, E. Chargaff, Editor, Academic Press, N.Y. 1:285 (1955).

7. R. F. Chen and R. L. Bowman, Science 147, 729 (1965).

8. M. N. McDermott and B. Novik, J. Opt. Soc. Amer. 51, 1008 (1961).

9. B. J. Benton, personal communication.

10. Mortensen, J.C. and Himes, F.L., Soil Organic Matter in Chemistry of the Soil, F. E. Bear, Editor, A.C.S. Monograph Series, Reinhold Publishing Corp., New York, Second Edition, pp. 206-241 (1964).

11. Bremner, J.M., J. Soil Science, 1:198 (1950).

12. Kyuma, K. and Kawaguch, K., Am. Soc. Agron. Abst., p. 25 (1962).

13. Saeki, H. and Azuma, J., Soil Plant Food , 6:49 (1960).